Membrane Binding Mechanism of Phosphoinositide Interacting Domains and Development of Their Inhibitors

A dissertation submitted to the
Indian Institute of Technology Guwahati as
partial fulfilment for the Degree of
Doctor of Philosophy in Chemistry

Submitted by

Sukhamoy Gorai

DEPARTMENT OF CHEMISTRY

INDIAN INSTITUTE OF TECHNOLOGY GUWAHATI

GUWAHATI-781039, ASSAM, INDIA

Dedicated

TO

My beloved Family

Contents

		Page No.
Statement		I
Certificate		II
Acknowledgements		III-IV
List of Abbreviations		V-VIII
Abstract		IX-XII
Chapter 1	Introduction	1-21
Chapter 2	Characterization of Phosphatidylinositols-Binding of Tks5-Phox Homology Domain and Role of its Hydrophobic Residues in Membrane-Binding	22-47
Chapter 3	Mechanistic Insights into the Phosphatidyl Inositol Binding Properties of Pleckstrin Homology (PH) Domain of Lamellipodin (Lpd)	48-66
Chapter 4	Inhibition of Phosphatidylinositol-3,4,5-trisphosphate Binding to AKT Pleckstrin Homology Domain by 4-Amino-1,2,5-oxadiazole Derivatives	67-93
Chapter 5	Insights into the Inhibitory mechanism of Triazole-Based Small Molecules on Phosphatidylinositol-4,5-bisphosphate Binding Pleckstrin Homology Domain	94-118
Conclusions and Scope for future work		119-121
Appendix		122-124
List of Publications		125

INDIAN INSTITUTE OF TECHNOLOGY GUWAHATI

DEPARTMENT OF CHEMISTRY

STATEMENT

I do hereby declare that the matter embodied in this thesis is the result of investigation carried out by me in the Department of Chemistry, Indian Institute of Technology Guwahati, Guwahati, Assam, India, under the guidance of Dr. Debasis Manna.

In keeping with the general practice of reporting scientific observations, due acknowledgements have been made wherever the work described is based on the findings of other investigators.

11.06.2015 Sukhamoy Gorai

IIT Guwahati (Roll No.-10612207)

INDIAN INSTITUTE OF TECHNOLOGY GUWAHATI

DEPARTMENT OF CHEMISTRY

DATE: 11.08.2015

CERTIFICATE

This is to certify that the thesis entitled ***"Membrane Binding Mechanism of Phosphoinositide Interacting Domains and Development of Their Inhibitors"***, is being submitted by **Mr. Sukhamoy Gorai (Roll No.-10612207)** for the award of degree of Doctor of Philosophy is an authentic record of the results obtained from the research work carried out under my supervision in the Department of Chemistry, Indian Institute of Technology Guwahati, India.

The results embodied in this thesis have not been submitted to any other University or Institute for the award of any degree.

Dr. Debasis Manna
(Thesis Supervisor)

Acknowledgements

I would like to thank all faculties, friends and family members who have helped me throughout my journey.

I wish to express my deep sense of gratitude to my thesis advisor, Dr. Debasis Manna for his expertise, guidance and excellence mentorship. His dedication and commitment to research and teaching is truly inspiring and remarkable.

I thank my doctoral committee members for their guidance and invaluable research expertise: Prof. Gopal Das, Prof. Biplab Mondal and Prof. Siddhartha Sankar Ghosh. Their insights and teachings, during my yearly progression were always enlightening. My honest regards to all the faculty of the Department of Chemistry for their motivation and encouragement.

A lot of what I have accomplished would not have been possible without the help of our collaborator, Dr. Manas Kumar Santra of National Centre for Cell Science; Pune, for giving me to study all the cellular experiments. I would like to thank Mr. Debasish Paul and other members in Dr. Manas Lab for their kind help during my cell study. Also, I would like to thank Dr. Biplab Bose and Prof. Siddhartha Sankar Ghosh who have provided me all instrumental facilities present at the DBT support program, Department of Biosciences and Bioengineering, IIT Guwahati. My sincere thanks also goes to Prof. Gopal Das for allowing me to perform monolayer experiment at Centre for Environment, IIT Guwahti.

I am heavily obliged to my former and present lab members, Dr. Narsimha, Rituparna Borah, Saurav Paul, Dipjyoti Talukdar, Subhankar Panda, Ashalata Roy, Abhishek Saha who have provided me insightful enjoyment and friendly working environment. I would also extend my thanks to my friends Mousumi, Najbul, Prasanta, Pankaj, Bappaditya, Krishnanjan, Subrata, Dr. Laxman, Radhakrishnan, Soumi, Manabda, Mitun, Subhamoyda, Sandipan, Thiyagarajan, Sudeep who have been exceptional support during my PhD.

I must not forget to thank IIT Guwahati for financial support and Department of Chemistry for giving me the opportunity to pursue my research work amidst such a wonderful environment.

None of this would have been possible without the love and endless support of my family. I express my deepest gratitude to my parents, Mr. Ajit Chandra Gorai and Mrs. Mamata Gorai, who are the great example of honesty and hard work. I learned lot of things from them. I am extremely grateful to my elder brothers, Mr. Krishna and Mr. Goutam Gorai. Without them it could have been impossible to complete this journey. Finally, I would like to thank to other family members specially Munni and Babu, two cute kids who are eagerly waiting for me back home.

Sukhamoy Gorai

List of Abbreviations

AKT	Protein kinase B
BTK	Bruton's tyrosine kinase
CHAPS	3-[(3-Cholamidopropyl)dimethylammonio]-1-Propanesulfonate
CISK	cytokine-independent survival kinase
C1/2	conserved region 1/2
DAPP1	Dual adapter for phosphotyrosine and 3-phosphotyrosine and 3-phosphoinositide
DMEM	Dulbecco's Modified Eagle Medium
DMSO	Dimethyl Sulfoxide
DNA	Deoxyribonucleic Acid
dNTP	Deoxyribonucleotide triphosphate
dPE	1,2-dioleoyl-sn-glycero-3-phosphoethanolamine-N-(5-dimethylamino-1-naphthalenesulfonyl)
DPH	1,6-diphenyl-1,3,5-hexatriene
DTT	Dithiothreitol
ENTH	Epsin1 N-terminal homology
ER	Endoplasmic reticulum
FAPP1	phosphoinositol-four-phosphate adapter protein 1
FRET	Fluorescence resonance energy transfer
FYVE	Fab1/YOTB/Vac1p/EEA1
GFP	Green Fluorescence Protein
GRB	Growth factor receptor-bound protein
GRP1	General receptor of phosphoinositides 1
GST	Glutathione S-transferase
GST	Glutathione S-Transferase
HEPES	4-(2-hydroxyethyl)-1-piperazineethanesulfonic acid
hr	Hour

HS1BP3	HCLS1 binding protein 3
IP_6	Inositol hexaphosphate
IPTG	Isopropyl β-D-1-thiogalactopyranoside
ITC	Isothermal titration calorimetric
kDa	Kilodalton
LB	Luria Broath
Lpd	Lamellipodin
mg	Milligram
min	Minute
ml	Milliter
mM	Millimolar
NBD-PE	1,2-diphytanoyl-sn-glycero-3-phosphoethanolamine-N-(7-nitro-2-1,3-benzoxadiazol-4-yl)
nM	Nanomolar
NMR	Nuclear Magnetic Resonance
n-OG	n-Octyl glucoside
PAGE	Polyacrylamide gel electrophoresis
PBS	Phosphate buffer saline
PC	1-Palmitoyl-2-oleoyl-*sn*-glycero-3-phosphocholine
PCR	Polymerase chain reaction
PDGF	Platelet Derived Growth Factor
PE	1-palmitoyl-2-oleoyl-*sn*-glycero-3-phosphoethanolamine
PEPP1	phosphoinositol-three-phosphate-binding PH domain protein 1
PH	Pleckstrin Homology
PI(3)P	phosphatidylinositol-3-phosphate
$PI(3,4)P_2$	Phosphatidylinositol-3,4-bisphosphate
PI(3,4,5)P3	phosphatidylinositol-3,4,5-triphosphate
$PI(3,5)P_2$	Phosphatidylinositol-3,5-bisphosphate
PI(4)P	phosphatidylinositol-4-phosphate

PI(5)P	phosphatidylinositol-5-phosphate
PI3K	Phosphatidylinositol 3-kinase
PIP	Phosphatidyl inositol
PIP_2 or $PI(4,5)_2$	phosphatidylinositol-4,5-bisphosphate
PKC	Protein kinase C
PLC	Phospholipase C
PMSF	Phenylmethanesulfonylfluoride
PS	1-palmitoyl-2-oleoyl-*sn*-glycero-3-phosphoserine
PTEN	Phosphatise and tension homolog
PX	Phox Homology
RFP	Red fluorescence protein
rpm	Revolutions per minute
s	Second
SDS	Sodium dodecyl sulphate
SH3	Src Homology 3
SPR	Surface Plasmon Resonance
Src	Sarcoma
TCN	Tricyclic nucleoside
Tks5	Tyrosine Kinase Substrate 5 SH3 domain
Tris	Tris(hydroxymethyl)aminomethane
WT	Wild type
π_c	Critical surface pressure
µg	Microgram
µl	Microliter
µM	Micrometer
IC_{50}	The concentration of an inhibitor which causes 50% inhibition
K_I	Inhibitor dissociation constant
K_a	Association constant
K_d	Dissociation constant

$K_I(IP_6)_{app}$	Apparent inhibitory dissociation constant

Amino Acid	3-letter code	1-lettere code	Amino Acid	3-letter code	1-lettere code
Alanine	Ala	A	Methionine	Met	M
Arginine	Arg	R	Phenylalanine	Phe	F
Asparagine	Asn	N	Proline	Pro	P
Cysteine	Cys	C	Selenocystein	Sec	S
Glutamic acid	Gln	Q	Serine	Ser	S
Glycine	Gly	G	Threonine	Thr	T
Histidine	His	H	Tryptophan	Trp	W
Isoleusine	Ile	I	Tyrosine	Tyr	Y
Leusine	Leu	L	Valine	Val	V

Nucleobase	Code
Adenine	A
Gunine	G
Thymine	T
Cytosine	C
Uracil	U

Abstract

The content of this thesis entitled **"*Membrane Binding Mechanism of Phosphoinositide Interacting Domains and Development of Their Inhibitors*"** have been divided into five chapters based on the results of experimental work carried out during the research period. The introductory chapter (**Chapter1**) describes the role of phosphoinositides (PIP) in cell signalling, several PIP binding domains including PX, PH domains and small molecule based non-lipid antagonists those are used as inhibitors in PIP-PH interactions. **Chapter 2** determines the roles of basic and hydrophobic residues of Tks5-Phox homology domain in membrane binding. In **Chapter 3,** we have determined the mechanistic insight into PIP binding properties of Lpd-PH domain. **Chapter 4** demonstrates the inhibition of phosphatidylinositol-3,4,5-trisphosphate binding to AKT pleckstrin homology domain by 4-Amino-1,2,5-oxadiazole derivatives. In **Chapter 5,** we have demonstrated the inhibitory mechanism of triazole-based small molecules on phosphatidylinositol-4,5-bisphosphate binding pleckstrin homology domain.

Phosphatidylinositol (PIP) and its seven phosphorylated derivatives are involved in several cellular events including membrane trafficking, cytoskeleton remodeling, membrane dynamics and others. Their functions and turn over are catalyzed by PIP-kinases and phosphatases. Deregulation of their functions are involved in several human disease like disorder of myotubular myopathy, type 2 diabetes, cancer and others. The roles of PIPs are mediated by a number of PIP binding modules including PX, PH and others which can specifically interact with PIP and transmits their signal at membrane-cytosol interface. It is important to understand how these PIP binding receptors differentially respond to specific PIP. In this regard, in order to understand the binding properties of PIP and PIP interacting domains, we choose Tks5-PX and Lpd-PH domain and successfully determined their membrane binding behaviours and also to perturb these interactions, we have developed PIP/PH domain interactions based small molecule antagonists.

Therefore, to elucidate the role of basic and hydrophobic residues of Tks5-PX domain in membrane binding, we quantitatively determined the binding parameters using a number of biophysical studies including surface plasmon resonance (SPR), fluorescence resonance energy transfer (FRET) and monolayer penetration analyses. It is important to note that Tks5 (Tyrosine kinase substrate with five Src homology 3 domains) in association with other protein binding partners and phospholipids regulates several important cellular functions and is crucial for invadosome formation, invasion in cancer cells, degradation of extracellular

matrix and progression of Alzheimer's disease. In cellular condition the N-terminal phox homology (PX) domain of Tks5 interacts with phosphatidylinositol-3,4-bisphosphate ($PI(3,4)P_2$) lipid and this interaction is essential for Tks5-induced invadosome formation. The biophysical measurements revealed that Tks5-PX domain has significant different PIP binding properties with stronger affinities for $PI(3,4)P_2$ and phosphatidylinositol-3-phosphate (PI(3)P) lipids. Extent of PIP-dependent monolayer penetrations by the PX domain also varies significantly and alters its membrane binding properties. Mutational studies revealed that presence of basic residues within the PIP-binding pocket and hydrophobic residues at the putative membrane binding surface of the PX domain are significant for its PIP-dependent membrane binding properties. Under normal growth conditions, cellular localization patterns of the PX domain and its mutants in A549 cells are consistent with their *in vitro* membrane binding properties. PX domain colocalizes with PI(3)P binding cellular marker at the early endosomal membranes and translocates to the plasma membrane upon stimulation with platelet-derived growth factor. Results implied that R42 and R93 residues are mainly responsible for PIP binding and L80 and F81 hydrophobic residues enhance membrane binding by partial membrane penetration.

As we have already mentioned earlier that PH domain also display similar PIP binding nature as of PX domain, hence in this regard, we have also determined the membrane interactions properties of Lpd-PH domain. It is reported that lamellipodia formation in mobile cells is regulated by Ena/vASP proteins which have crucial role in actin dynamics, cell polarity and motility. Lamellipodin (Lpd), an Ena/VASP protein plays important role in lamellipodial protrusion formation. The PH domain of Lpd interacts with the membrane containing $PI(3,4)P_2$ phosphoinositide and regulates cellular functions. This interaction is essential for Lpd dependent cell migration. However, the molecular mechanism that underlies how the PH domain of Lpd specifically recruits to $PI(3,4)P_2$ remains unclear. Our biophysical results show that PH domain of Lpd strongly interacts with $PI(3,4)P_2$ containing liposomes without any membrane penetration. Mutational studies demonstrate the presence of cationic residues within the PIP binding site of Lpd-PH domain is essential in membrane binding. The translocation patterns of Lpd-PH domain and mutants in platelet-derived growth factor (PDGF) stimulated A549 cells are in good agreement with our *in vitro* binding measurements. Our results suggest that R32 and R34 amino acid residues play major role in $PI(3,4)P_2$ containing membrane binding.

Based on this interaction, several kinases activate which is crucial for their cellular functions. As for example, phosphatidylinositol-3-kinases (PI3K) is an important cell signalling pathways which is the key regulator of several proteins function. PI3K signaling pathways are frequently deregulated which is directly linked with different human cancers. AKT is a phosphatidylinositol (PIP) binding serine/threonine kinase enzyme and a key component of PI3K-signalling pathway. Several efforts have been made to perturb the activities of AKT enzyme; however, selectivity issue remains a key challenging point. Pleckstrin homology (PH) domain of AKT strongly interacts with the membrane localized PIPs and activates the enzyme. Several attempts are underway for the development of small molecules, which can specifically inhibit the PIP/PH-domain interaction to ascertain an alternate approach for the development of drug(s) for PI3K-AKT-signalling pathway. This proposed approach is highly beneficial because of easy synthesis of small molecules and low side effects. In this regards, we used a series of small molecule antagonists (**GPI**s) for PI(3,4,5)P_3/PH-domain interaction and determined their inhibitory effect by using competitive-surface plasmon resonance (SPR) analysis (IC_{50} ranges from 1.85 to 16.35 μM for PI(3,4,5)P_3/AKT1 PH-domain binding assay). To elucidate their binding selectivity, we also used PI(3,4,5)P_3, PI(3,4)P_2, PI(4,5)P_2 specific PH-domains. For further understanding of their PH-domain inhibition mechanism, we also performed various physicochemical analyses. The results showed that these water-soluble compounds do not significantly interact with the model membranes. The oxadiazole and N′-hydroxy moieties of the compounds are essential for their exothermic interaction with the PH-domains and their bindings do not alter the secondary structure of the PH-domain. Potent compounds show moderate effect on phosphothreonine (308) level of AKT enzyme.

With continuing PIP/PH domain interaction based inhibitor development, we also developed 1,2,3-triazol-4-yl methanol containing small molecule (**CIPs**) as antagonists for PI(4,5)P_2/PH-domain interaction and determined their inhibitory effect by using competitive-SPR analysis (IC_{50} ranges from 53 to 159 nM for PI(4,5)P_2/PLCδ1-PH domain binding assay). We also used PI(3,4,5)P_3, PI(3,4)P_2, PI(4,5)P_2 specific PH-domains to determine binding selectivity of the compounds. Various physicochemical analyses showed that the compounds have weak affect on fluidity of the model membrane but, strongly interact with the PLCδ1-PH domains preferably through its PIP binding site. The 1,2,3-triazol-4-yl methanol moiety and nitro group of the compounds are essential for their exothermic interaction with the PH-domains. Potent compound can efficiently displace PLCδ1-PH domain from PM to cytosol in A549 cells.

Overall our study lead us to propose membrane binding properties of Tks5-PX and Lpd-PH domain which could be used for therapeutic target for further biomedical research. Detailed membrane binding parameters were measured using SPR, FRET-based competitive binding, monolayer and cellular localization studies. In addition, we have also developed PIP/PH domain interaction based small molecule antagonists. The oxadiazole and 1,2,3-triazol-4-yl methanol moiety containing compounds selectively inhibit $PI(3,4,5)P_3$/AKT-PH and $PI(4,5)P_2$/PLCδ1-PH-domain interactions respectively. Further, this idea can be extended for PIP/PH-domain interactions based drug development.

Chapter 1

Introduction

1.1 Phosphoinositide: A key regulator in biological cell membrane

Cellular membranes are selectively permeable lipid bilayers, which separate cellular compartments from their environment. It is composed of numerous lipids, ion channels, proteins and other biomolecules that play important role in different cellular functions. Each cellular compartment is composed of specific lipid compositions that play important roles in segregating the inner machinery as well as transmitting signals via membrane-cytosol interfaces and through membrane bilayers. Interactions of proteins with these membrane containing-lipid molecules play an important role in regulating these cellular functions. It is well documented that properties of lipid head group, alkyl chain length, degrees of unsaturation and others greatly influence the functions of proteins through specific lipid-protein interactions. On the other hand, several functions of proteins also depend upon the self-association properties including thickness, fluidity, shape and packing of lipids bilayers. Therefore, study of lipid-protein interaction is considered as an emerging research area to understand how they involve in several cell signalling events.[1-6]

Most abundant membrane lipids are phosphatidylethanolamine (PE), phosphatidylcholine (PC), phosphatidylserine (PS), cholesterol, phophatidic acid (PA), sphingomyelin and phosphatidylinositol (PIP). Among the all lipids, PIPs are less abundant in cellular membranes but regulate a wide variety of cellular events. The structural anatomies of PIPs are very similar to that of other phospholipids except the presence of an extended polar head group, *myo-inositol.* The free hydroxyl groups at D3, D4 and D5 positions of the *myo-inositol* ring are readily phosphorylated and dephosphorylated by the action of inositol-kinases and phosphatases, respectively. Seven different phosphorylated isoforms play pivotal role in cell signalling, cell survival, growth, vesicular transport and other cellular functions.[4,9] These PIP lipids alter the physical properties, including charge and fluidity of cell membranes and/or act as binding partner of proteins. Each of these PIP lipids are localized at different cellular membranes and considered as marker of specific membranes. [5,7] phosphotidylinositol-3-phosphate (PI(3)P), and phosphotidylinositol-4,5-biphosphate ($PI(4,5)P_2$) are considered as the marker of early-endosomal membranes and plasmamembranes of eukaryotic cells, respectively. The polar headgroups of PIPs provide the

intrinsic charge and interact with the proteins though electrostatic interactions. This interaction is crucial for localization of proteins to the specific membranes as well as metabolization into different lipids, such as different PIPs, diacylglycerol (DAG), phosphatidic acid (PA) and others. Endoplsmic reticulum (ER) is the main source for production of PIP lipids. However, plasma membrane also takes part in PIPs synthesis, where different classes of inositol-kinases and phosphatases are involved in the synthesis of different PIP isoforms. In general, membrane translocation of proteins occurs due to the interaction between substrate proteins with the activated receptors and others through protein-protein interaction. However, recent studies demonstrate that protein-lipid interaction is also essential for specific sub-cellular localization of signalling proteins. Lipid binding domains directly interact with specific lipids and allow localization to the specific membrane/compartment site for their activation/proper functions, without perturbing regular protein-protein/protein-small molecule interactions.[7,8] Electrostatic interactions play a major role in protein-lipid interaction where polar head group of lipids specifically coordinates with protein. In few cases these interactions enhance the degree of membrane translocation by the partial membrane penetration of hydrophobic residues present on the binding surface. The translocation of a particular protein at the specific membrane gives us the idea of this complex lipid-protein interaction process which has been generally shown by the GFP or other tagged fluorescence probe with the protein. Use of these fluorescent tagged domains reveals the site of localization of specific lipids. Certain lipid–binding domains show higher affinity for certain lipids including PIPs which even indicates site of transient/persistent lipid productions. These lipid-protein interaction mechanism can be summarized as initial diffusion and nonspecific, long-range electrostatic interactions followed by specific interactions with lipids and/or partial membrane penetration through hydrophobic residues.[10-13] Structural analysis of the lipid binding domains in presence of their interacting partners, provide a detailed insight into the lipid-protein interactions. Most of the lipid binding domains have specific binding pockets and precisely interact with lipid head groups. Few well characterized domains like AP180 amino terminal homology (ANTH), protein kinase C conserved region 2 (C2) and others do not have proper lipid binding site but preferentially interact with specific lipid head groups.[14, 15] Majority of lipid binding modules including phox homology (PX), pleckstrin homology (PH), Fab1/YOTB/Vac1/EEA1 (FYVE), protein kinase C conserved region-1 (C1), FERM, Epsin1 N-terminal homology (ENTH), PDZ, BAR and tubby domains have specific lipid and/or ligand binding site.[10, 11, 16-23] Whereas some proteins play important role in signalling

either utilizing the protein surface to interact with membrane or covalently attach with the membrane residing lipid molecules. Therefore, these interactions are crucial for the site-specific targeting of many signalling and membrane-trafficking proteins.

Depending upon specificity lipid-protein interactions could be of higher to lower affinities. Typically, this interaction is highly specific and involve in stereo-specific recognition of lipid head groups. On the other hand low or non-specific interactions occur through other parameters including charge, curvature and amphiphilicity.[12, 19] Sometimes oligomeriztion also enhance membrane binding affinities. As an example, monomeric PH domain of dynamin interacts with lipid in millimolar range, but the dimeric form shows exceptionally higher binding (ranging from micromolar to sub-millimolar). Membrane binding affinity could be also enhanced by membrane insertion of hydrophobic residues present on the binding surface of the protein. Well known membrane binding domains containing hydrophobic residues are C1, PH and PX and increase 10-20 fold higher affinity to the specific lipids due to the membrane penetration. The reduction of electrostatic potential is critical for membrane penetration, especially for PIP binding modules. In the absence of lipids, charged surface of proteins are surrounded by water molecules. Interaction of lipids with charged proteins reduce the electrostatic potential on the protein surface, which allows the surface-exposed hydrophobic residues to penetrate into the cellular membranes.

1.2 Phosphoinositides in membrane dynamics and cell signalling

Initially PIP research was focused on only $PI(4,5)P_2$ and later, the role of phosphoinositides in cell signalling was established in 1975. PIPs are only 15% of the all the phospholipids present in eukaryotic cells.[24] Still it is very crucial in all aspect of cellular functions including proliferation, survival, signalling, ion transport, metabolism gene expression, exocytosis, cytoskeleton dynamics, membrane trafficking and others. Deregulation of their functions is associated with several disorders like autoimmune, cancers and cardiovascular disease.[25-28] Phosphoinositides and its soluble products inositol phosphates work in parallel in signalling and constitutive functions. $I(1,4,5)P_3$ is the hydrolyzed product of $PI(4,5)P_2$ and controls the intracellular Ca^{2+} signalling which is associated with gene transcription, protein phosphorylation, nuclear export and RNA editing.[29, 30] The PIP-signalling is mediated by a number of proteins. To understand their role in different cellular functions, understanding the overall mechanism is highly beneficial.

Current research of particular interests is the derivatives with phosphate groups at the D3, D4, and/or D5 positions of the D-myoinositol ring. The seven derivatives of PIPs are

PI(3)P, phosphatidylinositol-5-phosphate (PI(5)P), phosphatidylinositol-4-phosphate (PI(4)P), phosphatidylinositol-3,4-biphosphate ($PI(3,4)P_2$), $PI(4,5)P_2$, phosphatidylinositol-3,5-biphosphate ($PI(3,5)P_2$), phosphatidylinositol-3,4,5-triphosphate ($PI(3,4,5)P_3$). Characteristically, each of the seven derivatives of PIPs are distributed in the specific compartments with a predominant localization in the corresponding membranes. Earlier it was thought that monophosphorylated phosphoinositides are the only precursors for multi-phosphorylated phosphoinositides. Later researchers demonstrated their individual role in cell signalling. PI(3)P is enriched primarily in early endosomes and multivesicular bodies (MVB). PI(3)P is generated either due to phosphorylation by class I and III phosphotidylinositol-3-kinase or due to dephosphorylation of $PI(3,4)P_2$ and $PI(3,4,5)P_3$ by phosphatidylinositol polyphosphate 3-phosphatase. The cellular PI(3)P level is controlled by phosphorylation, dephosphorylation or degradation in the lysosome and precisely plays role in endosomal functions.[7, 8, 31, 32] Generally PX domain and FYVE domain containing proteins are recruited to the endosomal PI(3)P and plays important role in membrane trafficking. It is reported that GFP fused FYVE domain is localized in early endosome, provided the information of enrichment of PI(3)P at the endosomal membrane. The PI(3)P is also precursor of another phophoinositide, $PI(3,5)P_2$ and $PI(3,4)P_2$ although maximum $PI(3,4)P_2$ is generated at plasma membrane. PI(3)P is phophorylated by the phophoinositide kinase (PIKfyve) at position D5 position to generate $PI(3,5)P_2$. Whereas phosphorylation at the position of D4 by the function of phosphoinositide kinase II gives rise a lesser amount of $PI(3,4)P_2$ at the endosome.

Phophoinositides $PI(4,5)P_2$ is the most abundant PIPs in the plasma membrane and takes part in several cellular events carried out at the cell surface. Cellular level of $PI(4,5)P_2$ or its metabolic products are significantly involved in transduction of extracellular signals. It is generated either phosphorylation at D5 position of PI(4)P by type I phosphoinositide kinase or phosphorylation at D4 position of PI(5)P by type II phosphoinositide kinase. Major portion of $PI(4,5)P_2$ is derived from PI(4) due to less abundant of PI(5)P in cell. $PI(4,5)P_2$ could be hydrolyzed by phospholipase C(PLC) and phospholipase A_2 (PLA_2), produced membrane bound diacyglycerol (DAG) and inositol 1,4,5-trisphosphate (IP_3). The hydrolyzed products of $PI(4,5)P_2$ are two potent second messengers, control other signalling pathway whereas the dephosphorylation plays role in controlling steady-state levels of $PI(4,5)P_2$ and turns off its signalling. Further the newly formed DAG is recognized by the C1 domains including PKC, Munc13 and others and translocate to the plasma membrane, inducing the phosphorylation on serine and threonine residues of the target proteins. This membarne

translocation is important to activate C1 domain and that of the intracellular Ca^{2+} and other phospholipid-binding C2 domain. Another hydrolyzed product IP_3 releases the Ca^{2+} ions from endoplasmic reticulum (ER) and maintains the cellular Ca^{2+} ions.[33-35]

Class I phosphoinositide 3-kinase phosphorylates at D3 position of $PI(4,5)P_2$, produces $PI(3,4,5)P_3$ that are very less abundant in resting cells. But the level of $PI(3,4,5)P_3$ is transiently increased upon stimulation with growth factors. A large number of proteins are recruited by $PI(3,4,5)P_3$ and are involved in signalling cascades. As an example GEFs and GAPs for GTPases are targeted by $PI(3,4,5)P_3$ and regulates the actin cytoskeleton remodelling. MToR, a serine/threonine protein kinase is also activated by the cooperative action of protein kinase PDK and AKT/PKB via $PI(3,4,5)P_3$ recruitment. In addition, dephosphorylation of $PI(3,4,5)P_3$ at the D3 and D5 positions is resulted to form $PI(4,5)P_2$ and $PI(3,4)P_2$ respectively, thus it facilities either to off signal or may extend the duration of $PI(3,4,5)P_3$ signalling. Therefore this metabolic pathway plays significant role in seval cellular functions.

Recent studies demonstrate that $PI(4,5)P_2$ is primarily involved in exocytosis and endocytosis process at the cell membrane. Critically it recruits both in *cis* on membrane proteins and in *trans* on vesicle proteins at the pre-fusion stage and in that way proceeds to the nucleation centre for an exocytosis apparatus.[36, 37] Milosevic and co-workers determined the pooling as well as secretion level of vesicles is highly depended on the level of $PI(4,5)P_2$ at the membranes. The hydrolyzed products of $PI(4,5)P_2$ also trigger the secretion of vesicles. On the other hand $PI(4,5)P_2$ and/or $PI(3,4,5)P_3$ play important roles in recruiting and regulating of endocytic proteins to the membrane. It is reported that fusion reaction is tightly mediated by endocytic clathrin proteins including AP180/CALM, AP-2, epsin and other endocytic factors (for an example dynamin) via interaction with phosphoinositides. Deposphorylation of phosphoionositides by the function of inositol-5 phosphatase takes place and removes the endocytic vesicles from the phosphoinositides.[38]

Endosomal biology (mostly in trafficking from and to the plasma membrane, lysosomes and plasma membrane) is primarily regulated by the phosphoinositides PI(3)P and $PI(3,5)P_2$. As described before PI(3)P is mostly found in early endosome and determinants its identity through interactions with PI(3)P binding proteins. Cellular level of PI(3) is maintained by the class III PI-3 kinase VPS34 as well as the sequential dephosphorylation of $PI(3,4,5)P_3$ by inositol phosphatases specific for the 5 and 4 position respectively. By the functions of Fab1P/PIKfyve kinase Phosphorylation takes place at D5 position of PI(3)P to form $PI(3,5)P_2$ which triggers budding of vesicles from late endosomes.

1.3 PX domain

The Phox Homology (PX) domain was originally identified in two cytosolic subunits, $p47^{phox}$ and $p40^{phox}$ of NADPH in 1996.[39] In general, PX domains are composed of ~100-120 amino acid residues with three α-helix followed by three β-sheets and a number of poly proline (PXXP) rich motifs. It is well documented that PX domain can interact with other SH3 domain containing proteins through its PXXP motif. PX domains are classified into three subclasses depending on their length amino acid sequences and presence of other motifs. In the **first category**, the PX domain containing proteins are of short polypeptide chain and PX domains itself represent more than half of the host protein sequences. **First category**, the PX domain contains Grd19p, SNX22, SNX23, SNX12, SNX3, SNX10, SNX24 and SNX26 proteins. **Second category** of PX domains contain longer flanking sequences, but lack of other characterized motifs and include yeast Mvp1p, Vps5p and mammalian SNX1, SNX2, HS1BP3 (haemopoietic-specific protein 1 (HS1) SH3 domain binding protein) and others. **Third category** of PX domains contains other well known domains including C1, C2, PH along with PX domain. A large number of PX domain containing proteins including, p40phox, p47phox, Bem1p, SNX18, FISH/Tks5, PI3K-C2α/β/γ, CISK, SNX25, Bem3p and others are associated with this category.[40] Recent studies demonstrated that the PX domain is a novel lipid binding module and its preferential interaction with PIPs allowed the effector proteins to regulate several cellular processes. As an example, PX domain of SNXs preferentially interacts with endosomal PI(3)P and regulate transportation from early-endosome to recycling-endosome and involved in signalling processes. Further studies showed that this endosomal membrane association were perturbed by mutants of PIP-interacting amino acids or by PI3Ks inhibitor and wortmannin.[41, 42]

Since most of the PX domains have been identified through database search, their cellular functions have not been fully elucidated. However, recent genetic and biochemical studies have suggested that HS1BP3, Tks5 and Bem3P PX domains play key role in diverse cellular processes, including T-cell activation, chemical signalling in the brain region, control of cell polarity, podosome formation. PX domain containing SNARE family of proteins mediate vesicle fusion that is, the fusion of vesicles with their target membrane bound compartments. The PX domain of yeast Vam7p protein plays an important role in docking and fusion at the vacuoles. The endosomal/vacuolar association takes place by direct interaction of N-terminal PX domain of Vam7p to membrane containing PI(3)P. Mechanistic studies revealed that membrane localization of the PX domain was completely abolished by

inactivation of yeast PI3K (Vps34p), suggests that PX domain of Vam7p targets vacuolar membrane via specific PI(3)P dependent manner.[43] The knowledge of PIP-PX domain interactions and their role in several cellular events are broaden by two separate studies which established the membrane binding mechanism of two cytosolic components (p40phox and p47phox) of NADPH oxidase. $p40^{phox}$-PX domain selectively interacts with vesicle containing PI(3)P whereas p47phox-PX domain preferentially interacts with $PI(3,4)P_2$ and stimulates NADPH oxidase activity in vitro.[44] It is also important to mention that PX domain preferably interact with PI(3)P whereas its interaction with other PIs are rare (Table 1.3.1). Only few PX domain selectively interacts with other PIPs rather than PI(3)P. Such as the PX domain of class II-PI3K preferentially interacts $PI(4,5)P_2$ and also studies show that CISK-PX domain selectively binds to $PI(3,5)P_2$, $PI(3,4,5)P_3$.

Table 1.3.1. Reported non-PI(3)P-binding PX domains

PX-domains	$p47^{phox}$	PI3K-C2α	Bem1p	PLD1	CISK	KIF16B (SNX23)
Preferred PIPs	$PI(3,4)P_2$	$PI(4,5)P_2$	PI(4)P	$P(3,4,5)P_3$ > PI(3)P > PI(5)P >> other PIPs	$P(3,5)P_2$ > $P(3,4,5)P_3$ > $P(4,5)P_2$	PI(3)P> $P(3,4)P_2$ > $P(3,4,5)P_3$

Homology sequence alignments of the PX domains show that most of the PX domains consist of number of subdomains or motif with conserved hydrophobic amino acid residues and PIP-interacting basic amino acid residues. Recently, NMR and crystallography studies successfully investigated the structural basis of several PX domains. Structural analyses revealed that the architecture of PX domain is flat and compact, consisting of three β-strands followed by three α-helices. Few PX domains (such as $p47^{phox}$) consist of additional α-helix (named as α1′) downstream of α1 helix. In general, two basic residues of majority of the PX domains are conserved in β3-α1 region as RR(F/Y)(S)(D/E)F sequence. Presence of two other conserved basic residues in the α2 helix of the PX domain constructs the PIP-binding site. The conserved hydrophobic residues present near the PIP-binding surface of PX domain also shows significant role in membrane binding. Through structural analyses, PIP-binding properties and biological activity studies demonstrated a probable PIP-dependent membrane binding mechanism of the PX domain, where PX domains first non-specifically interact with the membrane surface then specifically interact with selective PIPs followed by membrane penetration through the hydrophobic residues present near the binding surface. Kinetics studies of PIP-PX domain interactions showed that mutants of these hydrophobic residues get

dissociated at a faster rate than the wild type PX domain, which suggests that hydrophobic residues play an important role in PIP-dependent membrane binding. The PX domains also interact with proteins like SH3 domain through its conserved proline-rich PXXP motif. PX domains of Tks5, HS1BP3, $p47^{phox}$ and others strongly interact with the SH3 domain of other or host protein through inter/intra molecular interactions.

PX domain containing proteins are also play a major role in cell signalling and/or cell survival. Ser/Thr kinase Cytokine-independent survival kinase (CISK) is distributed in endosome via PI(3)P- PX domain interaction and regulates in interleukin-3-dependent survival mechanisms in haematopoietic cells.[45,46] Biological studies revealed that CISK and AKT proteins display phophorylation of both Bcl-xl/Bcl-2 associated death promoters (BAD) due to PIP-dependent membrane interactions through their PX/PH domains, respectively. It is well documented that several PX domain containing proteins play an important role in phosphorylation and hydrolysis of phospholipids. PI3Ks, which spatially and temporally regulates the diverse cellular processes by phosphorylation of the 3′-OH of PIPs also regulates activation and membrane recruitment of the cytosolic $p40^{phox}$, $p47^{phox}$ and $p67^{phox}$ proteins (Figure 1.3.1).

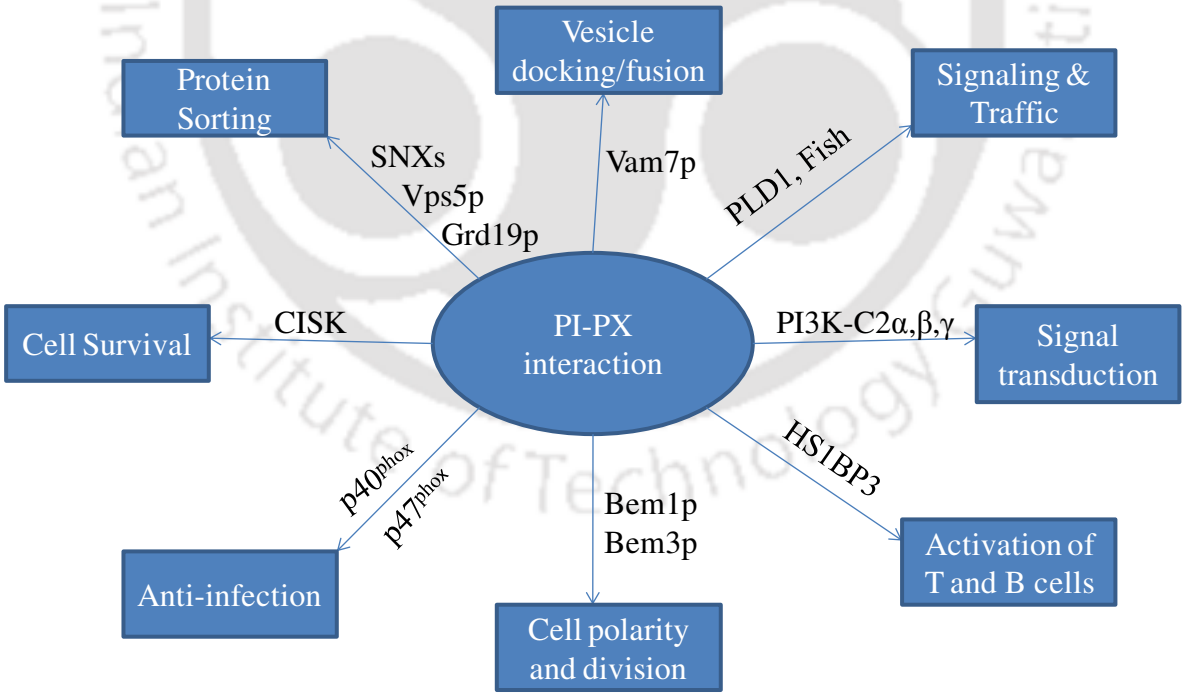

Figure 1.3.1: Diverse cellular functions regulated by PIP-PX domain interactions.[38]

1.4 PH domain

The PH domain was first identified as a novel PIP-interacting motif of approximately 120 amino acid residues. It is the 11^{th} most abundant domain found in human genome and most

functionally diverse-phospholipid binding module that has not been completely characterized yet. PH domains have been identified in various proteins involved in cell signalling, cytoskeleton dynamics and metabolism. To date there are more than 250 human proteins which contain one or more PH domains. Out of them, only10-20 % PH domains exhibit high affinity and specificity for PIPs, whereas a majority of the characterized PH domains bind weakly to PIPs with little or no selectivity. Based upon binding affinities and specificities, PH domains are classified into four major groups.[47, 48] PH domains of BTK, GRP1, and Ras-GAP1 show high affinity (with $K_D < 50$ nm) to PI(3,4,5)P_3 and classified as **Group I** PH domains. The PH domains of Gap1^{IP4BP}, mSos-1 and N-terminal Tiam-1 are also classified as **Group I** PH domains. The PH domain of PLCδ belongs to **Group II** PH domains and exhibits high affinity for PI(4,5)P_2, the most abundant PIPs in the cellular membranes. However, these PH domains exhibit much weaker binding affinity for PI(4,5)P_2 lipids (2-4 folds) than that of **Group I** PH domains for PI(3,4,5)P_3 lipids. The **Group III PH** domains show dual character in PIP binding properties. AKT/PKB, PDK1, Dapp1 and others belong to this class and preferentially interact with PI(3,4)P_2 and PI(3,4,5)P_3.[49] The PH domains of ARNO, cytohesin-1 and GRP1 interact with PI(3,4)P_2 and/or PI(3,4,5)P_3. The PH domains with low PIP binding affinities (with $K_D > 1$ μm) are classified into **Group IV** and dynamin-PH domain belongs to this group. Recent developments revealed that TAPP1and 2 (tandem PH domain containing protein 1 and 2 respectively), PEPP1(phosphoinositol-three-phosphate-binding PH domain protein 1), centaurin-β2 and FAPP1(phosphoinositol-four-phosphate adapter protein 1) preferentially interact with PI(3,4)P_2, PI(3)P, PI(3,5)P_2 and PI(4)P respectively.

Structural analyses revealed that PH domains contain seven β-sheets followed by one α-helix. To date, more than 100 high resolution 3D-structures of PH domains are available in Protein Data Bank website. Macias et al. in 1994 first reported the structure of the PH domain of β-spectrin using homonuclear NMR technique and the same year Fesik and co-workers solved the PH domain of pleckstrin using heteronuclear NMR technique. They find out the presence of common core known as canonical core-fold with different loop regions in the NMR structures of the PH domains. The basic core structure of proteins consist of a pair of nearly orthogonal N-terminal four β-sheets with three anti-parallel strands close to a collapsed β-barrel and appears as two sandwiched β-sheets (β1-β4, β5-β7) followed by C-terminal α-helix.[50] The carboxy- and amino-termini are present on the similar side, but protrude in opposite directions. One long α-helix is located in carboxy-terminus of the structure and packed against one edge of the β-sheet which stabilizes the structural

orientation through helix-sheet interaction. Homology sequence alignment of several PH domains illustrate that three loop regions (β1/β2, β3/β4, β6/β7) connecting the β-sheets are conserved. In addition, the PIP interacting basic residues in this region are conserved in Group I-III PH domains but not in Group IV, suggesting the key role of these conserved residues in PIPs binding. Due to the abundance of high basic residues in β-barrel region and a number of acidic residues in α-helix, the overall charge of the PH domain makes it dipolar in nature. The electro positive surface at the open-end of the β-barrel region accommodates the ligands or PIP headgroups.

PH domains of BTK, GRP1, AKT proteins have drawn much attention due to their higher binding affinities and specificities for PI3K product, PI(3,4,5)P_3. The crystal structure of BTK-PH domain (1B55) shows that the head group of PI(3,4,5)P_3 interact with the cationic groove in a similar fashion as that of PLCδ PH domain with PI(4,5)P_2. The 3- and 4- phosphates of PI(3,4,5)P_3 and 5- and 4- phosphates of PI(4,5)P_2 lipids interact in a similar fashion with BTK and PLCδ PH domains, although the interacting loops of the respective PH domains, β1/β2 and β3/β4 are somewhat distinct. The orientation of these interactions primarily depends on both composition and length of β1/β2 loop, which differs dramatically among PH domains. In case of BTK PH domain, β1/β2 loops consists of 11 amino acids which makes the binding surface more flatten. Whereas short chain of 5 amino acid residues present in the β1/β2 loops of PLCδ-PH domain form a complete binding pocket for both 4- and 5- phosphate interaction.[51, 52] Presence of an extended β6/β7 loop in few PH domains ruled out the above hypothesis. Likewise, although GRP1-PH domain has relatively short β1/β2 loop but the orientation of interaction patterns are similar as BTK-PH domain because of having 20 extra amino acid residues in the β6/β7 loop and preferentially interacts with PI(3,4,5)P_3. Combining this extra amino acid residues form a β hairpin structure and complete the pocket for 5-phosphate with short β1/β2. Interestingly, PH domain of Dapp1 specifically interacts with PI(3,4,5)P_3 but the binding pattern is little bit different than the GRP1 PH domain. Although in both cases β6/β7 loop contributes in PI(3,4,5)P_3 binding but the Dapp1-PH domain essentially interacts with 4-phosphate instead of 5-phosphate due to the too short loop length is unable to form β hairpin structure.

Isolated PH domains and/or the host proteins are generally cytoplasmic peripheral proteins. In response to PDGF, PI(3,4)P_2 and PI(3,4,5)P_3 generate at the plasma membrane and several PH domains transiently translocate to the membrane. The translocation studies of GFP or other fluorescence tagged PH domains and their host proteins support the formation

and disappearance of different PIPs at the cellular membranes. Full length GRP1 and its 2G splice variant PH domain translocate from cytosol to plasma membrane in response to stimuli, like insulin or epidermal growth factor hormone. Similar translocation pattern were also observed for AKT/PKB and BTK-PH domains. Their membrane translocation could be completely abolished either by mutation of PIP interacting amino acid residues or by using PI-3 kinase inhibitor, wortmanin. This translocation results are in good agreement with their *in-vitro* PIP-binding studies. Therefore, PIP binding is necessary and sufficient for membrane translocation and subsequent cellular functions of the PH domain containing proteins. However, in few cases protein-protein interactions also play a key role in membrane translocation. The PH domain of OSBP weakly interacts with PI(4)P and localize at the Golgi apparatus. Binding studies with PIP-binding mutants of OSBP-PH domain also showed its localization at the Golgi apparatus.[53] This localization pattern is due to the interaction between OSBP-PH domain and Golgi GTPase Arf1 protein. In addition of lipid-proteins interactions, the carboxy-terminal polybasic sequence of Cytohesin-1 and ARNO-PH domains cooperatively targets the membrane.

1.5. Small molecules inhibitors of PIP/PH interaction

The PI3K signalling pathway plays various roles in cellular functions including survival, differentiation, invasion and growth. Insulin or growth factor activation of PI3K regulates the production of $PI(3,4,5)P_3$ and $PI(3,4)P_2$. Cellular $PI(3,4,5)P_3$ level is transiently and tightly regulated by PTEN (phosphatise and tension homology domain) enzyme which play a critical role in several cytosolic and nuclear functions. Deregulation of this kinase and phosphatase is directly or indirectly associated with human disease including cancers. PTEN is frequently mutated in disease state and consequently increase the $PI(3,4,5)P_3$ level leading to over activity of PI3K related signalling pathway. Thus, PI3K signalling pathway is crucial and considered as an attractive therapeutic target in numerous cancers. A number of proteins containing PH, PX and others lipid binding domains are highly regulated and activated through interacting with the PI3K products phosphatidylinositol lipids. AKT/PKB (Protein kinase B) is a downstream signalling protein of the PI3K enzyme. The PH domain of AKT specifically bind with membrane residing $PI(3,4,5)P_3$ and get over-activated in different types of cancers including pancreatic, skin and prostate cancers. AKT is a ser/Thr kinase enzyme and a member of cAMP dependent protein kinase A/G/C super family of protein kinases, and share similar structural sequence homology within their catalytic domain. In mammalian cell, AKT exists in three isoforms, AKT1, AKT2 and AKT3 and their chromosomal localization

are identified as 14q32, 19q13, and 1q44, respectively. Full activation of AKT protein is mediated by membrane recruitment via PIP/PH domain interaction, followed by phosphorylation at two crucial amino acid residues, Thr308 and Ser 473 residing at kinase domain and C-terminal hydrophobic motif respectively. PIP dependent membrane recruitment of AKT PH domain alter its conformation and expose the amino acid residues, Thr308 and Ser473 which are further phosphorylated by phosphoinositide-dependent kinase 1 (PDK1) and phosphoinositide-dependent kinase 2 (PDK2) enzymes, respectively. AKT activation is also mediated by known DNA activated protein kinase (DNA-PK), rapamycin complex 2 (mTORC2), and ataxia telangiectasia mutated kinase (ATM). The loss of PTEN activity results in hyper-activation of AKT and increase in phophorylation in downstream targets including GSK3-β proteins.[54-57]

A number of other PH domain containing proteins are also frequently activated and do proper functioning through the PI3K pathway. A cytoplasmic tyrosine kinase, BTK and ITK are known to specifically interact with PI(3,4,5)P_3 lipid through their PH domains and crucial for B and T cell development. Like AKT protein, BTK also get frequently mutated and loss their proper activity, resulting a number of disorders including lymphocyte autoimmunity or allergy/ hypersensitivity and malignancies. Although, the ITK deficiency is much less in humans but the mutation of functional amino acid residues causes susceptibility to severe, frequently fatal, Epstein–Barr virus infections. Activated BTK/ITK stimulates a number of downstream signals including PLC isoenzyme activation, cell proliferation, apoptosis, survival and differentiation.[57-60] Upon stimulation, PLC enzyme binds to PI(4,5)P_2 containing plasma-membrane through its PH domain and hydrolyze the phosphodiester bond. (DAG). Consequently, it generates two important downstream signalling molecules, I(1,4,5)P_3 [IP_3] and diacyglycerol (DAG). These second messengers subsequently activate the transcription factors NF-κB and NF-AT through several intermediate steps and over activation of NF-κB critically promotes the tumour growth. For these reasons few research groups are involved in developing small molecule which can specifically inhibit the PIP/PH domain interactions.

In general catalytic domain of AKT, BTK, PLC and others are considered as the target to develop inhibitors for regulating these enzymes. However, most of the catalytic domain based inhibitors have several drawbacks. In most of the cases catalytic domains are high homologous which is accounted for the lack of selectivity. For this selectivity problem, the small molecules can also regulate the cellular functions of non-targeted proteins. As an example the development of AKT kinase inhibitors (for catalytic domain) to target and treat

cancers are effective but experience selectivity problems resulting in an unwanted side effects, including myelosuppression, skin rash and stomatitis and others. Meanwhile mechanistic studies demonstrated that highly specific PIP/PH-domain interactions can regulate activities of the effector proteins. It is also described that small molecules can alter the protein-lipid interactions, because of the presence of well defined binding pocket of most of the lipid binding modules of the effector proteins. It is also reported that small molecule inhibitors for protein-lipid interactions are advantageous over usual approaches due to lower side-effects and rational design with comparatively simple structures and functions. On the other hand lipid based drug development is also problematic due to low solubility and permeability in cellular environment. Recently Prof. Meuillet's group have successfully been developed lipid based AKT-PH domain inhibitors, DPIEL which strongly prevents the membrane translocation and activation as well as reduced phosphorylation level of AKT protein.[63]

The PH-Domain as a target for synthetic small molecules-

As mention earlier PH domain is unique to AKT and others proteins, which offers selective advantage among the protein kinases and make the PH-domain an alternative and attractive drug target. Several natural and synthetic compounds specifically target the PH domains. These compounds bind with the PH domains through similar mode as of PIP/PH interaction. Efforts are undergoing to develop selective and potent inhibitors for preventing these PIP/PH interactions. Here, couple of PH domain targeted synthetic small molecules which are in clinical trial or used in biophysical study, have been described.

TCN Analogues-

Tricyclic nucleoside (TCN) was developed as an inhibitor for DNA synthesis and also had antitumor and antiviral activity. Recently, Yang and co-workers demonstrate that this small molecule selectively interact with AKT without hindering the activities of other A/G/C family related regulatory pathways, including activation of phosphatidylinositol 3 -kinase, serum-and glucocorticoid-inducible kinase, phosphoinositide dependent kinase-1, protein kinase C, protein kinase A, signal transducer and activators of transcription 3 and others.[61] Considerable inhibition was reported in downstream effects of AKT enzyme, where it acts as a substrate for more than 20 others proteins. The TCN analogue (Figure 1.5.1), API-2 (1μM) showed remarkable effect of inhibiting the phosphorylation levels of tuberlin leading to stabilization and up-regulation of tuberin. Further studies revealed that this potent compound

potentially inhibits tumour growth in high expressed AKT overexpressing cells in xenograft nude mice, but fails in low AKT expressing tumour cells. Although, this compound acts as potential antitumor agent but the use of this compound in clinical trial was limited due to a number of side effects including hypertriglyceridemia, hepatotoxicity, hyperglycemia and thrombocytopenia.

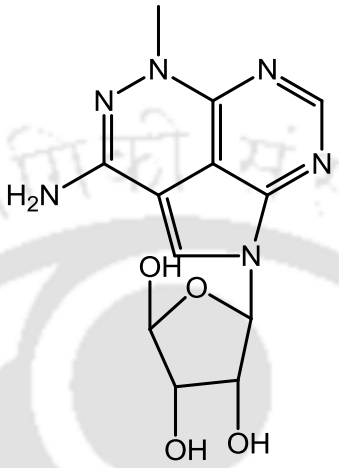

Figure 1.5.1. Structure of TCN

Benzenesulfonamide and its analogs- Recently, Ahad and co-workers developed a series of benzenesulphonamide based potent compounds (Figure 1.5.2) which selectively inhibit the AKT-PH/PI(3,4,5)P_3 interactions.[62] They developed 47 different benzenesulfonamide substrates for their study and determine their inhibition ability by SPR based competitive binding assay and tested the activities of the compounds in human BxPC-3 pancreatic cancer cell line. However, no significant binding (K_i > 50 µM) was observed in case of compounds with hydrogen atoms at positions R_1, R_2, and R_3 and an amino or acetamido substituent at R_4

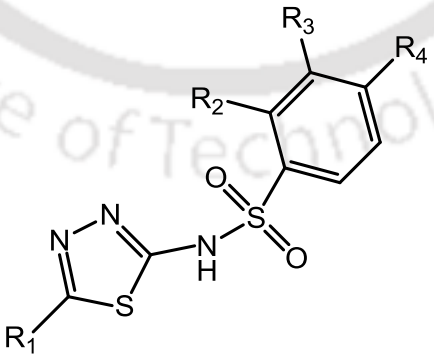

Figure 1.5.2. Structure of Benzenesulfonamide

position, respectively. But remarkable binding (K_i ~ 10 µM) was observed with variable substituent at R_1 position only. Alkyl substituent at the position R_4 of these compound

showed relatively higher binding affinity for AKT-PH domain that mimic the PI(3,4,5)P_3 binding of phosphate group at C-3 by interacting with Arg23, Arg25, and Lys14 residues.

DPI (1-[(R)-2,3-bis(hexadecanoyloxy)propyl hydrogen phosphate]) and its analogs- Meuillet and co-workers descried a novel strategy to inhibit AKT-PH domain activation by lipid based inhibitors, DPI and its functional analogs (Figure 1.5.3).[63] DPIs strongly interact with AKT-PH domain and inhibit the membrane translocation in PDGF treated mouse NIH3T3 cells. Compounds were designed in such a way that must not have D-3-hydroxy group in myo-inositol ring, preventing the opportunity of phosphorylation by PI3K. Among all the DPIs, Molecular modelling and in-silico docking studies showed that DPIEL (ether lipid analogue) strongly interacts with AKT-PH domain. In vitro binding studies showed that these potent compounds specifically interact with AKT-PH domains without disturbing the function of other PH domain containing proteins in cellular environment and inhibit its function with high IC_{50} value (ranging from 1.5-27.4 μM) but fells to inhibit a membrane-bound myristylated-AKT expressed in NIH3T3 cells.

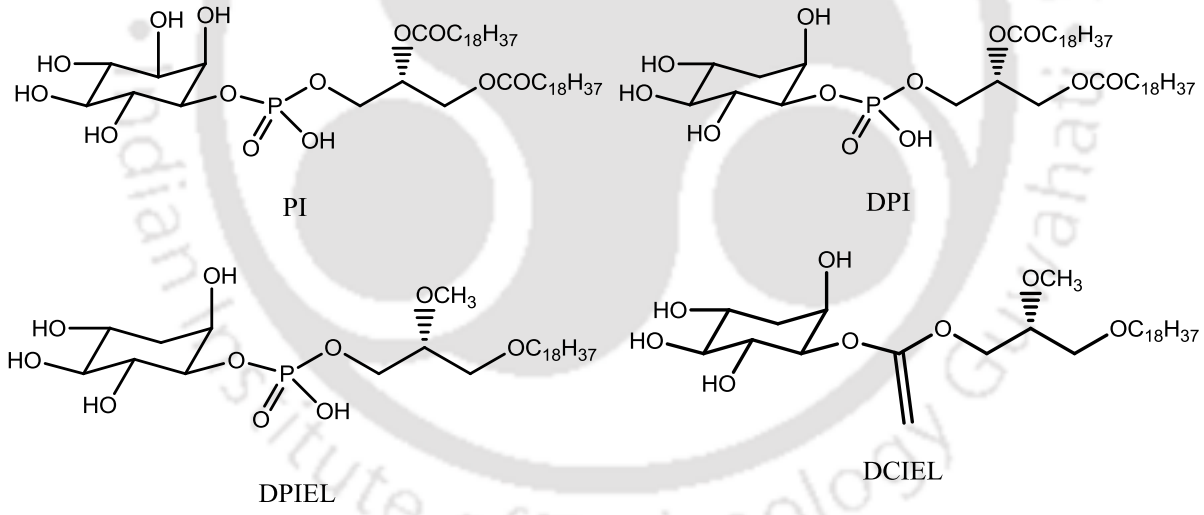

Figure 1.5.3. Structure of DPI and its analogues

PITenins (PITs) and its analogs-

PITenins or PITs (Figure 1.5.4) are a class of non-lipid and non-phosphoinositide based small molecules with high selectivity for PI(3,4,5)P_3 binding of the PH domains.[64] In vitro binding studies and cellular activity studies showed that these potent compounds significantly inhibit the PI(3,4,5)P_3/AKT-PH domain interaction (IC_{50} ranges from 13.4 to 31μM) and tumour growth. They also reported that these potent compounds selectively inhibit PI(3,4,5)P_3-dependent PI3K-PDK1-AKT signalling pathway. Among the PITs, PIT-1

showed significant antitumor activity with perturbation in membrane translocation of AKT enzyme.

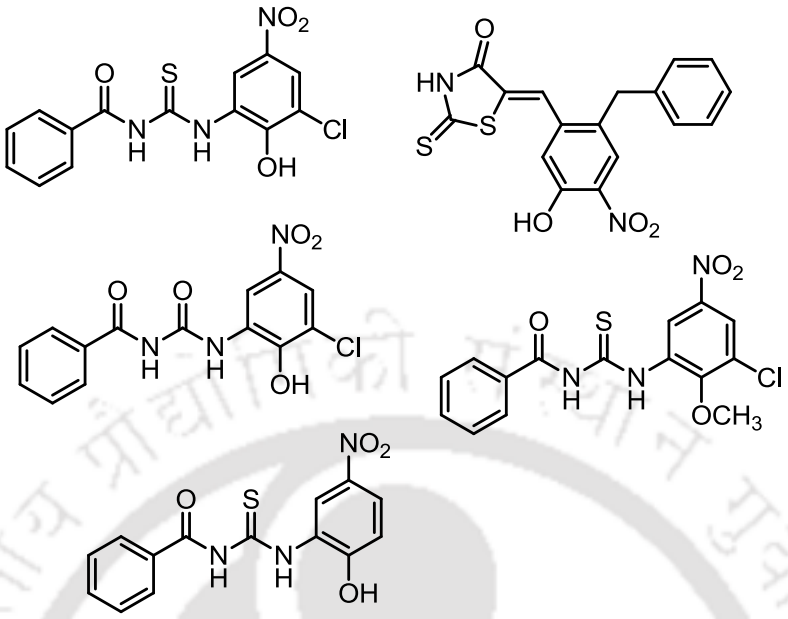

Figure 1.5.4. Structure of PITenins (PITs) and its analogues.

Inhibitors of PLC

There are only few inhibitors of PLC enzyme reported so far in various literatures. Neomycin (Figure 1.5.5A) and U73122 (Figure 1.5.5B) are generally used as inhibitor of PLC enzyme. Neomycine is a high positive charged (+4.5) polyamine compound.[65] Thus it has large affinity for membranes with negatively charged lipids (preferentially for polyphosphoinositides). Therefore, neomycin could block the PLC functions indirectly by rendering these lipids unavailable as for the substrate to activate their functions. On the other hand maleimide containing U73122 is widely used as PLC inhibitor in cell study.[66] But there are no reports whether this potent compound has been studied in molecular level. Recently Klein and co-workers studied the interaction of U73122 with PLC in a simple, cell-free, mixed micellar system.[67] Surprisingly, they found out that U73122 compound acts an activator rather being a inhibitor of PLC enzyme in cell free system. In contrast, U73122 acts as inhibitor due to block the functions of PLC enzyme indirectly under cellular environment. The maleimide moiety is highly reactive to thiols, such as cystine residues of cellular proteins, resulting in covalent modification of a number of sulfhydryl groups on hPLCβ3 protein.

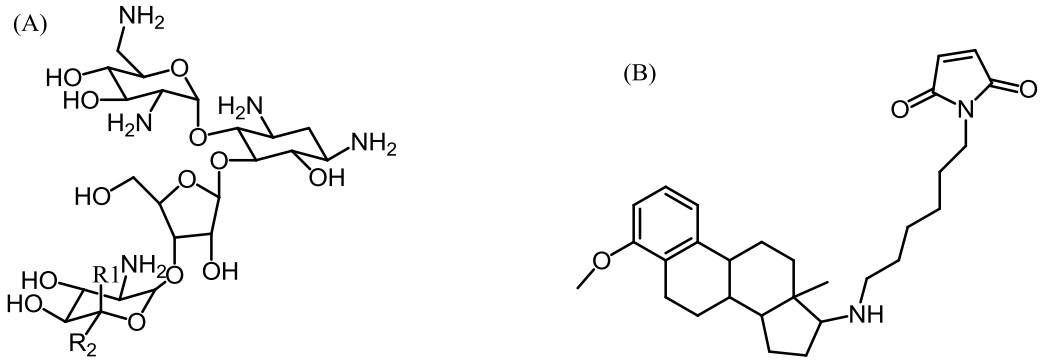

Figure 1.5.5: Structure of neomycine (A) and U73122 (B).

Concluding Remarks

Phosphatidylinositol and its seven phosphorylated isoforms are involved in several cellular signaling processes. Their functions are mediated by a number of proteins specifically lipid binding domains that tightly regulate by lipid-protein interactions. There are many reports where lipid-protein interactions have been successfully characterized in molecular level. A number of in-vitro biophysical studies as well as membrane translocation study in cell have been employed. Mutational studies provide the idea of exact role of interacting residues as well as the role of hydrophobic residues in membrane interaction. To date PIP-dependent membrane binding nature of only eleven PIP-binding domains including conserved region 1(C1) domain, conserved region 2 (C2) domain, phox homology(PX) domain, pleckstrin homology (PH), Fab1/YOTB/Vac1p/EEA1 (FYVE), AP180 N-terminal homology (ANTH), Epsin1 N-terminal homology (ENTH), PDZ, FERM, BAR and tubby domains have been thoroughly characterized. Out of several of PIP-interacting proteins only few proteins have been mechanistically characterized for their membrane binding properties. Therefore, mutational study is the key step to characterize the lipid-protein interactions. Here we have successfully characterized the membrane binding properties of Tks5-PX and Lpd-PH domain. Mutational study as well as other biophysical studies including FRET-based competitive binding study, SPR and monolayer study demonstrate the PIP-binding specificity and affinity and also determine the role of basic residue and the hydrophobic residues present at the binding surface. Cellular localization study is good correlates with our *invitro* binding study. Overall, our results demonstrate the mechanistic insights into the PIP-binding properties of Tks5-PX domain and Lpd-PH domain.

On the other hand deregulation of lipid-protein interactions and their functions led to a number of disorders including cancer. PI3K pathway, which is associated with AKT signalling, is considered as an attractive drug target because of its numerous roles in cellular

events that are directly or indirectly related with different kind of disease. Efforts are underway to develop potent inhibitors for PIP/PH domain interactions. For example, benzensulfonamide, API, DPI, PITs based small molecules have developed and determined their inhibition by biophysical methods as well as in cancer cell lines. In this study, we also developed a series of small molecules which specifically interact with AKT-PH and PLCδ-PH domain. SPR based competitive binding assay shows that 4-amino-N′-hydroxy-1,2,5-oxadiazole-3-carboximidamide moiety-based small molecule antagonists (**GPI**s) potentially inhibit the PI(3,4,5)P_3/AKT-PH interactions and the phosphorylation level of AKT decrease in cellular environment. 1,2,3-triazol-4-yl methanol based small molecules (**CIP**s) potentially interact with PLCδ-PH domain. SPR based competitive binding study shows that these potent compounds selectively inhibits the PI(4,5)P_2/ PLCδ-PH domain interactions and displaces the PLCδ-PH domain from the membrane in cellular environment. Overall, our studies demonstrate that these compounds could interact with the PIP-binding PH-domains and inhibit their membrane recruitment. These studies also illustrate the feasibility of further development of 4-amino-N′-hydroxy-1,2,5-oxadiazole-3-carboximidamide and 1,2,3-triazol-4-yl methanol moiety-based small molecule antagonists of PIP-signalling.

References

1. B.H. Falkenburger, J.B. Jensen, E.J. Dickson, B.C. Suh and B. Hille, *J. Physiol.*, 2010, **588**, 3179-3185.
2. T. Bala, Z. Szentpetery and Y.J. Kim, *Physiology (Bethesda)*, 2009, **24**, 231-244.
3. O. Cremona and P. De Camilli, *J. Cell Sci.*, 2001, **114**, 1041-1052.
4. G. Di Paolo and P. De Camilli, *Nature*, 2006, **443**, 651-657.
5. R. Behnia and S. Munro, *Nature*, 2005, **438**, 597-604
6. Z. Jiang, R.E. Redfern, Y. Isler, A.H. Ross and A. Gericke, Chem Phys Lipids. 2014, **182**, 52-61.
7. J.H. Hurley and T. Meyer, *Curr. Opin. Cell Biol*., 2001, **13**, 146-152.
8. T. Bala, *J. Cell Sci*., 2005, **118**, 2093-2104.
9. T.F Martin, *Annu Rev. Cell Dev. Biol*., 1998, **14**, 231-264.
10. D. Manna, A. Albanese, W. Sun Park and W Cho, *J. Biol. Chem.*, 2007, **282**, 32093-32105.
11. R.V. Stahelin, F. Long, K. Diraviyam, K.S. Bruzik, D. Murray, and W. Cho, *J. Biol. Chem.*, **277**, 26379-26388.
12. R.V. Stahelin, F. Long, B.J. Peter, D. Murray, P. De Camilli, H.T. McMahon and W. Cho, *J. Biol. Chem.*, 2003, **278**, 28993–28999.
13. R.V. Stahelin, A. Burian, K.S. Bruzik, D. Murray and W. Cho, *J. Biol. Chem.*, 2003, **278**,14469-14479.
14. A. Silkov, Y. Yoon, H. Lee, N. Gokhale, E. Adu-Gyamfi, R.V. Stahelin, W. Cho and D. Murray, *J. Biol. Chem*., 2011, **286**, 34155-34163.
15. L. Bittova, M. Sumandea and W. Cho, *J. Biol. Chem*., 1999, **274**, 9665-9672
16. M.A. Lemmon, *Nat. Rev. Mol. Cell. Biol*., 2008, **9**, 99-111.
17. W. Cho and R.V. Stahelin, *Annu. Rev. Biophys. Biomol. Struct*., 2005, **34**, 119-151.
18. W.D. Heo, T. Inoue, W.S. Park, M.L. Kim, B.O. Park, T.J. Wandless and T. Meyer, *Science*, 2006, **314**, 1458-1461.
19. Y. Yoon, X. Zhang and W. Cho, *J. Biol. Chem*., 2012, **287**, 34078-34090.
20. D.C Bosanquet, L. Ye, K.G. Harding and W.G. Jiang, Int J Mol Med, 2004, 34, 3-12..
21. M.E. Ivanova, G.C Fletcher, N. O'Reilly, A.G Purkiss, B.J. Thomson and N.Q. Mcdonald, *Acta Crystallogr D Biol Crystallogr*. 2015, 71, 555-564.
22. W. Nunomura, P. Gascard, H. Wakui and Y. Takakuwa, *Biochem Biophys Res Commun*, 2014, **446**, 434-440.
23. K. Moravcevic, C.L. Oxley and M.A. Lemmon, *Structure*, 2012, **20**, 15-27.
24. A. Zachowski, Biochem J. 1993, **294**, 1-14.
25. M. Wishart and J.E. Dixon, *Trends Cell Biol*., 2002, **12**, 579-585.
26. J.R. Halstead, K. Jalink and N. Divecha, *Trends Pharmacol. Sci*., 2005, **26**, 654-660.
27. J. Laporte, F. Blondeau, A. Buj-Bello and J.-L. Mandel, *Trends Genet*., 2001, **17**, 221-228.
28. D. Noack, J. Rae, A.R. Cross, B.A. Ellis, P.E. Newburger, J.T. Curnutte and P.G. Heyworth, *Blood*, 2001, **97**, 305-311.
29. C.A. Barlow, R.S. Laishram and R.A. Anderson, *Trends in Cell Biol*., **20**, 25-35.

30. Z.H. Shah, D.R. Jones, L. Sommer, R. Foulger, Y. Bultsma, C. D'Santos and N. Divecha, *FEBS Journal*, 2013, **280**, 6295–6310.
31. M.A. Lemmon, *Traffic*, 2003, **4**, 201–-213.
32. H.C. Birkeland and H. Stenmark, *Curr. Top. Microbiol. Immunol*., 2004, **282**, 89-115.
33. R.F. Irvine, *Nat. Rev. Mol. Cell Biol.,* 2003, **4**, 349–360.
34. K. Goto, Y. Hozumi and H. Kondo, *Biochim. Biophys. Acta*, 2006, **1761**, 535–541.
35. N. Chalhoub and S.J. Baker, *Annu. Rev. Pathol*., 2009, **4**, 127–150.
36. M.R. Lackner, S.J. Nurrish and J.M. Kaplan, *Neuron*, 1999, **24**, 335-346.
37. J.S. Rhee, A. Betz, S. Pyott, K. Reim, F. Varogueaux, I. Augustin, D. Hesse, T.C. Sudhof, M. Takahashi, C. Rosenmund,and N. Brose, *Cell*, 2002, **108**, 121-133.
38. I. Milosevic, J.B. Sorensen, T. Lang, M. Krause, G. Nagy, V. Haucke, R. Jahn and E. Neher, *J. Neurosci.*, 2005, **25**, 2557-2565.
39. C.P. Ponting, *Protein Sci*., 1996, **5**, 2353-2357.
40. Y. Xu, L.F. Seet, B. Hanson and W.Hong, *Biochem. J*., 2001, **360**, 513-530.
41. A. Arcaro and M.P. Wymann, *Biochem. J*., 1993, **296**, 297-301.
42. B. Vanhaesebroeck, S.J. Leevers, A. Khatereh, J. Timms, R. Katso, P.C. Driscoll, R. Woscholski, P.J. Parker and M.D. Waterfield, *Annu. Rev. Biochem*., 2001, **70**, 535-602.
43. M.L. Cheever, T.K. Sato, T. de Beer, T.G. Kutateladze, S.D. Emr and M. Overduin, *Nat. Cell Biol*., 2001, **3**, 613-618.
44. F. Kanai, H. Liu, S.J. Field, H. Akbary, T. Matsuo, G.E. Brown, L.C. Cantley and M.B. Yaffe, *Nat. Cell Biol*., 2001, **3**, 675-678.
45. D. Liu, X. Yang and S. Zhou, *Curr. Biol*., 2000, **10**, 1233-1236.
46. J. Xu, D. Liu,G. Gill and Z. Songyang, *J Cell Biol*. 2001, **154**, 699–706.
47. L.E. Rameh, A.-K. Arvidsson, K.L. III Carraway, A.D. Couvillon, G. Rathbun, A. Cromptoni, B. VanRenterghem, M.P. Czech, K.S. Ravichandran, S.J. Burakoff, D.S. Wang, C.S. Chen and L.C. Cantley, *J. Biol. Chem*., 1997, **272**, 22059-22066.
48. S. Dowler, R.A. Currie, D.G. Campbell, M. Deak, G. Kular, C.P. Downes and D.R. Alessi, *Biochem. J*., 2000, **351**, 19-31.
49. S. Dowler, R.A. Currie, C.P. Downes and D.R. Alessi, *Biochem. J*., 1999, **342**, 7-12.
50. J. Yan, W. Wen, W. Xu, J.F. Long, M.E. Adams, S.C. Froehner and M. Zhang, *EMBO J,* 2005, **24**, 3985-3995.
51. J.P. DiNitto and D.G. Lambright, *Biochim Biophys Acta*, 2006, **1761**, 850-867.
52. K.M. Ferguson, M.A. Lemmon, J. Schlessinger and P.B. Sigler, *Cell*, 1995, **83**, 1037-1046.
53. M. Lenoir, M. Grzybek, M. Majkowski, S. Rajesh, J. Kaur, S.B. Whittaker,U. Coskun and M. Overduin, *J. Mol. Biol*., 2015, **427**, 966-981.
54. G. Songa, G. Ouyang and S. Bao, *J. Cell. Mol. Med*., 2005, **9**, 59-71.
55. R. Yao and G.M. Cooper, *Science*, 1995, **267**, 2003-2006.
56. R. Chen, O. Kim, J. Yang, K. Sato, K.M. Eisenmann, J. McCarthy, H. Chen and Y. Qiu, *J. Biol. Chem*., 2001, **276**,31858-31862.
57. H.G. Wendel, E. De Stanchina, J.S. Fridman, A. Malina, S. Ray, S. Kogan, C. Cordon-Cardo, J. Pelletier and S.W. Lowe, *Nature*, 2004, **428**, 332-337.

58. J.J. Cohen, R.C. Duke, V.A. Fadok and K.S. Sellins, *Annu. Rev. Immunol*., 1992, **10**, 267-293.
59. C.B. Thompson, *Science*, 1995, **267**, 1456-1462.
60. D.J. Rawlings, D.C. Saffran, S. Tsukada, D.A Largaespada, J.C. Grimaldi, L. Cohen, R.N. Mohr, J.F. Bazan, M. Howard, N.G. Copeland, N.A. Jenkins and O.N. Witte, *Science*, 1993, **261**, 358-361.
61. L.L. Wortring, J.L. Roti, J.L. Hudson, J.E. Passiatore, K.Z. Borysko, R.D. Newcomb and L.B. Townsend, *Nucleosides and Nucleotides,* **6**, 95-109.
62. A.M. Ahad, S. Zuohe, L. Du-Cuny, S.A. Moses, L.L. Zhou, S. Zhang, G. Powis,E.J. Meuillet and E.A. Mash, *Bioorganic & Medicinal Chemistry*, 2001, **19**, 2046-2054.
63. E.J. Meuillet, D. Mahadevan, M. Berggren, R. Williams, A. Coon, A.P. Kozikowski and G. Powis, *Mol Cancer Ther*., 2003, **4**, 389-99.
64. B. Miao, I. Skidan, J. Yang, A. Lugovskoy, M. Reibarkh, K. Long, T. Brazell, K.A. Durugkar, J. Maki, C.V. Ramana, B. Schaffhausen, G. Wagner, V. Torchilin, J. Yuan and Alexei Degterev, *PNAS*, 2010, **107**, 20126-20131.
65. J. Schacht, *Journal of Neurochemistry*, 1976, **21**, 1119-1124.
66. J.E. Bleasdale, G.L. Bundy, S. Bunting, F.A. Fitzpatrick, R.M. Huff, F.F. Sun and J.E. Pike, *Adv Prostaglandin Thromboxane Leukot Res*., 1989, **19,** 590-603.
67. R.R. Klein, D.M. Bourdon, C.L. Costales, C.D. Wagner, W.L. White, J. D. Williams, S.N. Hicks, J. Sondek and D.R. Thakker, *J. Biol. Chem*., 2011, **286**, 12407-12416.

Chapter 2

Characterization of Phosphatidylinositols-Binding of Tks5-Phox Homology Domain and Role of its Hydrophobic Residues in Membrane-Binding

In this chapter, we describe a through mechanistic investigation of PIP induced membrane binding of Tks5-PX domain. Differential PIPs binding properties was quantitatively determined by FRET based competitive binding assay, kinetics SPR measurements, monolayer penetration analyses. Biological significance of their PIP binding parameters was tested by cellular localization studies in A549 cancer cells. All together the results lead us to propose new membrane docking mechanisms that provide insights into membrane interacting and translocation mechanism of the Tks5-PX domain and precise role of PI(3)P and PI(3,4)P_2 in membrane binding of Tks5-PX domain.

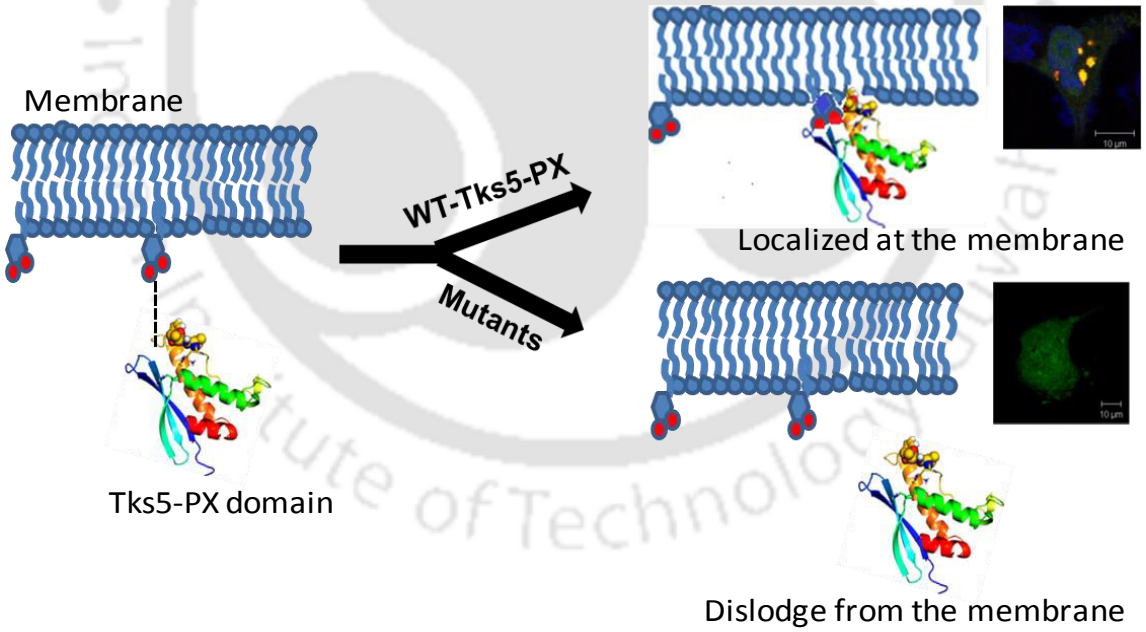

2.1. Background and Focus of the Present Work

It is well documented that occurrence and increase of distance metastasis is the most important reason of cancer cell motility and mortality. The enhanced motility of malignant tumor cells allows them to invade adjoining tissues through podosomes/invadopodia, a protrusive membrane structure. Hence, preventing the spread of cancer cells is considered as an alternative therapeutic approach for the treatment of various types of cancers.[1-5] The invadopodia formation by the cancer cells also promotes cell migration along with extracellular matrix degradation. Tks5 (tyrosine kinase substrate 5) is one of the essential proteins that assists the invasiveness of cancer cells and also progression of different diseases like Alzheimer's, inflammation and others.[6, 7] Cooperative action of tyrosine kinase substrate with five Src homology 3 domains (Tks5) and Src tyrosine kinase promotes extracellular matrix degradation by the cancer cells. It is important to mention that the expression level of Tks5 is very high in cancer cells in comparison with normal cells.[3, 6, 8, 9]

Tks5 was first recognized as a Src adaptor protein and crucial for the linking cell surface receptors to the effector proteins for biological relevance. It acts as a scaffolding protein and interacts with both proteins and lipids.[10] Tks5 protein contains one amino-terminal phox homology (PX) domain followed by five SH3 domains, several polyproline-rich motifs and a number of probable phosphorylation sites.[11] It is reported that the PX, SH3 and several polyproline rich motifs of Tks5 protein are involved in lipid-protein and/or protein-protein interactions.[12, 13] Among five SH3 domains of Tks5, two amino-terminal SH3 domains are important for association with other SH3 domains containing novel binding partner, like Ras/Rho guanine nucleotide exchange factor, Son of sevenless-1(Sos1) and metalloproteins like ADAM12 and ADAM19.[14, 15] Neurotoxic effect of amyloid β peptide in Alzheimer's disease is directly related with the interaction of carboxy-terminal SH3 domain of Tks5 and ADAM12 protease. This interaction may regulate t he enzymatic activity of ADAM proteases. Tks5 also acts as an organizer protein that allows NOX1– or NOX3– dependent reactive oxygen species (ROS) generation and ROS localization.[16]

It is well documented that Tks5 is a cytoplasmic protein but it localizes to podosomes in Src-transformed and various cancer cell lines. Tks5 is required for podosome formation and PX domain is crucial for its podosome localization.[6, 13, 17] Homology sequence alignment shows that like other conventional PX domain containing proteins Tks5-PX domain also contains several conserved regions, including a proline-rich stretch and a number of basic residues with overall hydrophobic character. It has highest amino acids sequence

homology with two cytosolic subunits ($p40^{phox}$ and $p47^{phox}$) of NADPH oxidase.[18] In general, PX domains are found in combination with protein binding SH3 domains and the host proteins are involved in cell signaling, (phospholipase D (PLD), PI 3-kinase (PI3K) and cytokine-independent survival kinase (CISK)), membrane trafficking (i.e., Mvp1p, Vps5p, Vam7p, Bem1p, Grd19p, sorting nexins (SNXs)) and others. Phosphorylated derivatives of phosphatidylinositol like phosphatidylinositol 3-phosphate (PI(3)P) and phosphatidylinositol 3,4-bisphosphate ($PI(3,4)P_2$) are their most common lipid binding partner of PX domains.[11, 18, 19]

Recent studies pointed out that Tks5-PX domain interacts with $PI(3,4)P_2$ lipid molecules. In Src-transformed cell lines Tks5 is localized in the membranes during invadopodium maturation phase, but not in initiation phase in breast carcinoma cells.[8] $PI(3,4)P_2$-dependent membrane recruitment of Tks5 protein through its PX domains is essential for its Src-dependent invadosome localization and its biological activities.[1, 6] Recruitment of Tks5 protein by both $PI(3,4)P_2$ lipid and Grb2 protein incite the actin polymerization at the invadosome.[20] It is also mentioned that green fluorescent protein fused-PX domain of Tks5 protein localized to discrete cytoplasmic punctate like structures in normal fibroblast cells, which indicates its PI(3)P binding capabilities.[3, 12] Hence, PIP-binding of the Tks5-PX domain plays an important role in cellular functions of Tks5 protein in different cellular conditions or diseases states. PIP binding specificities of Tks5-PX domain was earlier determined by protein-lipid overlay assay, this makes it difficult to quantitatively measure its PIP-binding specificity and affinity and predict which PIP will have stronger binding affinity for Tks5-PX domain under a certain condition. In spite of well documented structural function relationship studies of Tks5-PX domain, a through membrane recruitment mechanism has not been described yet. In general weak-nonspecific electrostatic interactions between anionic lipids like phosphatidylserine and cationic groove of the protein allow PX domains to interact with the membrane and then specific PIP binding and/or partial membrane penetration allow them to reside at the membrane for activation of the host proteins, signal transduction and other biological functions.[9] PIP binding protein modules generally contain a large number of cationic residues. As a result PIP-binding to these cationic grooves generates electrostatic potential alteration and/or neighbouring conformational changes, which allow these protein modules like PX domain to penetrate the membrane. The PX domain of $p40^{phox}$ and $p47^{phox}$, KIF16B and other proteins are known to significantly penetrate the membrane in PIP-dependent manner due to the presence of hydrophobic residues close to their PIP binding sites.[11, 18, 19, 21] For this reason

membrane penetration measurement along with quantitative PIP-specificity determination is essential to understand their membrane interaction mechanism.

2.2 Results and Discussion

PIP Binding Properties of the PX Domain of Tks5:

The PIP-binding capability of Tks5-PX domain was recently mentioned by a qualitative protein-lipid overlay assay with higher binding affinity for $PI(3,4)P_2$ and PI(3)P lipids. Further inspection of reported PIP-array data revealed that Tks5-PX domain also bind to other PIPs but with less affinities.[12] However, the PIP binding affinity and specificity of the PX domain of Tks5 has not been quantitatively determined to understand the detail mechanism of PIP dependent-membrane binding properties of Tks5. This creates doubt in describing definite PIP-binding partner of Tks5-PX domain, during different cellular conditions/diseases states. In this regard, we quantitatively determined the binding properties of Tks5-PX domain to liposomes containing different PIPs (PC/PE/PS/PIP (57:20:20:3)) by fluorescence resonance energy transfer (FRET)-based competitive binding assay and surface plasmon resonance (SPR) analysis.

Fluorescence Resonance Energy Transfer-Based Competitive Binding Assay— We used a FRET-based competitive binding assay for quantitative measurement of PIPs binding affinities and specificities of the Tks5-PX domain under liposomal environment (PC/PE/PS/dPE/PIP (57:19:20:1:3)). Phytic acid (IP_6) was used as competitive inhibitor for this assay.[23, 24] Surface exposed Trp-residue (W32) of the Tks5-PX domain act as the FRET donor, and a low density of membrane-embedded dansyl probe of the dPE lipid serve as the acceptors. Displacement of Tks5-PX domain from its PIP-specific membrane bound state to the bulk phase by IP_6, results in decrease in FRET signal in a concentration-dependent manner. Figure 1A illustrates representative isotherms of the protein-to-membrane FRET assay in the presence of IP_6 as competitive inhibitor. Apparent inhibitory constant [$K_I(IP_6)_{app}$] values calculated for different PIP containing liposomes are listed in Table 2.2.1.

Surface Plasmon Resonance Analysis— We also quantitatively measured the binding affinities and specificities of the PX domain to the liposome containing $PI(3,4)P_2$ and PI(3)P lipids (PC/PE/PS/PIP (57:20:20:3)) using real-time SPR analysis.[22] The protein was passed over the liposome-coated L1 sensor chip at a flow rate of 30 μL/min and real-time measurement of association and dissociation phase was used to measure the binding affinity

values.[23] Figure 2.2.1B and 2.2.1C describes representative SPR sensorgrams for binding of Tks5-PX domain to PC/PE/PS/PI(3,4)P_2 (57:20:20:3) and PC/PE/PS/PI(3)P (57:20:20:3) liposomes. The association (k_a) and dissociation (23) rate constants and binding affinities for protein-membrane interaction can be easily determined and compared using 1:1 binding model with one-step binding pattern (P + M → PM).(22) K_d values calculated various PIP containing liposomes are listed in Table 2.2.1.

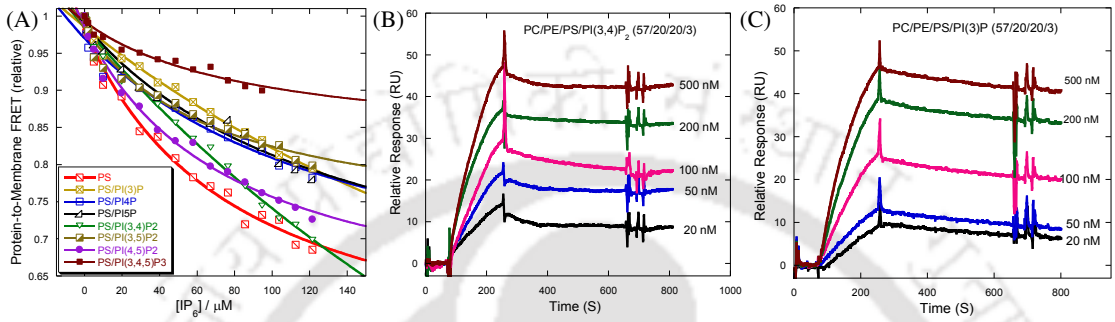

Figure 2.2.1. Competitive displacement assay for Tks5-PX domain (1 μM) bound to PC/PE/PS (60:20:20) and PC/PE/PS/PIP (57:20:20:3) liposomes. The bound complex was titrated with the IP_6 as competitive inhibitor (A). Kinetic SPR sensorgrams for Tks5-PX domain interacting with the PC/PE/PS/ PI(3,4)P_2 (57:20:20:3) (B) and PC/PE/PS/PI(3)P (57:20:20:3) (C) liposomes immobilized of sensor chip L1. A 20 mM HEPES buffer at pH 7.4 containing 160 mM KCl, was used for all measurements. The SPR sensorgrams are shown after background correction for binding to the control surface coated with PC/PE/PS (60:20:20) liposome and BSA (40 μL of 0.1 mg/mL in the running buffer). Flow rate was kept at 30 μL/min.

Calculated $K_I(IP_6)_{app}$ and K_d values of the Tks5-PX domain showed that Tks5-PX domain have stronger binding affinity for PI(3,4)P_2 and PI(3)P lipids and their binding affinity difference is negligible. The $K_I(IP_6)_{app}$ values for PI(3,4)P_2 and PI(3)P lipids are 470 and 422 μM, respectively. Results revealed a weak affinity for PI(4)P and PI(5)P but little or no affinity for other PIPs. The measured K_d values (from SPR analysis) of Tks5-PX domain for PI(3,4)P_2 and PI(3)P lipids are 2.87 and 3.43 nM, respectively. Our FRET analysis with PC/PE/PIP (77:20:3) liposomes also showed similar PIP-binding pattern, suggesting that selective PIP-binding is crucial for membrane interaction of Tks5-PX domain. A similar pattern of PI(3,4)P_2 and PI(3)P binding affinity and specificity was observed for liposomes with different PIP concentration. Therefore our FRET and SPR analysis quantitatively measure the PIP binding affinity and specificity of Tks5-PX domain, which provide a new insight into how this PX domain would respond to both PI(3,4)P_2 and PI(3)P more effectively than other PIPs in different cellular conditions.

Identification of the PIP-binding Site of the Tks5-PX Domain:

To understand how PI(3,4)P_2 and PI(3)P lipids interact with the PX domain of Tks5, we first generated *in silico* model structure and designed mutated PX domains for further quantitative binding analysis. A multiple sequence alignment of the Tks5-PX domain with p47-, p40 and other PX domains was also performed to find the sequence conservation, structural relationship and PIP binding properties. The model structure of PX domain of Tks5 was generated using the maximum homologues sequence as template by Modeller 9v7 software. Suitable templates were chosen by blasting the Tks5-PX protein sequence into protein data bank of NCBI using PSI-blast and blast the same sequence into the structure prediction meta-server. In both cases it was found that p47-PX (PDB code: 1kq6) showed highest amino acid sequence homology with the Tks5-PX domain (Figure 2.2.2). To generate the energy minimized suitable structure we followed the following path: two models were generated using two different softwares to get maximum quality model. Initially the model quality was verified using PROCHECK online server. Then all models were energy minimized by Swiss PDB VIEWER 4.0.1 (Swiss Institute of Bioinformatics, Switzerland) and again checked the structural quality of the model by the PROCHECK

Table 2.2.1. Apparent inhibitory constants [$K_I(IP_6)_{app}$] for Tks5-PX domain binding to PC/PE/PS (60:20:20) and PC/PE/PS/PI (57:20:20:3) liposomes determined membrane-to-protein FRET analysis[a]

Liposome	$K_I(IP_6)_{app}$ (μM)	
	PX-WT	PX-R42A/R93A
PC/PE/PS	61 ± 8	47 ± 11
PC/PE/PS/PI(3)P	422 ± 11	22 ± 3
PC/PE/PS/PI(4)P	151 ± 9	-
PC/PE/PS/PI(5)P	142 ± 7	-
PC/PE/PS/ PI(3,4)P_2	470 ± 19	67 ± 7
PC/PE/PS/ PI(3,5)P_2	74 ± 5	-
PC/PE/PS/ PI(4,5)P_2	79 ± 5	-
PC/PE/PS/ PI(3,4,5)P_3	90 ± 5	-

[a]All measurements were performed in 20 mM HEPES buffer at pH 7.4 containing 160 mM KCl. IP_6 was used as inhibitor of membrane-to-protein interactions. Protein, 1 μM. Values represent the mean ± SD from triplicate measurements.

program. To determine the location of PIP binding site, we inspected the surface electrostatic potential distribution and homology sequence analysis of Tks5-PX domain and look for

cationic groove on the surface of the protein. We identified a cationic groove comprising of R42, R43, K78, R82, R83 and K93 residues, which may be directly involved in interaction with the head group of anionic PIPs (Figure 2.2.2). The model structure also revealed the presence of three hydrophobic residues (I79, L80 and F81) on the membrane binding surface of the PX domain surrounding the PIP binding site. Molecular docking analysis of PI(3,4)P_2 and PI(3)P with Tks5-PX domain also suggested that the cationic groove could accommodate the PIP molecule and the basic residues directly interact with the phosphate groups of PIPs (Figure 2.2.3). Therefore, we mutated those residues to Ala-residue individually or in combination and measured their effect on PIP binding properties under similar experimental condition as of with wild type Tks5-PX domain. Calculated $K_I(IP_6)_{app}$ and K_d values of the mutants are summarized in Table 2.2.2 and Table 2.2.3, respectively. The binding parameters obtained from SPR analyses shows that single mutants R42A, R43A, K78A and R93A separately showed 1.7 to 11-fold lower binding affinity for both of these PIPs than WT-PX domain. The results also showed that R42A and R93A mutations plays a significant role in PI(3,4)P_2 and PI(3)P containing liposome binding. The double mutant, R42A/R93A shows significantly lower binding affinity for both PI(3,4)P_2 and PI(3)P containing liposomes than WT. Kinetic SPR analysis showed that R42A/R93A mutant

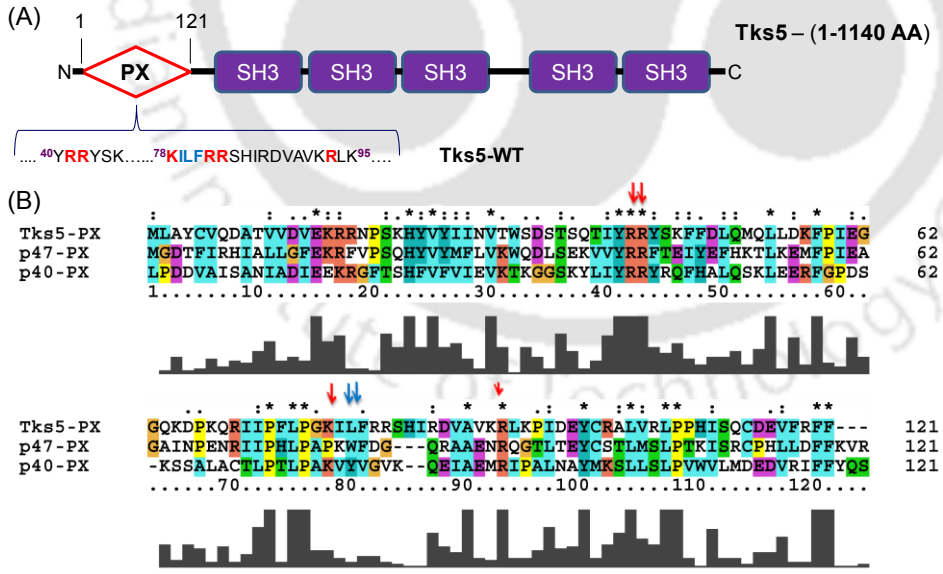

Figure 2.2.2. A schematic representation of the full-length Tks5 structure (A). Amino-acid sequence alignment of the Tks5, p47 and p40-PX domains are shown using Clustal X program. PX domain residues forming the cationic patch and hydrophobic cluster at its base are labelled with red and blue arrows, respectively (B).

have 51 and 67-fold lower binding affinity for PI(3,4)P_2 and PI(3)P lipids, respectively than WT-PX domain under similar experimental conditions (Table 2.2.3). Another double mutant R82A/R83A also showed only 2.7 to 7-fold lower PIPs binding affinities than WT-protein. The other double and triple mutants R43A/R93A and R43A/K78A/R93A showed only 4-16 fold lower PIP binding affinity than WT-PX domain (Table 2.2.3). $K_I(IP_6)_{app}$ values also showed that double mutant R42A/R93A have stronger effect on PI(3,4)P_2 and PI(3)P lipid binding abilities (Table 2.2.2). This clearly indicates that both R42 and R93 strongly interact with the head groups of PI(3,4)P_2 and PI(3)P lipids.

Table 2.2.2. Apparent inhibitory constants [$K_I(IP_6)_{app}$] for Tks5-PX domain and mutants binding to PC/PE/PS/PI (57:20:20:3) liposomes determined membrane-to-protein FRET analysis[a]

Protein	PC/PE/PS/PI(3)P	Fold change in $K_I(IP_6)_{app}$	PC/PE/PS/PI(3,4)P_2	Fold change in $K_I(IP_6)_{app}$
	$K_I(IP_6)_{app}$ (μM)		$K_I(IP_6)_{app}$ (μM)	
PX-WT	422 ± 11	1	470 ± 14	1
PX-R42A	156 ± 18	2.7	345 ± 24	1.4
PX-R93A	142 ± 15	2.9	147 ± 12	3.2
PX-R78A	150 ± 12	2.8	282 ± 29	1.7
PX-R42A/R93A	22 ± 3	19	67 ± 7	7
PX-R82A/ R83A	290 ± 14	1.5	180 ± 20	2.6
PX-I79A	110 ± 33	3.8	144 ± 14	3.3
PX-L80A/ F81A	118 ± 17	3.6	50 ± 11	9.4

[a]All measurements were performed in 20 mM HEPES buffer at pH 7.4 containing 160 mM KCl. IP_6 was used as inhibitor of membrane-to-protein interactions. Protein, 1 μM. Values represent the mean ± SD from triplicate measurements.

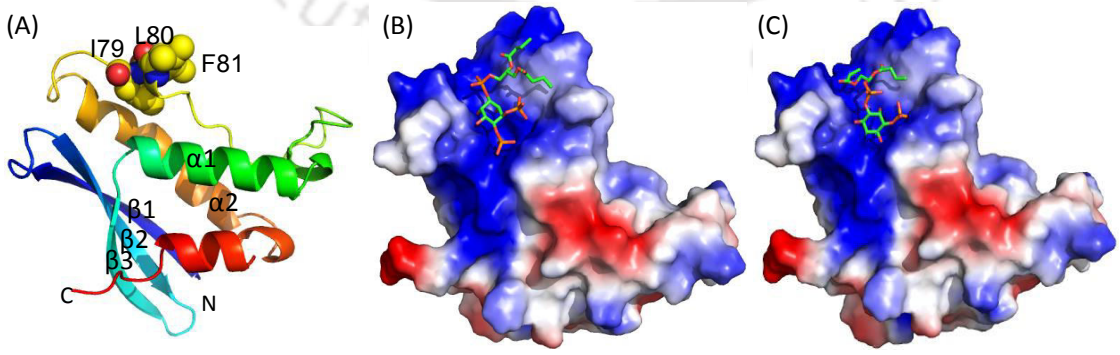

Figure 2.2.3. Model structure of Tks5-PX domain. Model structure of Tks5-PX domain is shown in ribbon diagram. Secondary structural units are shown in different colors and labeled. Probable membrane-penetrating hydrophobic residues are shown in spheres and labeled (A). Surface representations of model structures of

Tks5-PX-PI(3,4)P_2 (B) and Tks5-PX-PI(3)P (C) complexes. Red and blue colours indicate negative and positive potentials, respectively calculated by PyMol software. PI(3,4)P_2 and PI(3)P are shown in stick representations.

We also determined the role of hydrophobic residues on PIP binding of the PX domain. The binding parameters obtained from both SPR and FRET analyses show that I79A and L80A/F81A mutants have significant effect on PIP binding. The mutants I79A and L80A/F81A showed 3.6 and 9.4-fold lower binding affinity (K_d values) for PI(3,4)P_2, and 3.9 and 3.5-fold lower binding affinity (K_d values) for PI(3)P, respectively than WT-PX domain under the similar experimental conditions. $K_I(IP_6)_{app}$ values for these hydrophobic mutants also showed similar effect on PI(3,4)P_2 and PI(3)P lipids binding affinities (Table 2.2.2). Collectively, these mutational analyses indicate that R42 and R93 constitute the main PIP binding site of the protein, whereas other cationic residues, including R43, K78, R82 and R83 are involved in formation of a cationic groove. Therefore, a network of hydrogen bond interaction between PIP-headgroup and the amino acid residues of the PX domain form a membrane bound complex. The hydrophobic residues present on the membrane binding surface also play a significant role in PIP-dependent membrane binding of the Tks5-PX domain, probably due to their membrane penetration ability.

Effect of PIP Binding on Membrane Penetration of Tks5-PX Domain:

Several studies reported that few PX domains significantly penetrate into the cell membrane in a PIP-dependent manner.[11, 28] The PIP-binding may induce a considerable change in electrostatic potential and/or local conformation of the membrane binding surface to allow PX domain to penetrate into the membrane. Cellular studies reported that Tks5 localize at the plasma membrane in Src-transfored cells during invadosome formation in PI(3,4)P_2 dependent manner.[3, 4, 29] Therefore, to verify if Tks5-PX domain has membrane penetrating ability and how PIPs affect its membrane penetration, we determined its lipid-monolayer (PC/PE/PS/PIP (57:20:20:3)) penetration ability in terms of surface pressure change. To effectively penetrate a cell membrane the critical surface pressure (π_c) of the protein should be around 31-35 dynes/cm for lipid monolayer.[22] Figure 2.2.4A describes the interaction properties of the PX domain monolayer composed of different phospholipids. The results showed that Tks5-PX domain has low membrane penetration ability to PC/PE/PS containing monolayer with π_c = 25-26 dyne/cm. However, inclusion of 3 mol% of PI(3,4)P_2 and PI(3)P to PC/PE/PS containing monolayer increase the π_c value of PX domain to 36-37 and 34-35 dyne/cm, respectively. This clearly suggest that the PX domain could penetrate the

cell membrane in PI(3,4)P_2 and PI(3)P dependent manner. PIP-dependent monolayer penetration ability of the PX domain is additionally supported by the result that the mutation of indispensable PIP binding resides (R42A/R93A) overturned its PI(3,4)P_2 and PI(3)P-dependent monolayer penetration properties. The π_c value of R42A/R93A mutant for PI(3,4)P_2 and PI(3)P containing monolayers were 27-28 and 25-26 dyne/cm, respectively, indicates that membrane penetration of Tks5-PX domain significantly contribute to its PIP-dependent membrane interaction properties. It is also important to mention that membrane penetration ability of Tks5-PX domain is slightly stronger in the presence of PI(3,4)P_2 than PI(3)P containing monolayer. We hypothesize that this differential membrane penetrating abilities of the Tks5-PX domain could be due to its binding orientation with the PIP molecules.

Table 2.2.3. Membrane binding parameters of Tks5-PX domain and mutants to PC/PE/PS/PI (57:20:20:3) liposomes determined by SPR analysis[a]

Protein	PC/PE/PS/PI(3)P	Fold change in K_d	PC/PE/PS/PI(3,4)P_2	Fold change in K_d
	K_d (M)		K_d (M)	
PX-WT	$(3.43 \pm 0.7) \times 10^{-9}$	1	$(2.87 \pm 0.3) \times 10^{-9}$	1
PX-R42A	$(9.15 \pm 0.4) \times 10^{-9}$	2.7	$(4.82 \pm 0.6) \times 10^{-9}$	1.7
PX-R93A	$(3.87 \pm 0.9) \times 10^{-8}$	11	$(1.68 \pm 0.7) \times 10^{-8}$	5.8
PX-R78A	$(3.28 \pm 0.6) \times 10^{-8}$	3	$(5.10 \pm 0.5) \times 10^{-9}$	1.8
PX-R42A/R93A	$(1.77 \pm 0.9) \times 10^{-7}$	51.6	$(1.93 \pm 0.8) \times 10^{-7}$	67
PX-R43A/R93A	-	-	$(1.23 \pm 0.6) \times 10^{-8}$	4
PX-R82A/R83A	$(9.22 \pm 0.5) \times 10^{-9}$	2.7	$(1.99 \pm 0.5) \times 10^{-8}$	7
PX-R43A/R93A/R78A	$(5.43 \pm 0.7) \times 10^{-8}$	15.8	$(1.74 \pm 0.6) \times 10^{-8}$	6
PX-I79A	$(1.34 \pm 0.8) \times 10^{-8}$	3.9	$(1.05 \pm 0.4) \times 10^{-8}$	3.6
PX-L80A/F81A	$(1.23 \pm 0.7) \times 10^{-8}$	3.5	$(2.71 \pm 0.3) \times 10^{-8}$	9.4

[a]All measurements were performed in 20 mM HEPES buffer at pH 7.4 containing 160 mM KCl. Values represent the mean ± SD from triplicate measurements.

Role of Hydrophobic Residues on PIP-dependent Membrane Penetration of Tks5-PX Domain-

To investigate the role of hydrophobic residues present along the surface of the PIP-binding site of the PX domain, we measured membrane binding kinetics by SPR analysis and monolayer penetration properties of the hydrophobic-mutants. It is demonstrated that membrane association of the peripheral proteins is first induced by nonspecific-electrostatic interactions, and then short range specific interaction and membrane penetration.[22, 30]

These results in a slow membrane dissociation rate of the membrane penetrating peripheral proteins. The model structure suggests that Tks5-PX domain has three prominently protruding hydrophobic residues, I79, L80 and F81 residues in the loop region close the PIP-binding site, suggesting their significant contribution in membrane penetration. It is important to note that $p47^{phox}$-PX domain also has hydrophobic residues, W80 and F81 at the similar region.[28] Therefore, Tks5-PX domain is expected to be as effective $p47^{phox}$-PX domain in terms of membrane penetration. To explore whether surface exposed hydrophobic residues are crucial for membrane penetration and prolonged membrane residence of the PX domain, monolayer penetration abilities and membrane interaction kinetics of the hydrophobic mutants and WT-PX domain were compared under similar experimental conditions.

Monolayer penetration data showed that WT-PX domain significantly penetrate PC/PE/PS/PI(3)P and PC/PE/PS/PI(3,4)P_2 containing lipid monolayers, but weakly penetrate PC/PE/PS lipid monolayer (Figure 2.2.4A). The π_c value of WT-PX domain for PI(3,4)P_2 and PI(3)P containing monolayer were 36-37 and 34-35 dyne/cm, respectively. Figure 2.2.4B and 2.2.4C clearly demonstrates that L80A/F81A mutant lost its monolayer penetration capability. The π_c value of L80A/F81A mutant for PI(3,4)P_2 and PI(3)P containing monolayer were 26-27 and 28-29 dyne/cm, respectively. This indicates that the L80A/F81A mutant has some degree of PIP-dependent membrane penetrating ability, but that may not be sufficient enough to penetrate membrane-bilayers under physiological conditions. The other hydrophobic mutant I79A also showed lower membrane penetration abilities. To check whether these monolayer penetration abilities of the Tks5-PX domain have any effect on membrane residence, SPR binding isotherms were reanalyzed. To compare membrane association and dissociation kinetics same concentration of proteins were injected to the L1 sensor chip

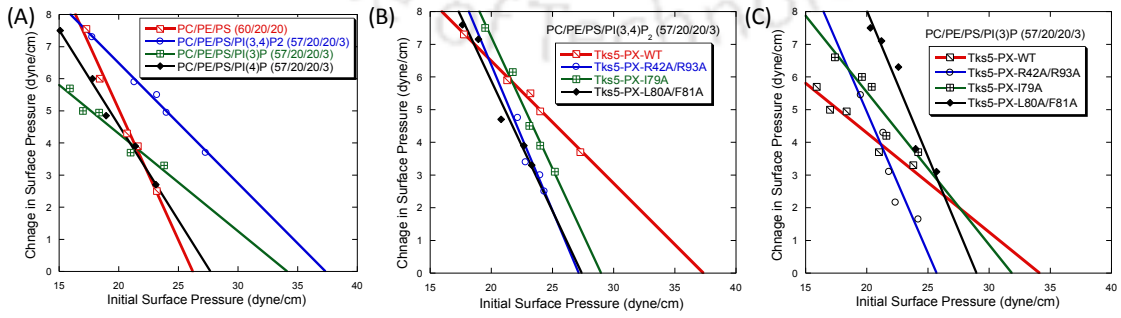

Figure 2.2.4. Interactions of Tks5-PX domain and mutants with monolayers of lipids. Interaction of Tks5-PX domain with PC/PE/PS (60:20:20), PC/PE/PS/PI(3,4)P_2 (57:20:20:3), PC/PE/PS/PI(3)P (57:20:20:3) and

PC/PE/PS/PI(4)P (57:20:20:3) monolayers (A). Interaction of Tks5-PX, R42A/R93A, I79A and L80A/F81A with PC/PE/PS/PI(3,4)P_2 (57:20:20:3) (B) and PC/PE/PS/PI(3)P (57:20:20:3) (C) monolayers.

coated with PIP-containing liposomes (PC/PE/PS/PIP (57:20:20:3)). The association rate constant (k_a) values of the proteins showed almost no difference. However, there are noticeable differences in dissociation rates of I79A and L80A/F81A mutants in comparison with the WT-PX domain (Figure 2.2.5). Membrane dissociation kinetics of the WT and mutants followed 1:1 binding model, hence the k_d values were calculated quantitatively. The k_d values of WT, I79A and L80A/F81A proteins are 1.14 x 10^{-4}, 3.75 x 10^{-4} and 9.48 x 10^{-4} (M), respectively (Figure 2.2.5). These results suggest that WT-PX domain resides in the membrane for longer time in comparison with the hydrophobic mutants, which is in accordance with their monolayer penetration abilities. Partial membrane dissociation of the hydrophobic mutants could be due to the PIP-induced membrane penetration of the other hydrophobic residues localized on their membrane-binding surface of the PX domain or their PIP binding properties. Monolayer penetration measurements also showed that PIP-mutant, R42A/R93A significantly lost its membrane penetration capabilities. This implies that both specific PIP-binding residues and membrane penetrating hydrophobic residues present on the membrane binding surface are necessary for its PIP-dependent membrane binding and neighbouring-hydrophobic residues containing loop region essentially participate in membrane binding.

Both basic and hydrophobic residues are important for subcellular co localization of Tks5- To investigate if the cellular membrane targeting activities of Tks5-PX domain are administered by their membrane binding properties under cellular environment, we examined PIP-mediated subcellular localization of **GFP**-fused Tks5-PX domain. Most of the PX domain, are localized in endosome and/or plasma membrane due its high binding specificity and affinity to PI(3)P and PI(3,4)P_2 lipids.[19, 28, 31, 32] It has been reported that PX domain of Tks5 localized to the punctuate structures in normal NIH3T3 cells, whereas in Src-transformed cells Tks5-PX domain co-localized with F-actin and assist in forming semi circle or dot like structure known as podosome.[3, 12] To examine the localization of wild type Tks5-PX in non-Src-transformed A549 cells, we transiently co-transfected GFP-fused PX domain along with RFP-fused tandem FYVE domain of Hrs protein, a specific cellular marker of PI(3)P lipid.[27] Tandem FYVE domain of Hrs protein generally showed a punctuate distribution pattern a typical of early endosome localization.[27, 33, 34] The cells

expressing both GFP-fused PX domain and RFP-fused FYVE domain were selected by visual inspection. All confocal images of the cells were collected after serum starvation to avoid any pre-localization at the plasma membrane of quiescent cells. In general more than 70% of cell population showed the expression of both PX domain and marker. We observed that, in most of the observed cells (90%) Tks5-PX domain localized to the punctuate structures along with PI(3)P marker RFP-FYVE protein which is in accordance with previous report (Figure 2.2.6). [12] This punctuate distribution pattern was not observed for EGFP alone in A549 cells (data not shown). This clearly suggest that the isolated PX domain strongly interact with the PI(3)P lipid. We also examine the localization pattern of EGFP-fused Tks5 full length protein in fixed A549 cells. However, Tks5 full length protein showed predominantly cytoplasmic distribution which is in good agreement with previous reports (Figure 2.2.6A).[12] This localization pattern of Tks5 full length protein clearly suggests that its PX domain is not accessible for interaction with PI(3)P lipid.

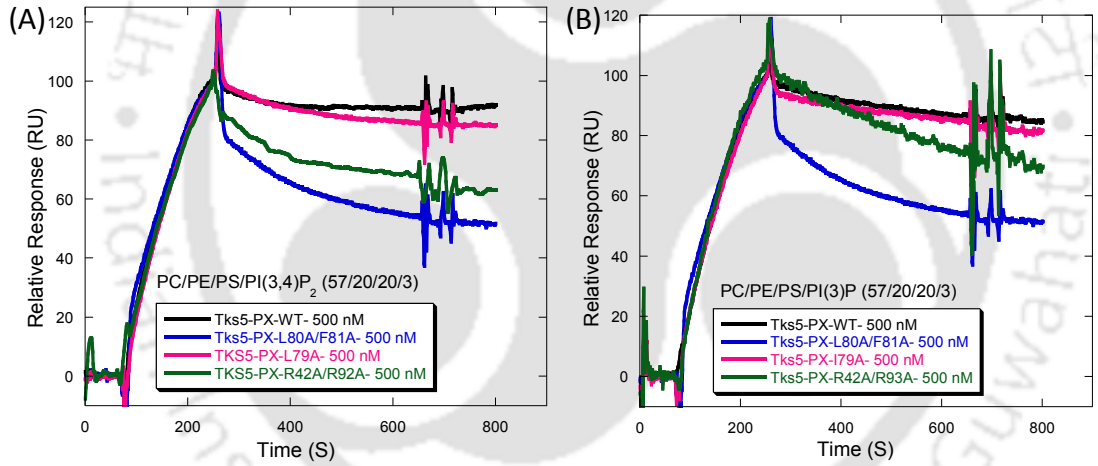

Figure 2.2.5. Kinetic SPR sensorgrams for Tks5-PX and mutants, L80A/F81A, I79A and R42A/R93A interacting with PC/PE/PS/PI(3,4)P_2 (57:20:20:3) (A) and PC/PE/PS/PI(3)P (57:20:20:3) (B) liposome. A 20 mM HEPES buffer solution, pH 7.4, with 0.16 M KCl, was used for all measurements.

Then, to examine the importance of PI(3)P-binding basic residues and membrane binding hydrophobic residues on its cellular localization pattern, we co-transfected GFP-fused PX domain mutants and RFP-fused tandem FYVE domain of Hrs protein in normal A549 cells.[8] It was observed that colocalization or the enrichment of PX domain mutants in subsequent membrane is greatly affected. The R42A/R93A mutant, which showed much reduced PIP-affinity exhibited predominantly cytosolic distribution under the similar conditions (Figure 2.2.6F) and expression of R42A/R93A mutant in A549 cells did not

change the cellular distribution pattern of tandem FYVE domain. However, the effects of other PIP-binding mutants on cellular localization pattern were not that obvious. The mutants R42A, R93A and K78A showed both early endosome and cytoplasmic localization but with different extents. This clearly suggest that the R42 and R93 residues of the isolated PX domain strongly interact with the PI(3)P lipid, whereas other positively charged present with the binding site assist PX domain to interact with the PI(3)P lipid. To understand the physiological significance of hydrophobic residues the PX domain in membrane binding and penetration, A549 cells were transfected with GFP-fused hydrophobic mutants I79A and

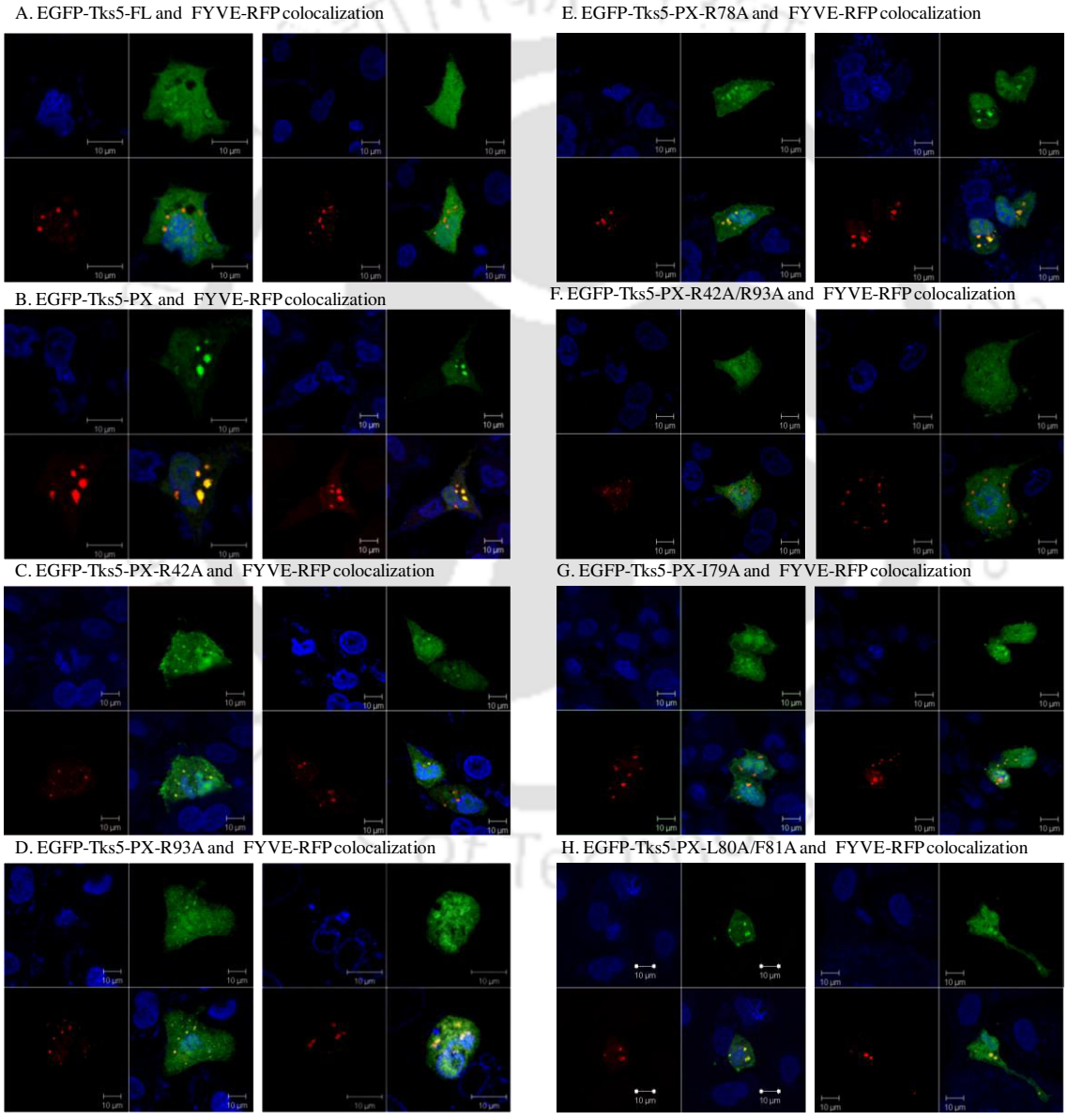

Figure 2.2.6. Subcellular localization of GFP-fused Tks5-PX domain and its mutants in A549 cells. Confocal images of fixed A549 cells transfected with RFP-fused tandom FYVE domain of Hrs protein and GFP-fused Tks5-full length (A), PX domain (B) and mutants of PX domain (C-H). Subcellular localization patterns in

A549 cells represents > 70% of cell populations that express similar levels both RFP-fused tandom FYVE domain of Hrs protein and GFP-fused Tks5-PX domain or mutants. Scale bars indicate 10 µm.

L80A/F81A, which showed significantly reduced membrane penetrating capability with moderate PIP-binding affinity. The cellular localization pattern clearly showed that the hydrophobic mutants predominantly localize at the cytoplasm. This support the findings that surface exposed hydrophobic residues of Tks5-PX domain are critical structural determinant of its endosomal localization.

Since $PI(3,4)P_2$ is reported as a lipid binding partner of the Tks5-PX domain in Src-transformed cells [3, 4] and essential for invadosome formation, we investigated $PI(3,4)P_2$ mediated subcellular translocation of PX domain and mutants upon platelet-derived growth factor (PDGF) stimulation in non-Src-transformed A549 cells. PDGF is reported to generate $PI(3,4)P_2$ at the plasma membrane.[22] Cells were fixed 5 min after PDGF (50 ng/mL) treatment. The confocal images showed that PX domain is localized to early endosomes in serum starved cells and localized to plasma membrane upon stimulation with PDGF (Figure 2.2.7B). The PIP-binding mutant R42A/R93A showed predominantly cytoplasmic distribution even after PDGF treatment (Figure 2.2.7C). The hydrophobic mutant L80A/F81A showed partial membrane localization after PDGF stimulation which is

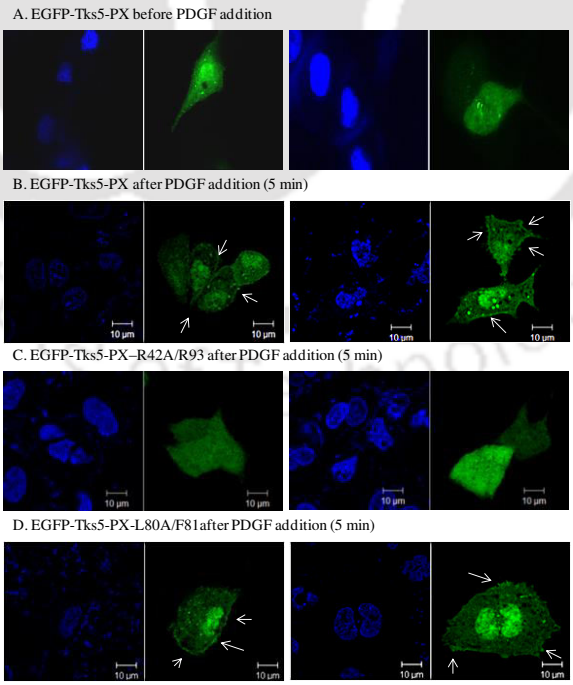

Figure 2.2.7. Membrane translocation of GFP-fused Tks5-PX domain and mutants in response to PDGF treatment in A549 cells. Confocal images of A549 cells transfected with Tks5-PX domain and mutants (A-D). Cells were first serum starved for 4 hours and then fixed 5 min after stimulation with 50 ng/mL of human

PDGF-BB. Subcellular localization patterns represents > 75% of cell populations that express similar levels of GFP-fused Tks5-PX domain or mutants.

consistent with their liposome binding patterns (Figure 2.2.7D). Overall, our results show that cellular localization patterns of the wild type and mutant PX domain of Tks5 are in accordance with their binding affinity for PI(3)P and PI(3,4)P_2 containing liposomes and more importantly PIP-dependent membrane penetration is crucial for its cellular localization patterns.

Discussion

It is well documented that Tks5 localizes at the cytoplasm of the normal fibroblasts cells and at the invadosomes in Src-transformed and cancer cells.[3, 8] The mechanism by which Tks5 regulates invasiveness of cancer cells also has been thoroughly investigated. The interaction of PX domain of Tks5 with PIPs is crucial for its cellular activities and localization. Evidences suggest that PI(3,4)P_2 is crucial for the co-localization of Tks5 protein with its protein binding partners at the invadosomes.[3] It is also mentioned that isolated Tks5-PX domain may be able to bind to PI(3)P at the endosomal membranes.[12] However, it is still remain unclear how the Tks5-PX domain is recruited to the cellular membranes. Reported PIP specificity and selectivity of Tks5-PX domain were also qualitative.[12] In this regard, present study describes quantitative PIP-binding parameters and a through cellular membrane binding mechanism of isolated Tks5-PX domain. It also provides strong evidences for PI(3)P-dependent endosomal localization of isolated Tks5-PX domain.

Our FRET-based competitive binding assay and SPR analyses clearly showed that the isolated Tks5-PX-WT domain strongly interacts with PI(3,4)P_2 and PI(3)P lipids with almost similar binding affinities through the same binding pocket. The binding specificities of Tks5-PX domain are in good agreement with the reported one.[12] Although, most of the PX domains prefer to interact to PI(3)P, whereas interaction of PI(3,4)P_2 is very rare.[11, 21] This anomaly may be due to the presence of different cationic residues within the PIP-binding site of the Tks5-PX domain. Homology sequence alignment showed that Tks5-PX domain is closely related to the $p47^{Phox}$-PX domain, which shows strong PI(3,4)P_2 binding properties.[18, 28] Slight preference of the PX domain for PI(3,4)P_2 over PI(3)P lipid may be due to the additional interaction of basic residues with D4-phosphate group. Model structure and homology sequence alignment identified that the R42, R43, K78, R82, R83 and R93 residues are probable PIP-binding residues of the PX domain. Our molecular docking

analysis predicted that R93 directly interacts with the D3-phosphate whereas D4-phosphate involves in interaction with R42 followed by K78 interaction with D1-phosphate of the inositol ring. Mutations of these residues significantly lower the PIP-binding affinities of the PX domain. SPR based binding affinity calculation showed that R93A mutation showed 11- and 5.8-fold binding affinity difference for PI(3)P and PI(3,4)P_2 lipids, where as R42A mutation showed 2.7- and 1.7-fold binding affinity difference for PI(3)P and PI(3,4)P_2 lipids, respectively. Whereas double mutant R42A/R93A showed 51.6- and 67-fold binding affinity difference for PI(3)P and PI(3,4)P_2 lipids, respectively. In addition, other basic residues like K78, R43, R82 and R83 are also responsible for such stronger PI(3)P and PI(3,4)P_2-binding properties of the PX domain. This strongly suggested that R93 and R42 preferentially interact with the D3- and D4-phosphate group, respectively, which is in accordance with the molecular docking analysis results.

Consistent with these findings, a significant portion of GFP-fused Tks5-PX-WT is co-localized with RFP-fused tandem FYVE domain in A549 cells. Hrs-FYVE domain is known as cellular marker of PI(3)P lipid. A punctuate distribution of PX and FYVE domains associated with early endosomal membranes was observed.[12] This co-localization is disrupted by mutation of PIP-binding residues. The double mutant R42A/R93A showed predominantly cytoplasmic distribution of PX domain. Therefore, PI(3)P binding is primarily responsible for the endosomal localization of isolated PX domain of Tks5 in A549 cells. On the contrary, full-length Tks5 protein showed predominantly cytoplasmic distribution pattern. This could be due to the non availability of the surface exposed PIP-binding site of the PX domain or the entire PX domain for membrane interaction. It is also demonstrated that the PX domain of Tks5 strongly interacts with its third SH3 domain and Src-dependent phosphorylation release this intramolecular interaction.[29] The importance of PI(3,4)P_2 binding and invadosomal localization of the PX domain of Tks5 in Src-transformed cells has been already demonstrated.[3, 4, 35] In this regard, rearrangement of the cellular localization pattern of the PX domain was also investigated upon PDGF treatment, which is known to produce PI(3,4,5)P_3/PI(3,4)P_2 at the plasma membrane.[22, 36] Isolated PX domain translocates to plasma membrane of A549 cells upon stimulation with PDGF. Our studies showed that Tks5-PX domain preferentially bind to PI(3,4)P_2 over PI(3,4,5)P_3. Hence, PDGF dependent PI(3,4)P_2 generation at the plasma membrane could be the driving force for the plasma membrane translocation. Whereas PIP-binding mutant, R42A/R93A failed to translocate to plasma membrane even after PDGF stimulation. Hence, PI(3,4)P_2 binding is

primarily responsible for the plasma membrane translocation of the isolated Tks5-PX domain in A549 cells.

Another important finding in this study is the PIP-induced membrane penetration of Tks5-PX domain, which has not been so far reported. Depending on the extent of membrane penetration $p40^{phox}$- or $p47^{phox}$-PX domains are termed as H- or I-type of proteins, whereas PLD-PX domain is described as S-type of protein.[11] Measurements with low PIP concentration (3% of the total lipid) showed that both PI(3)P and PI(3,4)P_2 significantly enhance the monolayer penetration ability of the Tks5-PX domain and allows only partial dissociation of Tks5-PX domain from bilayer surface coated on SPR sensor chip. However, a very weak membrane penetration was observed in the absence of PIP lipids. The π_c values of the PX domain for PI(3)P and PI(3,4)P_2 containing monolayer penetrations were 34 and 37 dyne/cm respectively. For membrane penetrating proteins the π_c values for monolayer penetration are within the range of 30-35 dyne/cm. PIP-binding mutants, in particular R42A/R93A showed significantly reduced membrane penetration capabilities. Therefore, both PI(3)P and PI(3,4)P_2 lipid would seem to induce the penetration of Tks5-PX domain into the cell membrane. Monolayer penetration measurements of $p47^{phox}$-PX and $p40^{phox}$-PX and other domains proteins showed that hydrophobic residues present at the membrane binding surface allow the PX domain to penetrate into the densely packed lipid monolayer. Monolayer penetration ability of the Tks5-PX domain was substantially reduced by hydrophobic mutants I79A and L80A/F81A. Kinetic-SPR measurements also showed faster membrane dissociation rate of I79A and L80A/F81A mutants than the Tks5-PX domain, which is in good agreement with the membrane penetration observation. Therefore, presence of hydrophobic residues close to the PIP-binding site allows the PX domain to interact strongly with the membrane. Similar membrane penetration properties were observed for $p47^{phox}$-PX domain.[28] Thus, Tks5-PX domain would be termed as H-type of protein like $p47^{phox}$-PX domain.[11] The results also point out that presence of a cluster of hydrophobic residues (I79, L80 and F81) near the PIP-binding site is crucial for adequately strong membrane penetration capability, as replacement of any of these residues considerably lower monolayer penetration. However, model structure of the PX domain didn't show fully surface exposed hydrophobic residues present at the circumference of PIP-binding site. We hypothesize that PIP-binding to the cationic groove of the Tks5-PX domain causes a local conformation change by reducing positive electrostatic potential and allow the hydrophobic residues to penetrate into the membrane without substantial dehydration penalty. A similar membrane penetration mechanism was also observed for $p47^{phox}$- and $p40^{phox}$-PX domains. It

is important to note that cellular localization pattern of the hydrophobic mutants also show significant differences with the WT-PX domain. This could be due to PIP-induced membrane penetration of the PX domain or binding to other proteins under cellular environment.

It is important to note that monolayer penetration data is not in complete agreement with cellular localization or translocation pattern. The π_c values of the L80A/F81A and R42A/R93A domain for PI(3,4)P_2 containing lipid monolayer penetration were similar, 27 dyne/cm. However, their binding affinities and cellular translocation patterns are quite different. This could be due to the different membrane-bound topology of the mutant under the experimental conditions. The SPR based binding affinity of the WT-PX domain for PI(3)P and PI(3,4)P_2 lipids are comparable but monolayer data showed stronger penetration capability for PI(3,4)P_2 containing membrane. This could be due to real preference of the WT-PX domain for PI(3,4)P_2 over PI(3)P lipid and/or different binding orientation under monolayer and bilayer environment.

It has been demonstrated that prolonged membrane residence of Tks5 protein is essential for podosome formation in Src-transfored cells and the presence of PX domain is critical for its invadosome localization.[3, 4] SPR sensorgrams and monolayer data revealed that membrane penetration of PX domain mediated by hydrophobic residues present close to the PIP-binding pocket plays a critical role in membrane residence of Tks5 protein from liposome and cell membranes. Therefore, PIP-binding and PIP-dependent membrane penetration through I79, L80 and F81 residues of the PX domain would be essential for Tks5-dependent invadosome formation. In addition, measurement of the depth of membrane penetration by the PX domain would provide more details about its membrane penetration and cellular activity; however, it is beyond the scope of this study. Due to the presence of number of basic and hydrophobic residues at the membrane binding surface the membrane docking mechanism of Tks-PX domain is little bit complex. We hypothesize that positively charges residues would allow the PX domain to bind to the membrane non-specifically and then specific PIP binding and subsequent membrane penetration would allow the PX domain to interact the membrane strongly. Tks5-PX domain is reported to interact with the SH3 domain [12]; hence protein-protein interaction may also play a significant role in PI(3)P and PI(3,4)P_2-mediated subcellular localization and cellular functions of Tks5 protein.

Conclusion

Overall, present study establishes that both PI(3)P and PI(3,4)P_2 lipids play a crucial role in membrane localization and/or translocation of the PX domain of Tks5. SPR and FRET based

studies systematically compared the PIP-specificity of the PX domain with slight preference for PI(3,4)P_2 over PI(3)P lipid. Monolayer penetration measurements revealed PIP-dependent membrane penetration ability of the PX domain. Mutational analyses describe detail mechanistic insights of the PIP-dependent membrane recruitment of the PX domain, which depends on PIP-binding affinity and hydrophobic interactions through a cluster of hydrophobic residues present close to the PIP-binding site. The membrane binding and penetrating properties are in good correlation with physiological functions of isolated PX domain that not only binds to early endosomal membrane but also translocate to plasma membrane in response to PDGF. The membrane localization of the Tks5-PX domain is crucial for its cellular activities.

2.3. Experimental Section

Materials- Phosphatidylinositol-3,4-bisphosphate (PI(3,4)P_2), Phosphatidylinositol-3,5-bisphosphate (PI(3,5)P_2) phosphatidylinositol-4,5-bisphosphate(PI(4,5)P_2), and phosphatidylinositol-3,4,5-triphosphate (PI(3,4,5)P_3), phosphatidylinositol-3-phosphate(PI(3)P), phosphatidylinositol-4-phosphate (PI(4)P), phosphatidylinositol-5-phosphate(PI(5)P), phosphatidylinositol (PIP) were purchased from Cayman Chemicals (Ann Arbor, MI). 1-Palmitoyl-2-oleoyl-*sn*-glycero-3-phosphocholine (PC), 1-palmitoyl-2-oleoyl-*sn*-glycero-3-phosphoethanolamine (PE), 1,2-dioleoyl-sn-glycero-3-phosphoethanolamine-N-(5-dimethylamino-1-naphthalenesulfonyl) (dPE) and 1-palmitoyl-2-oleoyl-*sn*-glycero-3-phosphoserine (PS) were purchased from Avanti Polar Lipids. Octyl glucoside was purchased from Fisher. The Pioneer L1 sensor chip was purchased from Biacore AB (Piscataway, NJ). Ultrapure water (Milli-Q system, Millipore, Billerica, MA) was used for the preparation of buffers.

Vector Construction and Mutagenesis— For bacterial expression, the cDNA of human Tks5-PX domain, and mutants, R42A, R43A, K78A, I79A, R93A, R42A/R93A, R43A/R93A, R82A/R83A, L80A/F81A and R43/K78A/R93A were subcloned into the pGEX-4T1 vector between the restriction sites *EcoRI* and *XhoI* with N-terminal glutathione S-transferase (GST) fusion. The cDNA of EGFP-fused full length Tks5, Tks5-PX was a generous gift of Professor Sara A. Courtneidge (Burnham Medical Research Institute). For mammalian expression, Tks5-PX domain mutants were generated by the overlap extension PCR using forward and reverse primers (appendix Table A4) and subcloned into pEGFP-N1

vector between the *XhoI* and *KpnI* restriction sites with N-terminus enhanced green fluorescence protein (EGFP). All constructs were transformed into DH5α cells for plasmid isolation. All plasmid DNA sequences were verified. GST constructs were transformed into E. coli BL21 (DE3) cells for protein expression. The cDNA of RFP-fused FYVE domain of Hrs protein was a generous gift of Professor Junying Yuan (Harvard Medical School).

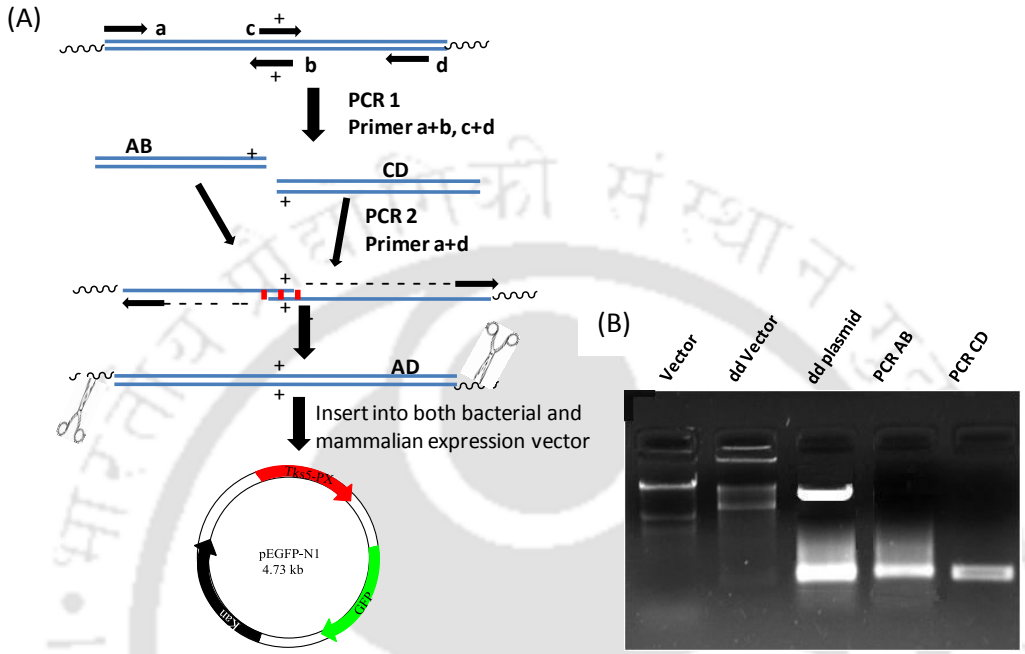

Figure 2.3.1. Schematic diagram of overlap PCR and subsequent digestion and ligation (A). Representative agarose gel image of Tks5-PX-R42A mutant.

Protein expression and purification— For protein expression in bacterial system, the GST-fused wild type Tks5-PX and mutants were individually transformed into BL21(DE3) bacterial cells, grown into 1liter Luria broth containing 100 µg/mL ampicillin at 37 ℃ with 120 rpm shaking until the absorbance reached approximately 0.7 at 600 nm.[12, 22] Cells growth was stopped keeping on ice for 10 minutes and added 500 µM isopropyl 1-thio-β-D galactopyranoside (IPTG) for induction of protein expression. After 14 hr incubation at 24℃, cells were pelleted down by centrifugation at 5000 × g and 4 ℃. Finally the cells were resuspended by adding 20 mL buffer containing 20 mM Tris, 160 mM Nacl, pH-8, 50 µM phenylmethylsulfonyl fluoride (PMSF), 2 mM dithiothreitol (DTT) and 0.1% Triton X-100. The resulting solution was sonicated and centrifuged for 30 min at 4 ℃**,** 48000 X g. Then supernatant was collected in a falcon tube and incubated 45 min at 80 rpm with 300 µl of glutathione s-transferase Tag^{TM} resin (GenScript). The solution was then passed through a pre-rinsed column. After three times washing with wash buffer (20 mM Tris,160 mM KCl,

pH 8), 20 mM 1mL reduced glutathione was added. Finally protein was eluted in five fractions using same composition wash buffer with reduced glutathione. Purity of the proteins was checked by SDS-PAGE gel electrophoresis (Figure 2.3.2). Buffer of the eluted proteins were exchanged to 20 mM Tris, 160 mM KCl, pH 8 using a HiTrap desalting column (GE Healthcare), and protein aliquots were kept at −80 °C until use.

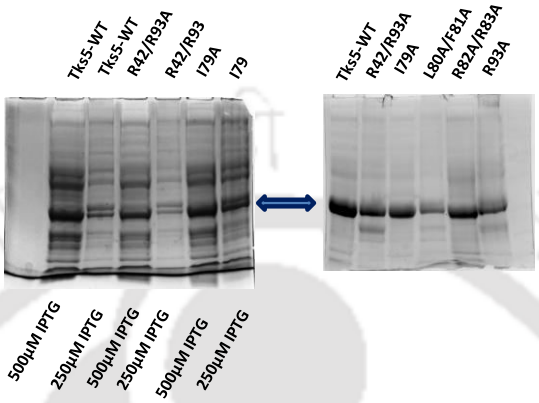

Figure 2.3.2. Representative SDS-PAGE gel of Tks5-PX domain and mutants. Left panel gel image indicates optimized condition of protein expression in different IPTG concentration. Right panel gel image indicates purified protein of Tks5 and mutants.

Förster resonance energy transfer-based competitive binding assay- Protein-to-membrane fluorescence resonance energy transfer (FRET)-based competitive binding assay was carried out using Fluoromax-4 spectrofluorometer at room temperature.[23, 24] The qualitative binding affinity and specificity of Tks5-PX domain and mutants to the PIP lipid was determined by this assay under liposomal environment. Membrane bound PX domain and mutants were displaced from liposomes by the addition of the competitive inhibitor inositol hexaphosphate (IP_6). The liposomes composed of PC/PE/PS/dPE (59:20:20:1 mol %)) and PC/PE/PS/dPE/PIP (57:19:20:1:3 mol %)) were used as control and for PIP, respectively. FRET signals were monitored at λ_{ex} = 284 nm and λ_{em} = 505 nm. The FRET signal due to PIP-dependent protein binding to the liposomes was corrected with non-specific fluorescence signal originated from control liposome (PC/PE/PS/dPE) and protein interactions. The stock solution of IP_6 was titrated into the sample containing protein (1 μM) and excess liposome (100 μM total lipid) in a buffer solution (20 mM Tris–HCl buffer, pH 7.4, containing 0.16 M NaCl) at room temperature. Plots of protein-to-membrane FRET as a function of IP_6 concentration were subjected to nonlinear least-squares-fit analysis using eq

(1) to calculate apparent equilibrium competitive inhibition constants ($K_I(IP_6)_{app}$) for IP_6. Where, [x] represents the total IP_6 concentration and ΔF_{max} represents the calculated maximal fluorescence change.[23, 24]

$$F = \Delta F_{\max}\left(1 - \frac{[x]}{[x] + K_I(IP6)_{app}}\right) + C \qquad (1)$$

Kinetic SPR measurements— To measure the PX domain binding affinity and specificity to the PIPs, we performed a real time surface plasmon resonance (SPR) measurements were performed (at 25 °C, in 20 mM HEPES buffer, pH 7.4, containing 0.16 M KCl, flow rate of 30 µL/min) using a two channel system. Lipid-coated L1 sensor chip was used in the Biacore-X 100 (GE Healthcare) systems.[22] Vesicles for SPR analysis were prepared at a concentration of 0.5 mg/mL in 20 mM HEPES buffer, pH 7.4, containing 0.16 M KCl, and were vortexed vigorously and passed through a 100-nm polycarbonate filter using an Avanti Mini-Extruder (Avanti Polar Lipids, Alabaster, AL) according to the manufacturer's protocol. After washing the sensor chip surface with the running buffer (20 mM HEPES, pH 7.4, containing 0.16 M KCl), PC/PE/PS/PIP (57/20/20/3) and PC/PE/PS (60/20/20) vesicles were injected at 5 µL/min to the active surface and the control surface, respectively, to achieve similar resonance unit values (3500-4500 response units). The levels of vesicle coating for both surfaces were kept at the minimum that is necessary for preventing the nonspecific adsorption to the sensor chips.[25] Non-specific adsorption of liposomes was washed out with 50 mM NaOH, until or unless the RU of the sensorgrams was observed constant. To minimize nonspecific adsorption the control surface was also coated with 40 µL of BSA (0.1 mg/mL in the running buffer) at a flow rate of 5 µL/min, and equilibrated for 20 min, before the injection of protein. For kinetic SPR measurements, the sensorgrams were obtained using five different concentration of each protein, monitoring association and dissociation phase for 180 sec. and 400 sec. respectively. After each experiment, lipid coated surface was regenerated using 50 mM NaOH. Data were analyzed with BIAevalution 3.0 software to determine the association (k_a) and dissociation (k_d) assuming 1:1 Langmuir binding model: protein (P) + protein binding site (M) on vesicle ↔ complex (PM).[22, 25] The dissociation constant [23] value was calculated using the following equation, $K_d = k_d/k_a$. Each fitting was checked their validation by residual plot and χ^2 value. All datas were reproduced three times to get more accurate means ± S.D.

Monolayer measurements— Ability of Tks5-PX domain and mutants to penetrate the phospholipid monolayer was measured by using Wilhelmy plate method.[22, 26] All measurements were performed using a 10 mL circular Teflon trough and Wilhelmy plate connected to a Langmuir–Blodgett trough (KSV NIMA). A lipid monolayer (prepared in hexane/ethanol (9:1, v/v)) consisting of desire lipid composition (PC/PE/PS with or without PI(3) or PI(3,4)P_2) was spread onto the subphase of buffer (containing 20mM HEPES, 160 mM KCl, pH-7.4) until the desired initial surface pressure (π_o) was obtained. Then it was allowed to stabilize the signal (for 15 min) and 100 µg of protein was injected into the subphase through the small hole on Teflon trough. The change in surface pressure ($\Delta\pi$) at a constant surface area was monitored for 60 min (with stirring the subphase at 60 rpm). $\Delta\pi$ was plotted versus π_0 and extra plotted to x -axis, yielding the critical surface pressure (π_c).

Subcellular localization study— Non-small cell lung cancer A549 cell lines were grown in RPMI-1640 (Gibco) containing 10% heat inactivated FBS along with penicillin and streptomycin at 37 $^{\circ}$C with 5% CO_2 under humid condition. The sub-confluent cells (0.5×10^6 cells/35 mm plate) were seeded on cover-slip one day prior the transfection. For colocalization sudy, EGFP-fused full length Tks5, Tks5-PX-WT, mutants and RFP-fused FYVE domain of Hrs protein (PI(3)P marker [27] were transfected in A549 cell line using polyethylenimin transfection reagent in Opt-MEM media. Media was changed at 24 hours post-transfection and then cells were fixed after 48 hours of transfection.[12] For PDGF-mediated stimulation studies of Tks5-PX-WT and mutants were also transfected using similar methods. Before the treatment with PDGF transfected cells were starved with serum free medium for 10 hours. Then media was replaced with fresh serum free medium followed by addition of human PDGF-BB (50 ng/mL) and incubated for 5 minutes. Then cells were fixed and prepared for immunofluorescence study.[22] Before confocal imaging all transfected cells were washed three times with phosphate-buffered saline (PBS) and then fixed by using 4% paraformaldehyde at room temperature for 15 min. Then cells were permeabilized with 0.1% Triton X-100 for 10 min. The permeabilized cells were again washed three times with PBS and then coverslips were mounted with mounting media containing DAPI (Santa cruz mounting medium) on a glass slide (Blue star). The subcellular localization of the proteins were observed with a Zeiss LSM 510 confocal microscope with an Axiovert 100 M inverted microscope operating with a 25 milliwatt argon laser tuned to 488 nm.

References

1. H.S. Leong, A. E. Robertson, K. Stoletov, S.J. Leith, C.A. Chin, A.E. Chien, M.N. Hague, A. Ablack, K. Carmine-Simmen, V.A. McPherson, C.O. Postenka, E.A. Turley, S.A. Courtneidge, A.F. Chambers and J.D. Lewis, *Cell Reports,* 2014, **8**, 1558-1570.
2. H.S. Leong, A.E. Robertson, K. Stoletov, S. J. Leith, C.A. Chin, A.E. Chien, M.N. Hague, A.L. Ablack, K.C. Simmen, V.A. McPherson, C.O. Postenka, E. A. Turley, S. A. Courtneidge, A. F. Chambers, and J.D. Lewis, *European Journal of Cancer*, 2014, **50**, 187-187.
3. T. Oikawa, T. Itoh and T. Takenawa, *Journal of Cell Biology,* 2008, **182**, 157-169.
4. D.A. Murphy, B. Diaz, P.A. Bromann, J.H. Tsai, Y. Kawakami, J. Maurer, R.A. Stewart, J.C. Izpisua-Belmonte, and S.A. Courtneidge, *PLoS One*, 2011, **6**, e22499.
5. H. Yamaguchi, J. Wyckoff, and J. Condeelis, *Curr Opin Cell Biol*,2005, **17**, 559-564.
6. S.A. Courtneidge, *Biochemical Society Transactions*, 2012, **40**, 129-132.
7. B. Blouw, D.F. Seals, I. Pass, B. Diaz, and S.A. Courtneidge, *Eur J Cell Biol*, 2008, **87**, 555-567.
8. V.P. Sharma, R. Eddy, D. Entenberg, M. Kai, F.B. Gertler and J. Condeelis, *Current Biology*, 2013, **23**, 2079-2089.
9. O. Thompson, I. Kleino, L. Crimaldi, M. Gimona, K. Saksela and S.J. Winder, *PLoS One*, 2008, **3**, e3638.
10. P. Lock, C.L. Abram, T. Gibson and S.A. Courtneidge, *EMBO J*, 1998, **17**, 4346-4357.
11. Y. Xu, L.F. Seet, B. Hanson and W.J. Hong, *Biochemical Journal*, 2001, **360**, 513-530.
12. C.L. Abram, D.F. Seals, I. Pass, D. Salinsky, L. Maurer, T.M. Roth and S.A. Courtneidge, *Journal of Biological Chemistry*, 2003, **278**, 16844-16851.

13. S.A. Courtneidge, E.F. Azucena, I. Pass, D.F. Seals and L. Tesfay, *Cold Spring Harb Symp Quant Biol*, 2005, **70**, 167-171.
14. A.C. Rufer, J. Rumpf, M. von Holleben, S. Beer, K. Rittinger and Y. Groemping, *J Mol Biol*, 2009, **390**, 939-950.
15. S.S. Stylli, R.B. Luwor, A.H Kaye, S.T. I, C.M. Hovens and P. Lock, *Oncol Rep,* 2014, **32**, 989-1002.
16. B. Diaz, G. Shani, I. Pass, D. Anderson, M. Quintavalle and S.A. Courtneidge, *Science Signaling*, 2009, **2.**
17. D.F. Seals, E.F. Azucena, I. Pass, L. Tesfay, R. Gordon, M. Woodrow, J.H. Resau and S.A. Courtneidge, *Cancer Cell*, 2005, **7**, 155-165.
18. D. Karathanassis, R.V. Stahelin, J. Bravo, O. Perisic, C.M. Pacold, W.W. Cho and R.L. Williams, *Embo Journal*,2002, **21**, 5057-5068.
19. R.V. Stahelin, F. Long, K. Diraviyam, K.S. Bruzik, D. Murray W.H. Cho, *Journal of Biological Chemistry*, 2002, **277**, 26379-26388.
20. T. Oikawa and T. Takenawa, *Cell Adh Migr*, 2009, **3**, 195-197.
21. R.D. Teasdale and B.M. Collins, *Biochemical Journal*, 2012, **441**, 39-59.
22. D. Manna, A. Albanese, W.S. Park and W. Cho, *J Biol Chem*, 2007, **282**, 32093-32105.
23. D. Talukdar, S. Panda, R. Borah and D. Manna, *J Phys Chem B*, 2014
24. J.A. Corbin, R.A. Dirkx and J.J. Falke, *Biochemistry*, 2004, **43**, 16161-16173.
25. W. Cho, L. Bittova and R.V. Stahelin, *Anal Biochem*, 2001, **296**, 153-161.
26. E. Adu-Gyamfi, S.P. Soni, Y. Xue, M.A Digman, E. Gratton and R.V. Stahelin, *J Biol Chem*, 2013, **288**, 5779-5789.
27. L. Zhang, J. Yu, H. Pan, P. Hu, Y. Hao, W. Cai, H. Zhu, A.D. Yu, X. Xie, D. Ma and J. Yuan, *Proc Natl Acad Sci USA,*2007, **104**, 19023-19028.
28. R.V. Stahelin, A. Burian, K.S. Bruzik, D. Murray and W. Cho, *J Biol Chem*, 2003, **278**, 14469-14479.
29. T. Oikawa, M. Oyama, H. Kozuka-Hata, S. Uehara, N. Udagawa, H. Saya and K. Matsuo, *J Cell Biol*, 2012, **197**, 553-568.
30. W. Cho and R.V. Stahelin, *Annu Rev Biophys Biomol Struct*, 2005, **34**, 119-151.
31. N.R. Blatner, M.I. Wilson, C. Lei, W. Hong, D. Murray, R.L. Williams and W. Cho, *EMBO J*, 2007, **26**, 3709-3719.
32. R.V. Stahelin, *J Lipid Res*, 2009, **50 Suppl**, S299-304.

33. S. Pankiv, E.A. Alemu, A. Brech, J.A. Bruun, T. Lamark, A. Overvatn, G. Bjorkoy and T. Johansen, *J Cell Biol*, 2010, **188**, 253-269.

34. S. Suetsugu, S. Kurisu and T. Takenawa, *Physiol Rev*, 2014, **94**, 1219-1248

35. M. Symons, *Curr Biol*, 2008, **18**, R925-927.

36. A. Hogan, Y. Yakubchyk, J. Chabot, C. Obagi, E. Daher, K. Maekawa and S.H. Gee, *J Biol Chem,* 2004, **279**, 53717-53724.

Chapter 3

Mechanistic Insights into the Phosphatidyl Inositol Binding Properties of Pleckstrin Homology (PH) Domain of Lamellipodin (Lpd)

This chapter determines the phosphoinositides binding properties of pleckstrin homology (PH) domain of lamellipodin (Lpd). To understand their interaction properties we quantitatively determined the binding parameters of Lpd-PH domain employing a number of biophysical studies including surface plasmon resonance (SPR), fluorescence resonance energy transfer (FRET)-based competitive binding assay, monolayer penetration measurements and cellular translocation study. Overall, these studies demonstrate an insight into how Lpd-PH domain regulates cellular signals in PI(3,4)P_2 dependent manner.

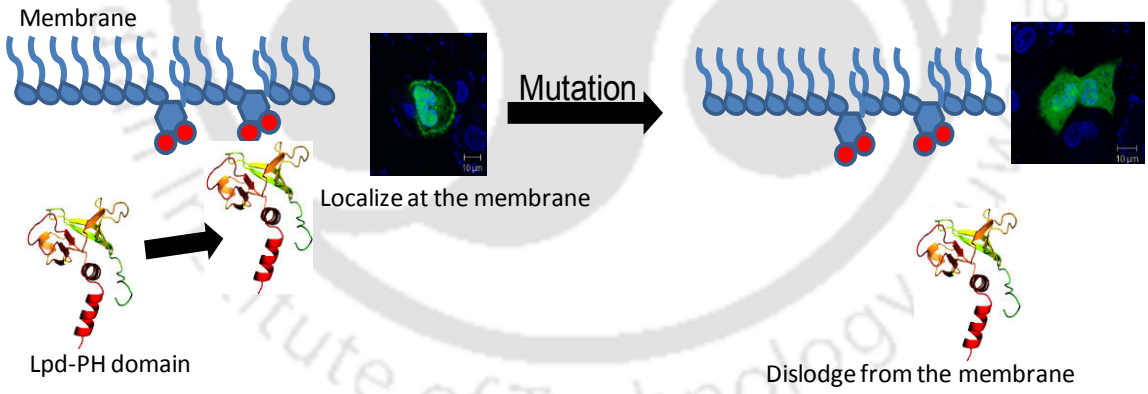

3.1. Background and Focus of the Present Work

Perturbation of actin-dependent cell migration and adhesion is associated with malignant cell metastasis and other diseases. Lamellipodin (Lpd) plays crucial role in actin-dependent cell migration and adhesion.[1, 2] Recently, cell motility and actin dynamics have been found to be associated with a group of adapter signaling proteins designated as MRL family (based on family members MIG-10/RIAM/Lpd), demonstrated to promote lamellipodia protrusion in fibroblasts.[3, 4] These proteins are recognized as a key convergence point that links upstream signaling with actin dynamics. It is well documented that Lpd acts as a junction point between upstream signaling pathways and cytoskeletal remodeling through its phosphotidylinositols (PIP) binding PH domain and Ras-superfamily proteins binding RA domain at the plasma membrane.[1, 8] High expression level of Lpd is observed in nerve, heart, brain, and ovary.[8] Lpd over expression augments lamellipodial projection velocity, a consequence detected when Ena/ vasodilator-stimulated phosphoproteins (VASP) are over expressed or stimulated at the plasma membrane. Ena/ VASP proteins also play crucial role in cytoskeleton rearrangement including migration, adhesion, cell-cell interaction and shape change. Lpd directly interacts with Ena/VASP via clusters of putative EVH1 binding site and recruits at lamellipodia and the tips of the filopodia. Pathogens like vaccinia and enteropathogenic E. coli (EPEC) use Ena/VASP molecules and Lpd as a tool to move them throughout inter or intra cells.[10, 16, 17] Reduced Lamellipodia formation efficiency was observed in Lpd knock-down cells but not in Ena/Vasp knock-down cells. This suggests the importance of Lpd in actin-cytoskelone dynamics. Like other FP4 motif containing proteins, Lpd also localize and recruits Ena/VASP proteins to the focal adhesion sites. Although, over expreesion of Lpd is dependent on Ena/VASP proteins but functional localization at the leading edge is completely independent.[3, 9, 15-18] Lpd is also considered as a potent therapeutic target for the treatment of cocaine abuse and toxicity for its catalytic activity of butylcholinesterase.[11, 19, 20] The Lpd is reported to localize at the ruffles in phosphoinositide 3-kinase (PI3-K) activated cells. The activation of PI3-K in response to growth factors and insulin stimulation leads to the generation of phosphatidylinositol 3-phosphate PI(3)P, phosphatidylinositol 3,4,5-trisphosphate [$PI(3,4,5)P_3$] and phosphatidylinositol 3,4-bisphosphate [$PI(3,4)P_2$].[21] These PIPs also play an important role in cell motility, signal transduction, membrane trafficking and cytoskeletal dynamics.[22]

Crystal structures of Lpd demonstrate the similar structural building block as MRL family protein. Like the analogues protein RIAM, Lpd also contain highly charged N-

terminus Ras-association (RA), pleckstrin homology (PH) domain, coil-coil region and a number of poly-proline motifs.[3, 5, 8] Furthermore, the C-terminus of Lpd consist proline rich eight possible SH3 binding sites followed by three profiling and six EVH1 binding sites. In mammalian system, RA and PH domains cooperatively regulates in both Ras-GTPase signaling and membrane translocation via RA and PH domain respectively.[6] Further structural analysis also revealed that Lpd oligomerize through intermolecular coil-coil interaction. This interaction is important for the recruit of Ena/VASP proteins; thereby leading to the binding of actin-filaments forming bundles.[5]

Structural analysis showed that like other PH domains, the Lpd-PH domain also contain a conserved structure comprising of seven β-sheets strands with variable loops, followed by one α-helix.[10, 12] Characteristically, PH domains exhibit high to-low specificity for the PIPs containing membrane. Sequence alignment and structure analysis revealed that Lpd-PH domain contains several positively charged residues on its membrane binding surface, which might be primarily responsible for its interaction with the anionic lipids like PIPs. Recent studies demonstrated that the PH domain of Lpd protein moderately interacts with the $PI(3,4)P_2$ and GFP-fused Lpd-PH domain localized at the ruffles in PDGF–stimulated cells. However, PIP-binding specificities were not measured quantitatively and PIP-dependent membrane binding mechanism is also known. Therefore, in this study we present a thorough understanding of the PIP-binding mechanism and PIP-dependent cellular localization of the Lpd-PH domain.

3.2. Results and Discussion

Phosphatidylinositol specificities of Lpd-PH Domain:

PH domains are one the common membrane binding modules with varying (weak to strong) affinities for PIP lipids and also involved in regulation of PIP level in different cellular compartments. PIP-dependent membrane binding of the PH domains serves as a common membrane translocalization function of the host proteins. RA-PH domain containing proteins like Grb and others also get anchored into the membrane in a PIP-dependent manner and facilitate the interactions of RA domain with Ras GTPases, which augments the signaling events.[6] Few studies already mentioned that Lpd-PH domain weakly interacts with PIPs. However, conflicting results have been reported regarding its PIP-specificities and binding affinities. Using various fluorescently labeled PIPs in a fluorescence-polarization assay

Jinhua Wu and coworkers recently reported that Lpd-cc-RA-PH domain have only lower affinities for PI(5)P, PI(3,4)P_2, PI(4,5)P_2 and PI(3,4,5)P_3 lipids (K_d in the range of 29-69 μM). Whereas Frank B. Gertler and coworkers performed protein-lipid overlay assay and showed that Lpd-PH domain specifically interacts with PI(3,4)P_2.[8, 5] In this regard, we quantitatively measured the PIP binding affinities and specificity of the isolated Lpd-PH domain using real time surface plasmon resonance (SPR) measurement and fluorescence resonance energy transfer (FRET)-based competitive binding analysis under liposomal environment.

Fluorescence Resonance Energy Transfer-Based Competitive Binding Assay— To determine the PIP-binding affinities and specificity of Lpd-PH domain, we employed FRET-based competitive binding assay under the liposomal environment (PC/PE/PS/dPE/PIP (57:19:20:1:3)). First Lpd-PH domain was equilibrated with liposomes and FRET signal was collected and then this lipid-protein interaction was perturbed by using competitive inhibitor, Phytic acid (IP_6) in a concentration dependent manner. The decrease in FRET signal at 505 nm was monitored to measure the apparent inhibitory constant [$K_I(IP_6)_{app}$] values. Surface exposed Trp-residue (W22, W31) of the Lpd-PH domain act as the FRET donor, and a low density of membrane-embedded, dansyl-PE (dPE) lipid serve as the acceptors. Figure 3.2.1A illustrates representative isotherms of protein-to-membrane FRET-assay. Calculated $K_I(IP_6)_{app}$ values for different PIP containing liposomes are listed in Table 3.2.1.

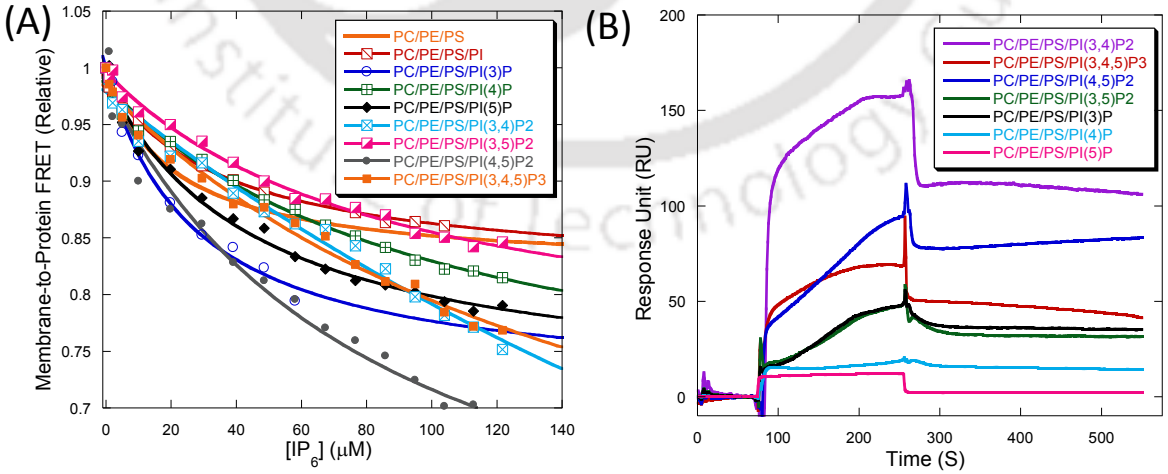

Figure 3.2.1. Competitive displacement assay for Lpd-PH domain (1 μM) bound to PC/PE/PS (60:20:20) and PC/PE/PS/PIP (57:20:20:3) liposomes. The bound complex was titrated with the IP_6 as competitive inhibitor (A). Representative kinetics SPR sensograms Lpd-PH domain interacting with the PC/PE/PS/PIP (57:20:20:3) liposomes (B).

Surface Plasmon Resonance Analysis— For further understanding of the Lpd-PH domain interactions with different PIPs and measurements of quantitative binding parameters, we also performed real-time SPR analysis using PIP-containing liposomes (PC/PE/PS/PIP_x (57:20:20:3)). The PIP binding affinities were calculated using both equilibrium- and kinetic-SPR analyses. For equilibrium-SPR measurements different concentrations of wild type (WT)-Lpd-PH domain was passed over the liposome-coated L1 sensor chip at a flow rate of 10 µL/min and real-time measurement of association phase was monitored for longer time (500 sec). Figure 3.2.2B describes representative binding isotherms of equilibrium-SPR measurements. Protein concentration dependent maximum SPR responses (after 500 sec) are plotted to calculate the binding affinities (K_{d1}) and are listed in Table 3.2.1. Figure 3.2.2A illustrates representative SPR sensorgrams for the binding of Lpd-PH domain to

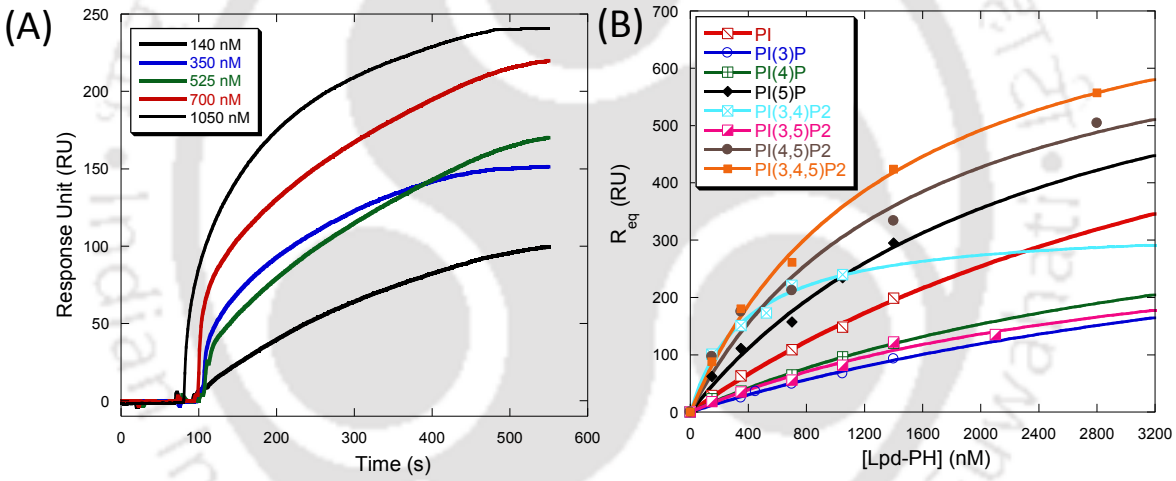

Figure 3.2.2. Representative equilibrium SPR sensorgrams for Lpd-PH domain interacting with the PC/PE/PS/PIP (57:20:20:3) liposomes immobilized on L1 sensor chip (A). PIPs binding isotherms were generated from the R_{eq} values after 500 sec in a concentration dependent manner (B).

PC/PE/PS/$PI(3,4)P_2$ (57:20:20:3) liposomes. We also performed kinetic-SPR analyses using PIP-containing liposomes (PC/PE/PS/PIP_x (57:20:20:3)). For kinetic-SPR analyses different concentrations of WT-Lpd-PH domain was passed over the liposome-coated L1 sensor chip at a flow rate of 30 µL/min and real-time measurement of both association and dissociation phase was monitored (Figure 3.2.1B). Calculated binding affinities (K_{d2}) and are listed in Table 3.2.1.

Calculated K_{d1} and K_{d2} values obtained from the SPR analyses are in good agreement with the $K_I(IP_6)_{app}$ values measured from the competitive-FRET analyses. The binding

parameters showed that the WT-Lpd-PH domain have sufficiently stronger binding affinity for PI(3,4)P_2 lipid. The K_{d1} and K_{d2} values of WT-Lpd-PH domain for PI(3,4)P_2 lipid are 388 nM and 3.80 × 10-9 M, whereas, the K_I(IP6)app value for PI(3,4)P2 lipid is 460 μM. However, the binding affinity of Lpd-PH domain for PI(3,4)P_2 is much weaker that the

Table 3.2.1. Binding parameters of Lpd-PH domain interaction with PC/PE/PS/PIP (57:20:20:3) liposomes were determined membrane-to-protein FRET analysis and SPR analyses[a]

Liposome	Lpd-PH WT		
	$K_I(IP_6)_{app}$ (μM)	K_{d1} (nM)	K_{d2} (M)
PC/PE/PI	37 ± 8	4886 ± 141	-
PC/PE/PS/PI(3)P	74 ± 7	5716 ± 365	-
PC/PE/PS/PI(4)P	101 ± 14	4035 ± 169	-
PC/PE/PS/PI(5)P	46 ± 7	2452 ± 115	-
PC/PE/PS/ PI(3,4)P_2	460 ± 32	388 ± 26	3.80×10^{-9}
PC/PE/PS/ PI(3,5)P_2	88 ± 14	3309 ± 152	-
PC/PE/PS/ PI(4,5)P_2	85 ± 23	1557 ± 148	2.08×10^{-8}
PC/PE/PS/ PI(3,4,5)P_3	171 ± 20	1390 ± 143	1.16×10^{-8}

[a]All FRET measurements were performed in 20 mM Tris buffer at pH 7.4 containing 160 mM NaCl. IP_6 was used as inhibitor of membrane-to-protein interactions. Protein, 1 μM was used for FRET analysis. All SPR measurements were performed in 20 mM HEPES buffer at pH 7.4 containing 160 mM KCl at 25 °C. Protein concentrations were varied for SPR analysis. Values represent the mean ± SD from triplicate measurements. K_{d1} values were calculated by nonlinear least squares fit analysis of the isotherm using $R_{eq} = R_{max}/(1 + K_{d1}/P)$. All SPR sensorgrams are shown after background correction for binding to the control surface coated with PC/PE/PS (60:20:20) liposome. Flow rate was kept at 10 and 30 μL/min for equilibrium and kinetic SPR analyses, respectively.

Tapp1-PH domain under the similar experimental conditions. The K_{d1} and K_{d2} values for Tapp1-PH domain under similar experimental conditions were 82 nM and 1.31 × 10^{-9} M, respectively. Tapp1-PH domain is considered as a cellular marker for PI(3,4)P_2 lipid. The Lpd-PH domain also exhibited a moderate binding affinities for PI(3,4,5)P_3 (~3 fold less), PI(4,5)P_2 (~5 fold less) lipids but weaker affinities for other PIPs. However, WT-Lpd-PH showed dissimilar kinetic patterns. Rate constants (k_a and k_d) could not be straightforwardly calculated and directly compared among the PIPs, because the sensograms for kinetic-SPR analyses for followed complex patterns of either one-step or two-step 1:1 binding models. The sensograms of WT-Lpd-PH binding to the PI(3,4)P_2, PI(4,5)P_2 and PI(3,4,5)P_3 lipids could be fitted using one-step 1:1 binding model. For this purpose, only the qualitative comparison of kinetic patterns was made for other PIP containing liposomes (Figure 3.2.1B).

Similar, we also measured the PIP-binding properties of Lpd-RA-PH domain. The $K_I(IP_6)_{app}$ values showed that like isolated PH domain, RA-PH domain also preferentially bind with the $PI(3,4)P_2$ containing liposome (805 μM) but with 1.75-fold stronger affinity (Table 3.2.2). Therefore, our FRET and SPR analyses clearly showed that Lpd-PH domain have higher specificity for $PI(3,4)P_2$ over

Table 3.2.2. Apparent competitive inhibition constants [$K_I(IP_6)_{app}$] of Lpd-RA-PH domain for IP_6[a]

	PI	PI(3)P	PI(4)P	PI(5)P	$PI(3,4)P_2$	$PI(3,5)P_2$	$PI(4,5)P_2$	$PI(3,4,5)P_3$
LPD-RA-PH	76 ± 9	122 ± 11	105 ± 12	119 ± 11	805 ± 36	111 ± 27	160 ± 24	261 ± 33

[a]All FRET measurements were performed in 20 mM Tris buffer at pH 7.4 containing 160 mM NaCl. IP_6 was used as inhibitor of membrane-to-protein interactions. Protein, 1 μM was used for FRET analysis.

other PIPs (Table 3.2.1). Collectively these quantitative binding parameters re-assess the PIP specificity and affinities of isolated Lpd-PH domain and provide a new insight into how Lpd-PH domain would respond to $PI(3,4)P_2$ formation more effectively than other PIPs under different cellular conditions.

Identification of the PIP-binding Site of the PH Domain: To identify the amino acids residues primarily involved in interactions with the $PI(3,4)P_2$ lipid, we analyzed the crystal structure of the Lpd-PH domain (4GN1) and amino acid sequences of the homologous PH domain (Figure 3.2.3). Surface electrostatic potential distribution calculation showed a cationic groove near the putative membrane binding surface. Interestingly, we identified a cationic groove comprising K24, K29, K79 and K96 as a non-canonical PIP binding site like β-spectrin-PH domain. Whereas another cationic groove comprising K28, K32 and R34 present at the regular canonical PIP-binding site of PH domains (Figure 3.2.4). Therefore, Lpd-PH domain may interacts with the PIP through the non-canonical binding site like β-spectrin-PH domain, or through regular canonical binding mode (Figure 3.2.4). Detailed structural analysis of Lpd-PH domain and β-spectrin-PH domain (1BTN) showed that L23 and D25 residues could prevent the PIP-head groups to interact with the Lpd-PH domain through its canonical binding site. To get initial information about the probable PIP-binding site, we performed molecular docking analyses with both short chain $PI(3,4)P_2$ lipid and $Ins(1,3,4)P_3$ molecule. However, the model structures revealed that both $PI(3,4)P_2$ and

Ins(1,3,4)P_3 have almost no preference for either canonical or non-canonical PIP-binding site. In this regards, we prepared a set of mutants for both the binding sites based on the crystal structure of the Lpd-PH domain. Cationic residues were mutated to Ala-residue either individually or in combination and their PI(3,4)P_2 binding affinities were measured by competitive-FRET and SPR analyses under the similar experimental conditions. Calculated binding parameters of the mutants are summarized in Table 3.2.3 and 3.2.4. The K_d values obtained from the SPR analyses show that single mutants K24A, K28A, R79A

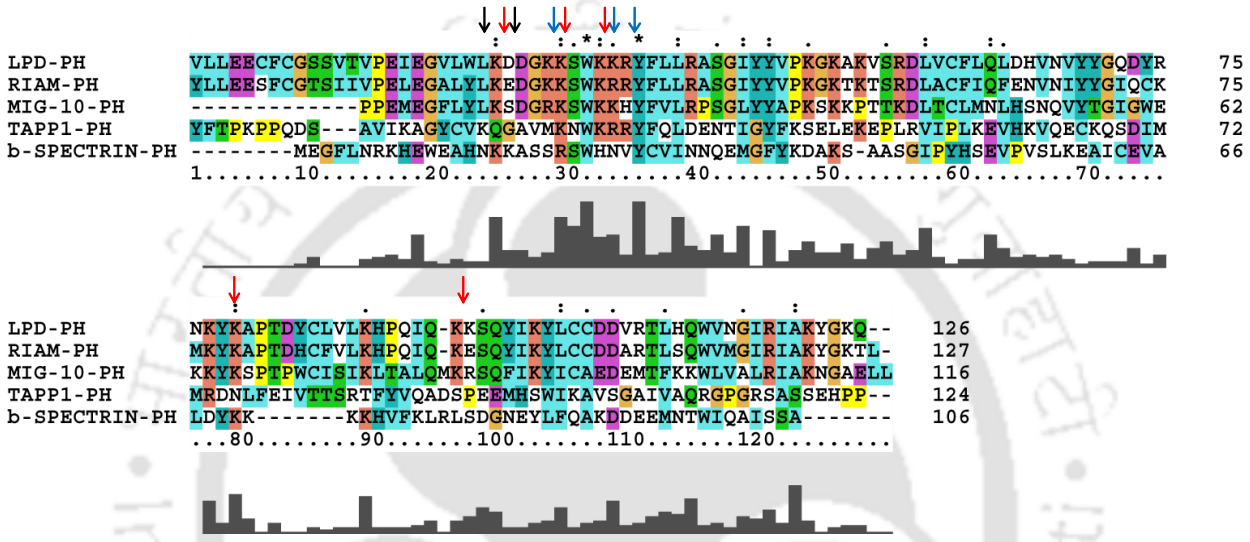

Figure 3.2.3. Amino-acid sequence alignment of PH domains of MRL protein family along with Tapp1 and β–spectrin are shown using Clustal-X program. Arrow indicates positions of the mutation.

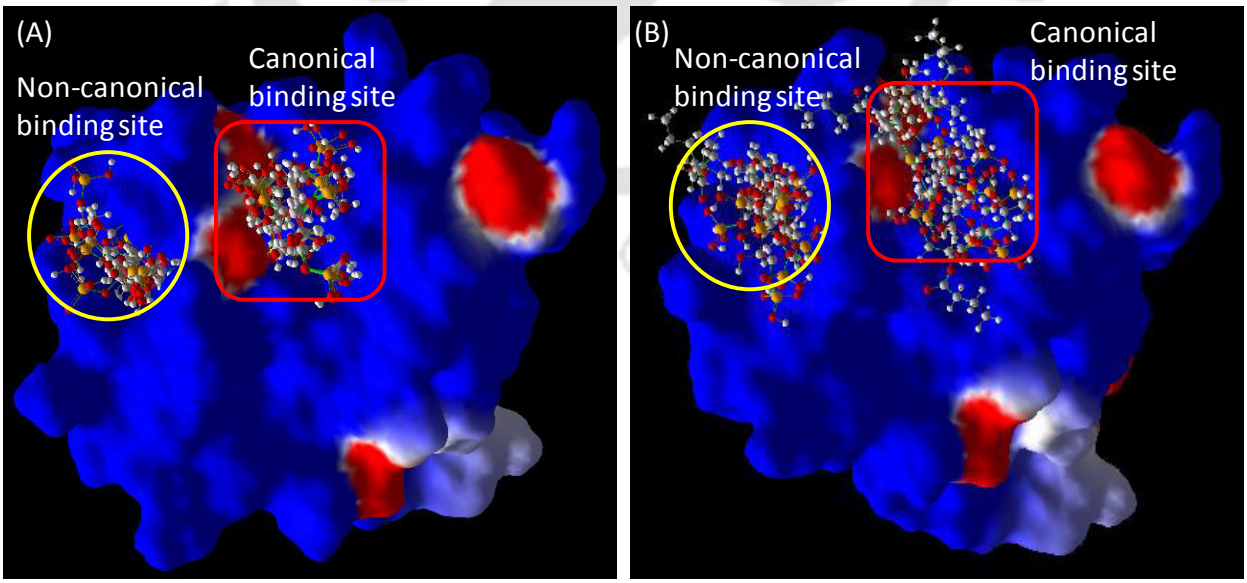

Figure 3.2.4. Model structure of ligand-bound Lpd-PH domain based on the crystal structure of mouse LPD-RAPH domain (4GN1). Surface representations of model structures of Lpd-PH domain docked with Ins(1,3,4)P_3 and PI(3,4)P_2 ligands. The modeled structures were generated using Molegro Virtual Docker, version 4.3.0.

separately showed 2.3-7 fold lower binding affinities for PI(3,4)P_2 lipid than WT-PH domain of Lpd protein. Whereas, double mutants K29/W31A and K32/R34A showed 2- and 24-fold

Table 2.3.3: Apparent inhibitory constants [$K_I(IP_6)_{app}$] for Lpd-PH domain and mutants binding to PC/PE/PS/PI(3,4)P_2 (57:20:20:3) liposomes were determined from protein-to-membrane FRET analysis[a]

Protein	$K_I(IP_6)_{app}$ (μM)	Fold change
PH (WT)	460 ± 32	1
PH-K24A	307 ± 20	1.5
PH-K29A/W31A	242 ± 31	1.7
PH-K79A	157 ± 23	2.9
PH-K96A	183 ± 12	2.5
PH-K28A	120 ± 27	3.8
PH-K32A/R34A	71 ± 12	5.7
PH-L23R/D25G	539 ± 39	-
PH-L23R/D25G/K29A	312 ± 25	-

[a]All measurements were performed in 20 mM Tris buffer at pH 7.4 containing 160 mM NaCl. IP_6 was used as inhibitor of membrane-to-protein interactions. Protein, 1 μM. Values represent the mean ± SD from triplicate measurements.

Table 2.3.4. Membrane binding affinity (K_{d2}) measurements by kinetic SPR analyses.

Protein	k_a ($M^{-1}S^{-1}$)	k_d (S^{-1})	K_{d2} (M)	Fold change
PH (WT)	4.30×10^4	1.62×10^{-4}	3.80×10^{-9}	1
PH-K24A	1.85×10^4	1.62×10^{-4}	8.76×10^{-9}	2.3
PH-K29A/W31A	1.17×10^4	4.13×10^{-4}	3.53×10^{-8}	8.7
PH-K79A	2.27×10^4	6.11×10^{-4}	2.69×10^{-8}	7
PH-K96A	3.58×10^4	4.84×10^{-5}	1.35×10^{-9}	2.8
PH-K28A	4.30×10^4	7.30×10^{-4}	1.70×10^{-8}	4.5
PH-K32A/R34A	4.70×10^3	4.40×10^{-4}	9.30×10^{-8}	24.5
PH-L23R/D25G	1.15×10^4	2.17 × 10-5	1.89×10^{-9}	-
PH-L23R/D25G/K29A	2.03×10^4	2.14×10^{-4}	1.06×10^{-8}	-

[a]All measurements were performed in 20 mM HEPES buffer at pH 7.4 containing 160 mM KCl. Values represent the mean ± SD from triplicate measurements.

lower binding affinities for PI(3,4)P_2 lipid, respectively that WT-PH domain. Similarly FRET-analyses also showed that double mutants K29/W31A and K32/R34A have 1.7- and 5.7-fold lower binding affinities for PI(3,4)P_2 lipid, respectively, than WT-PH domain. Other

mutants show moderately reduced affinity for PC/PE/PS/PI(3,4)P_2 liposomes. Collectively, these mutational data indicate that both K32 and R34 residues strongly interact with the headgroup of PI(3,4)P_2 lipid and cationic Lys28, Lys32 and Arg34 constitute the PIP-binding site of the Lpd-PH domain.

Membrane Penetration of Lpd-PH Domain- PIP-dependent membrane interactions of the FYVE, PH, PX, and ENTH-domains are associated with frequent membrane penetration due to adjustment in electrostatic surface potential and/or local conformational changes of the proteins. However, most of the reported PH domains have no significant membrane penetration ability. To date, only the PLCδ1, Tapp1 and Dapp1-PH domains have been

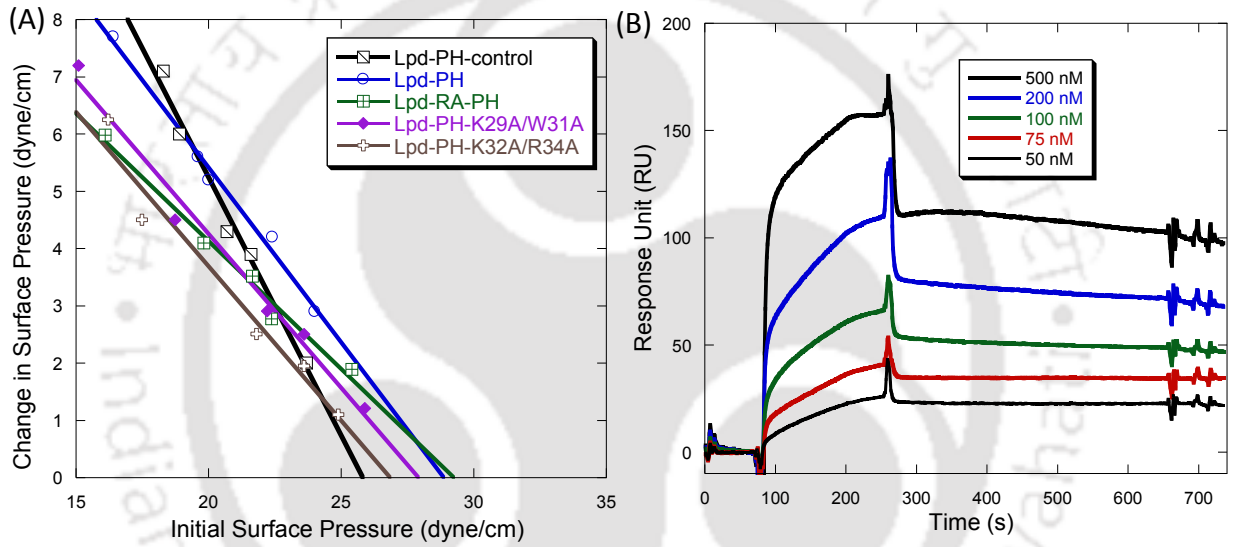

Figure 3.2.5. Interaction of WT-Lpd-PH domain with PC/PE/PS (60:20:20), PC/PE/PS/PI(3,4)P_2 (57:20:20:3) containing monolayer were measured by Langmuir trough technique (A). Kinetic SPR sensorgrams for WT-Lpd-PH interacting with PC/PE/PS/PI(3,4)P_2 (57:20:20:3) liposome (B). All measurements were carried out in 20 mM HEPES buffer at pH 7.4 containing 160 mM KCl at at 25 °C temperature.

reported to have a significant membrane penetrating activity.[23-25] Cellular studies reported that PIP-binding of the PH domain and protein binding of the RA at the plasma membrane plays a significant role in Lpd-dependent upstream cell signalling and cytoskeleton remodeling. However, it is unclear whether PIP-dependent membrane binding of the PH or RA-PH domains of Lpd protein is supported by membrane bilayer penetration. Therefore, to understand the membrane penetration ability of Lpd-PH domain, we measured the surface pressure of the above wild type Lpd-PH and Lpd-RA-PH domains into the lipid monolayers. Protein was injected at the sub-phase and the change of surface pressure ($\Delta\pi$) was monitored against a given initial surface pressure (π_0). In general, $\Delta\pi$ is inversely proportional to π_0 of

the phospholipid monolayer, and an extrapolation of $\Delta\pi$ *vs* π_0 yields π_c, which specifies an upper limit of π_0 that a protein can penetrate. The surface pressure of cell membranes and large unilamellar vesicles has been estimated to be 31–35 dynes/cm to be able to penetrate into the cellular membranes. Thus, for a protein to effectively penetrate a particular cell membrane (or large vesicles), it should have the π_c value above this range for the monolayer whose lipid composition mimics that of the cell membrane. Figure 3.2.5A shows that the π_c values of the Lpd-PH domain for PC/PE/PS (60:20:20 in mol %) and PC/PE/PS/PI(3,4)P_2 (57:20:20:3 in mol%) lipid monolayers are 26–27 and 29-30 dynes/cm, respectively. This π_c value indicates that Lpd-PH domain weakly penetrates into the lipid monolayer and this penetration ability could not be sufficient enough to penetrate into densely packed lipid bilayers or cell membranes. The inability of Lpd-PH domain to penetrate cell membrane is further supported by the kinetic SPR analysis (Figure 3.2.5B). The kinetic SPR analyses indicates that the interaction of Lpd-PH domain with PI(3,4)P_2 containing liposome follows a two step dissociation phases with certain conformational changes or other complex dissociation pathways.

Cellular Translocation of the Isolated PH Domain and Mutants- To explore the significance of PIP-dependent membrane binding properties of the PH domain and mutants under cellular environment, we monitored PDGF-mediated translocations of GFP-fused LPD-full length, LPD-RAPH, LPD-PH and mutants in A549 cells. PDGF is reported to produce PI(3,4)P_2 and PI(3,4,5)P_3 transiently at the plasma membrane. The cells expressing similar levels of GFP-fused PH domain/mutants were selected by visual inspections and used for PDGF-dependent translocation measurements. Serum-starvation was carried out to reduce the pre-localization of PH domain or mutants at the plasma membrane. Then the serum-starved cells were treated with 50 ng/mL of PDGF-BB and the confocal images of the fixed cells were collected (Figure 3.2.6). In general >70% of cell population showed similar behaviours with respect to membrane translocation of PH domains. Cellular images showed that a significant fraction of LPD-full length protein or LPD-RAPH and LPD-PH domain proteins translocated to the plasma membrane in a PDGF-dependent manner in A549 cells (Figure 3.2.6).

To further explore the significance between *in vitro* membrane binding properties of LPD-PH domain and their cellular membrane translocation, we measured the cellular localization pattern of the mutants after PDGF stimulation (Figure 3.2.6). Interestingly, the membrane translocation property of the PH-K32A/R34A mutant was almost abolished under

the similar experimental conditions. However, the membrane translocation efficiencies of the other mutants are not that significant. Although, K29A/W31A, K79A and K28A mutants showed 3 to 7-fold differences in PI(3,4)P_2 binding affinities under liposomal environment, but cellular translocation patterns are not that significantly different under cellular environment. This also suggest that the PI(3,4)P_2-lipid preferentially interact with the Lpd-PH domain through its canonical binding site. Overall plasma membrane translocation behaviours of the PH domain and mutants are in good agreement with our *in vitro* binding parameters.

A. EGFP-Lpd-Full length before PDGF treatment

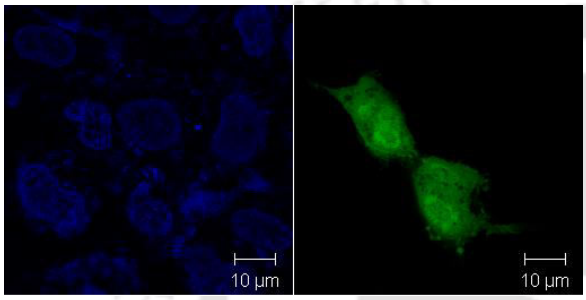

B. EGFP-Lpd-Full length after PDGF treatment (5 min)

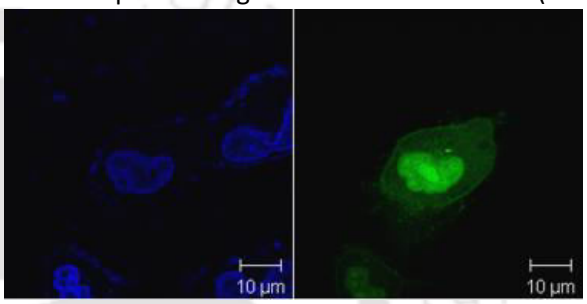

C. EGFP-Lpd-RAPH before PDGF treatment

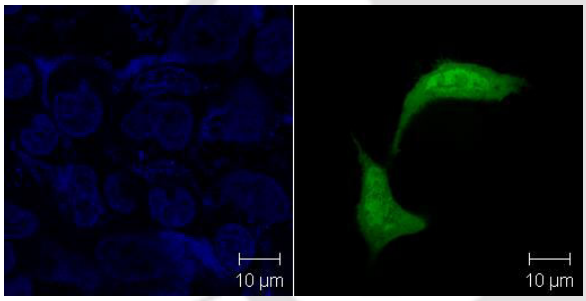

D. EGFP-Lpd-RAPH after PDGF treatment (5 min)

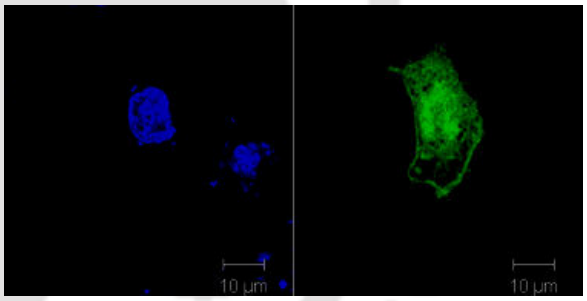

E. EGFP-Lpd-PH before PDGF treatment

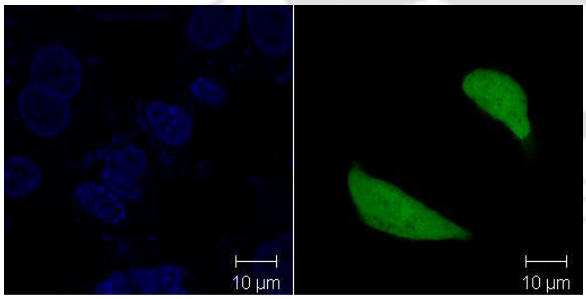

F. EGFP-Lpd-PH after PDGF treatment (5 min)

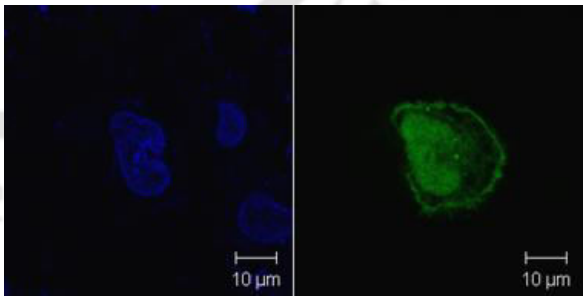

G. EGFP-Lpd-PH –K24A before PDGF treatment

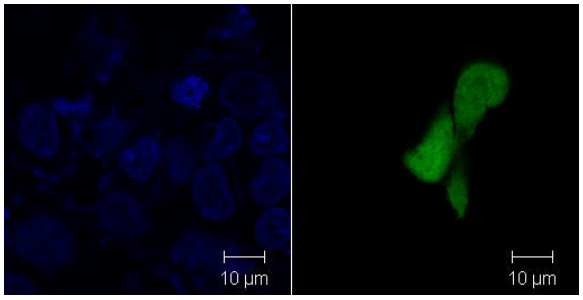

H. EGFP-Lpd-PH-K24A after PDGF treatment (5 min)

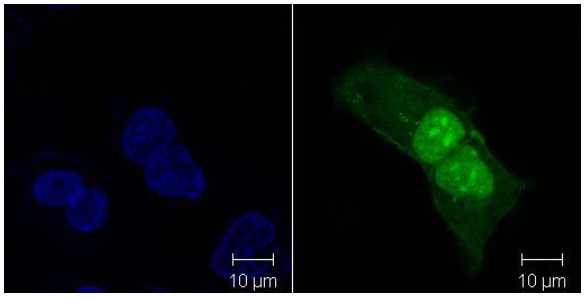

I. EGFP-Lpd-PH –K29A/W31A before PDGF treatment

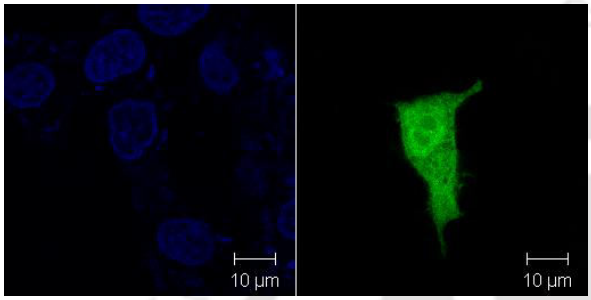

J. EGFP-Lpd-PH-K29A/W31A after PDGF treatment (5 min)

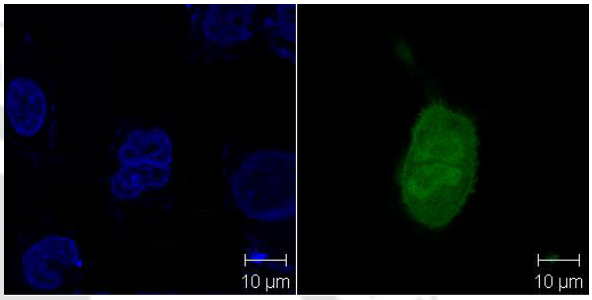

K. EGFP-Lpd-PH –K79A before PDGF treatment

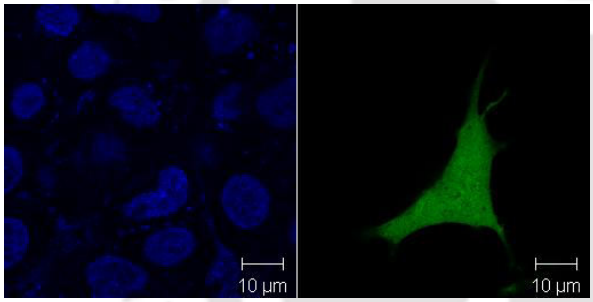

L. EGFP-Lpd-PH-K79A after PDGF treatment (5 min)

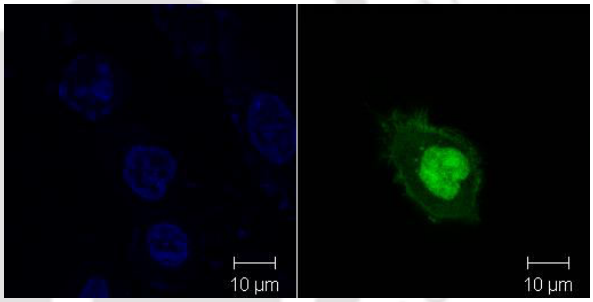

M. EGFP-Lpd-PH –K28A before PDGF treatment

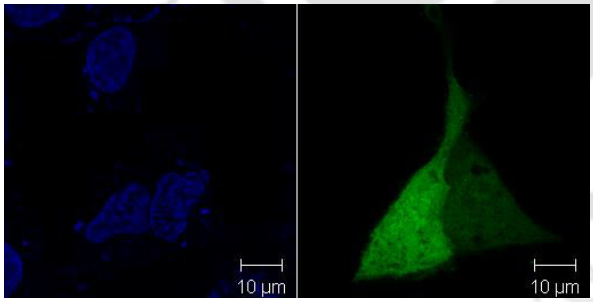

N. EGFP-Lpd-PH-K28A after PDGF treatment (5 min)

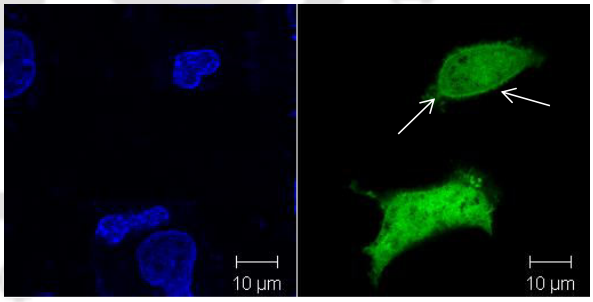

O. EGFP-Lpd-PH –K32A/R34A before PDGF treatment

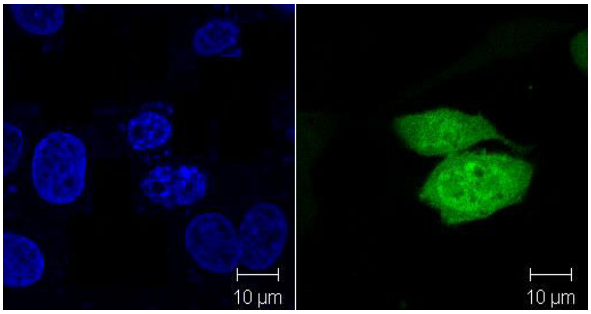

P. EGFP-Lpd-PH-K32A/R34A after PDGF treatment (5 min)

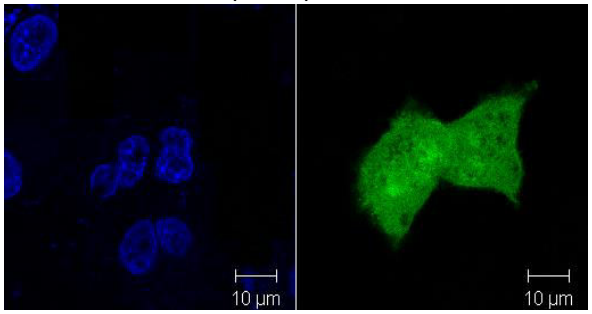

Figure 3.2.6. Translocation measurements of GFP-fused Lpd-PH domain and mutants in response to PDGF treatment. Translocation of GFP-fused Lpd-full length, Lpd-RAPH and Lpd-PH domain and mutants individually transfected into A549 cells were measured before (A, C, E, G, I , K, M and O) and 5 min after (B, D, F, H, J, L, N and P) the PDGF-BB treatments (50 ng/mL).

Discussion- It is well documented that PIPs divergently mediate signalling pathways in a spatially and temporarily specific manner. Several reports described that most of the PIPs specifically recruits a number of effectors proteins to respective cellular membranes and play crucial role in several cellular functions. But there are insufficient studies to understand the binding nature of signalling molecules that are specifically recruited by PIPs under specific conditions. The present study describes the *in vitro* PIP-binding affinity and specificity of Lpd-PH domain and determines its significance under cellular environment. It also demonstrates the PIP-dependent membrane binding mechanism of the isolated PH domain. Our initial measurements of protein-to-membrane FRET-based competitive binding assay showed that Lpd-PH domain strongly interact with the $PI(3,4)P_2$ containing membrane. However, this PH showed only 2.7 and 5-fold weaker affinities for $PI(3,4,5)P_3$ and $PI(4,5)P_2$ lipids containing membranes, respectively. Using SPR analyses, we also found that Lpd-PH domain has significantly stronger affinity for $PI(3,4)P_2$ containing liposomes. Both equilibrium- and kinetic-SPR analyses showed that $PI(3,4)P_2$ binding affinities are 3 to 5-fold stronger than $PI(3,4,5)P_3$ and $PI(4,5)P_2$ lipids under the similar experimental conditions. This binding preference for $PI(3,4)P_2$ lipid could be due to the proper fitting of the headgroup into the cationic groove with preferential interactions for D3- and D4-phosphate groups of the myo-inositol ring. In order to understand the significance of this invitro $PI(3,4)P_2$ lipid binding preference, we performed cellular translocation studies of the GFP-fused Lpd-full length, Lpd-RA-PH and Lpd-PH domain proteins in A549 cells in the absence and presence of PDGF. Confocal measurements clearly showed that GFP-fused Lpd-PH domain predominantly translocated to the plasma membrane of the A549 cells upon stimulation with PDGF. PDGF is known to transiently produce $PI(3,4)P_2$/$PI(3,4,5)P_3$ at the plasma membrane. This supports our binding parameters measured by both FRET and SPR analyses.

For further understanding of the $PI(3,4)P_2$ binding mechanism of the Lpd-PH domain mutational analysis of the cationic residues were performed. Homology sequence alignment and the reported crystal structure (PDB code: 4GN1) identified that K24, K28,

K29, K32, R34, K79, and K96 cationic residues could be the probable PIP-binding residues of Lpd-PH domain. However, further detailed analysis of Lpd-PH domain crystal structure revealed that K28, K32 and K34 forms a canonical PIP-binding site of the PH domain, whereas K24, K29, K79 and K96 residues constitute a non-canonical PIP-binding site for the Lpd-PH domain like that of β–spectrin protein.[26] Our molecular docking analyses with short chain (n = 4) PI(3,4)P_2 and Ins(1,3,4)P_3 showed that the PH domain can interact with both the cationic grooves. Mutational studies of the cationic residues showed their significant role in PIP-dependent membrane interactions. Kinetics-SPR based binding affinity calculation showed that K32A/R34A mutation showed over 25-fold binding affinity difference where as K28A mutation showed ~5-fold binding affinity difference with the WT-Lpd-PH domain for PI(3,4)P_2 lipid binding. Whereas other mutants showed only 2-7-fold binding affinity difference for PI(3,4)P_2 lipids. This clearly suggests that K32/R34 preferentially interact with the headgroup of PI(3,4)P_2 lipid. Based on our molecular docking results we presume that D3-phosphate and D4-phosphate preferentially interacts with K32 and R34 whereas K28 could be responsible for its interaction with D1-phosphate of the PI(3,4)P_2 lipid. Membrane translocation studies with the mutants showed that the double mutant K32A/R34A predominantly localize at the cytoplasm in the PDGF stimulated A549 cells. The other mutants showed partial membrane localization under the similar experimental conditions.

Another significant observation from our PIP-dependent membrane binding studies is the partial membrane penetration of the Lpd-PH domain in a PI(3,4)P_2-dependent manner. Although our monolayer penetration measurements shows that the monolayer penetration ability of the Lpd-PH domain get enhanced in the presence of PI(3,4)P_2 lipid, but the extent of penetration might not be significant enough to penetrate biological membranes. It is reported that only few PH domain like DAPP1-PH domain could penetrate into the biological membrane significantly.[25] Therefore, membrane interaction of Lpd-PH domain takes place primarily due to specific interactions with the headgroup of PI(3,4)P_2 lipid.

It is important to mention that there is some considerable discrepancy between our *in vitro* PIP-binding affinity data and reported data. Recently, Professor Jinhua Wu and coworkers determined the PIP-binding specificity and affinity of Lpd-cc-RA-PH domain using fluorescent polarization (FP) assay and found no specificity. But our biophysical studies suggest that isolated Lpd-PH domain strongly interacts with PI(3,4)P_2 lipid which is in accordance with previously reported PIP-binding speficity measured by protein-lipid overlay assay. Professor Frank B. Gertler and coworkers also showed that Lpd-PH domain

localize at the ruffles in PDGF-stimulated Rat2 fibroblasts. Very often this kind of discrepancy arises due to the binding parameters measured using different experimental design (e.g fluorometric, lipid dot blot, vesicle-pelleting, SPR and others) and conditions. Therefore, it is difficult to directly compare with reported affinities data. Our quantitative measurements of binding affinities and cellular localization studies are well correlated and were measured thoroughly and systematically. Our *in vitro* binding studies showed that Lpd-PH domain preferentially interact with the $PI(3,4)P_2$ lipid, over other PI3-kinase products like $PI(3,4,5)P_3$ and PI(3)P lipids. However, both FRET and SPR analyses showed that $PI(3,4)P_2$ had only ~3-fold stronger binding preference over $PI(3,4,5)P_3$ lipid. PDGF is also reported to produce both $(3,4)P_2$ and $PI(3,4,5)P_3$ lipid at the plasma membrane. Therefore, in addition to $PI(3,4)P_2$, $PI(3,4,5)P_3$ can also assist in membrane translocation of Lpd protein under different cellular conditions.

Conclusion: Taken together all results in the present study establishes that Lpd-PH domain strongly interacts with $PI(3,4)P_2$ lipid containing membrane without membrane penetration and is sufficient for membrane localization. *In vitro* binding studies systematically determined the PIP-specificity of the PH domain for $PI(3,4)P_2$ over other lipids. Mutational based PIP-binding affinity and specificity measurements demonstrate detail membrane docking properties of Lpd-PH domain. Our in vitro binding measurements are in good correlation with the cellular localization of the isolated Lpd-PH domain. This indicates that the kinetics of PI-mediated cellular membrane recruitment of this PH domain is governed, to a large extent, by their membrane binding properties. This would also help in account for different cellular functions and regulation of this protein. Furthermore, our results should form the foundation of systematic and quantitative assessment of different cellular membrane translocation properties of a large number of PH domains and their host proteins.

3.3. Experimental procedure-

Materials- As described in chapter 2, section 2.3.

Vector Construction and Mutagenesis- For bacterial expression, the cDNA of Lpd-PH , Lpd-RA-PH, Lpd-PH domain mutants, D25G/ L23R, D25G/L23R/K29A, K29A/ W31A, K79A, K24A, K32A/ R34A. K96A were subcloned into the vector pGEX-6P-1 between the *EcoRI* and *BamHI* restriction sites with N-terminal glutathione S-transferase (GST) fusion. The cDNA of full length Lpd-PH-GFP and Lpd-RAPH-GFP were the kind gift from Dr. Matthias Krause (King's College London). Lpd-PH domain mutants were generated by the

overlap extension PCR using forward and reverse primers (appendix Table A5)and subcloned into pEGFP-N1 vector between the *KpnI* and *XhoI* restriction sites with N-terminus enhanced green fluorescence protein (EGFP). All constructs were transformed into DH5α cells for plasmid isolation. All plasmid DNA sequences were verified. All GST constructs were transformed into E. coli BL21(DE3) cells for protein expression.

Protein expression and purification- As described in chapter 2, section 2.3.

FRET measurements- As described in chapter 2, section 2.3.

SPR measurements- As described in chapter 2, section 2.3.

Monolayer penetration measurement- As described in chapter 2, section 2.3.

Cellular translocation measurements- As described in chapter 2, section 2.3.

Molecular docking analysis- Molecular docking was performed using the model structure of LPD-PH domain using Modeller 9v7. The model structure was generated using the crystal structure of LPD-RAPH domain (Protein Data Bank code: 4GN1). The energy minimized three-dimensional structure of ligands was prepared by using the GlycoBioChem PRODRG2 Server (http://davapc1.bioch.dundee.ac.uk/prodrg/). The GROningen MAchine for Chemical Simulations (GROMACS) library of three-atom combination geometries employing a combination of short molecular dynamics simulations and energy minimizations was utilized for the conversion of 2D molecular structures to 3D structures. Ligand-protein docking was performed with using the Molegro Virtual Docker software, version 4.3.0 (Molegro ApS, Aarhus, Denmark). The binding site was automatically detected by the docking software and restricted within spheres with radius of 15 Å. During virtual screening, the following parameters were fixed: number of runs 10, population size 50, crossover rate 0.9, scaling factor 0.5, maximum iteration 2,000 and grid resolution 0.30. The docked results were evaluated on the basis of moledock and re-rank score. The poses were exported and examined with *PyMOL* software.

References:

1. M. Krause, E.W. Dent, J.E. Bear, J.J. Loureiro and F.B. Gertler, *Annu Rev Cell Dev*, 2003, **19**, 541-564.
2. G.P. Colo, E.M. Lafuente and J. Teixido, *Eur J Cell Biol*, 2012, **91**, 861-868.
3. E.M. Lafuente, A.A. Van Puijenbroek, M. Krause, C.V. Carman, G.J. Freeman, A. Berezovskaya, E. Constantine, T.A. Springer, F.B. Gertler and V.A. Boussiotis, *Dev Cell*, 2004, **7**, 585-595.
4. J.P. Wynne, J. Wu, W. Su, A. Mor, N. Patsoukis, V.A. Boussiotis, S.R. Hubbard and M.R. Philips, *J Cell Biol*, 2012, **199**, 317-330.
5. Y.C. Chang, H. Zhang, M.L. Brennan and J. Wu, *Protein Cell*, 2013, **4**, 211-219.
6. R.S. Depetris, J. Wu and S.R. Hubbard, *Nat Struct Mol Biol*, **16**, 833-839.
7. P. Rodriguez-Viciana, C. Sabatier and F. McCormick, *Mol Cell Biol*, 2004, **24**, 4943-4954.
8. M. Krause, J.D. Leslie, M. Stewart, E.M. Lafuente, F. Valderrama, R. Jagannathan, G.A. Strasser, D.A. Rubinson, H. Liu, M. Way, M.B. Yaffe, V.A. Boussiotis and F.B. Gertler, *Dev Cell*, 2004, **7**, 571-583.
9. J.E Bear, T.M. Svitkina, M. Krause, D.A. Schafer, J.J Loureiro, G.A Strasser, I.V. Maly, O.Y. Chaga, J.A. Cooper, G.G. Borisy and F.B. Gertler, *Cell*, 2002, **109**, 509-521
10. S. Dowler, R.A. Currie, D.G. Camppbell, M. Deak, G. Kular, C.P. Downes and D.R. Alessi, *Biochem J*, 2000, **351**, 19-31.
11. S. Gruenheid and B.B Finlay, *Nature*, 2003, **422**, 775-781.
12. J.M. Kavran, D.E. Klein, A. Lee, M. Falasca, S.J. Isakoff, E.Y. Skolnik and M.A. Lemon, *J Biol Chem*, 1998, **273**, 30497-30508.
13. W.A. Kimber, L. Trinkle-Mulcahy, P.C. Cheung, M. Deak, L.J. Marsden, A. Kieloch, S. Watt, R.T. Javier, A. Gray, C.P. Downes, J.M. Lucocq and D.R. Alessi, *Biochem J*, 2002, **361**, 525-536.

14. J.J. Lourereiro, D.A. Rubinson, J.E. Bear, G.A. Baltus, A.V. Kwiatkwski and F.B. Gertler, *Mol Biol Cell*, 2002, **13**, 2533-2546.
15. K. Niebuhr, F. Ebel, R. Frank, M. Reinhard, E. Domann, U.D. Carl, U. Walter, F.B. Gertler, J. Wehland and T. Chakraborty, *EMBO J*, 1997, **16**, 5433-5444.
16. K. Rottner, B. Behrendt, J.V. Small and J. Wehland, *Nat Cell Biol*, 1999, **1**, 321-322.
17. F.B. Gertler, K. Niebuhr, M. Reinhard, J. Wehland and P. Soriano, *Cell*, 1996, **87**, 227-239.
18. B. Drees, E. Friederich, J. Fradelizi, D. Louvard, M.C. Beckerle and R.M. Golsteyn, *J Biol Chem*, 2000, **275**, 22503-22511.
19. F. Frischknecht and M. Way, *Trends Cell Biol*, 2001, **11**, 30-38.
20. H. Li, L.M. Schopfer, P. Masson amd O. Lockridge, *Biochem J*, 2008, **411**, 425-432.
21. L.E. Rameh and L.C. Cantley, *J Biol Chem*, 1999, **274**, 8347-8350.
22. G.D. Paolo and P.D. Camilli, *Nature*, 2006, **443**, 651-657.
23. S. Tuzi, N. Uekama, M. Okada, S. Yamaguchi, H. Saito and H. Yagisawa, *J Biol Chem*, 2003, **278**, 28019-28025.
24. F.M. Flesch, J.W. Yu, M.A. Lemmon K.N. Burger, *Biochem J*, 2005, **389**, 435-441.
25. D. Manna, A. Albanese, W.S. Park and W Cho, *J Biol Chem*, 2008, **282**, 32093-32105.
26. M. Hyvonen, M.J. Macias, M. Nilges, H. Oschkimat, M. Saraste, M. Wilmanns, *EMBO J*, 1995, **14**, 4676-4685.

Chapter 4

Inhibition of Phosphatidylinositol-3,4,5-trisphosphate Binding to AKT Pleckstrin Homology Domain by 4-Amino-1,2,5-oxadiazole Derivatives

In this study, we describe the development of 4-Amino-1,2,5-oxadiazole-based antagonists, **GPIs** for PI(3,4,5)P_3-PH-domain binding. We determined their inhibitory effect by using competitive-surface plasmon resonance (SPR) analysis (IC_{50} ranges from 1.85 to 16.35 µM for PI(3,4,5)P_3/AKT1 PH-domain binding assay). Our studies also demonstrate that the potent compounds do not show significant cytotoxicity and induce reduction of phosphorylated AKT expression level in MDA-MB-231 cancer cell lines.

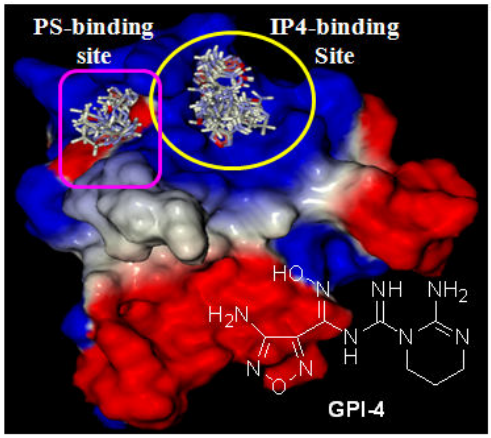

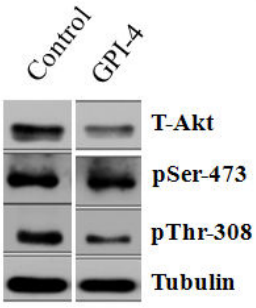

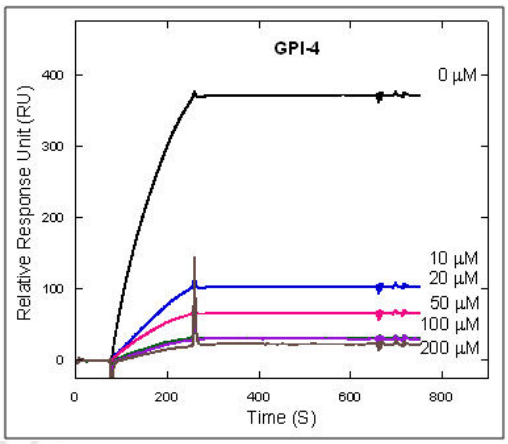

4.1 Background and Focus of the Present Work

The phosphatidylinositol-3-kinases (PI3K) dependent cell signalling pathway is directly linked with several human diseases. Upregulation of PI3K-pathway plays an important role in carcinogenesis, whereas down-regulation is linked with type-II diabetes. In this regard, PI3K-signalling pathway is considered as potential therapeutic target for the treatment of these diseases.[1-4] In responses to growth factor and hormone stimulation the PI3K enzyme phosphorylate phosphtidylinositol-4,5-bisphosphate ($PI(4,5)P_2$) to generate phosphtidylinositol-3,4,5-trisphosphate ($PI(3,4,5)P_3$) at the plasma membrane. The $PI(3,4,5)P_3$ generation recruits several proteins to the plasma membrane through their interaction with lipid-binding modules. The $PI(3,4,5)P_3$ signalling is terminated due to the dephosphorylation of $PI(3,4,5)P_3$ by the phosphatase and tensin homolog (PTEN) protein. $PI(3,4,5)P_3$-dependent membrane association of the lipid binding modules are necessary and sufficient for activation and proper functioning of the effector proteins, including AKT. These $PI(3,4,5)P_3$ binding proteins are generally cytosolic in unstimulated cells and recruited to the cellular membranes through PIP-binding module mediated binding to newly generated $PI(3,4,5)P_3$ lipid.[2-6]

To date there are a number of PIP-binding modules, including phox homology (PX), pleckstrin homology (PH) domain and others that have been reported as binding partners of $PI(3,4,5)P_3$.[7, 8] PH-domains are one of the systematically characterized PIP-binding modules and exhibit a broad range of binding specificities. Interestingly, majority of the PH-domains of the effector proteins bind to the membrane containing $PI(3,4,5)P_3$, $PI(3,4)P_2$ and $PI(4,5)P_2$ lipids with high affinity. $PI(3,4,5)P_3$ selectively regulates several PH-domain containing proteins including AKT, GRP and BTK that mediate a wide verity of cellular process.[9, 10] In particular, the AKT protein plays an important role in cell proliferation, survival, metabolism and others. Activation of AKT is achieved through $PI(3,4,5)P_3$-binding to its PH domain followed by PDK dependent phosphorylation at the membrane. Intramolecular interaction between lipid binding domain and kinase domain is also important in maintaining cellular level of the effector protein in its inactive state. For an example, AKT activation proceeds after PIP-binding at the inner plasma membrane that dislodges the PH-domain from kinase domain.[11-13]

In general direct inhibition/activation of enzyme through its catalytic domain is considered as potential approach for drug development. However, the activities of the enzymes should be systematically regulated in the cells, since direct activation/inhibition could also incite side-effects by perturbing the other up/down-stream pathways.[14, 15] As

an example the development of AKT kinase inhibitors (for catalytic domain) to target and treat cancers are effective but experience selectivity problems resulting in an unwanted side effects, including myelosuppression, skin rash and stomatitis and others.[15, 16] In the mean time mechanistic studies described that highly specific PIP/PH-domain interactions can regulate activities of the effector proteins.[2, 14, 15, 7] It is also described that small molecules can alter the protein-lipid interactions, because of the presence of well defined binding pocket of most of the lipid binding modules of the effector proteins. It is also reported that small molecule inhibitors for protein-lipid interactions are advantageous over usual approaches due to lower side-effects and rational design with comparatively simple structures and functions. In this regard, selective PH domains with true lipid specificity regarded as an alternate approach in designing selective inhibitors for enzymes.[2, 15, 18-20]

Regulations of enzyme activities by inhibiting the PIP/PH domain interactions have not been considerably described yet. We have recently demonstrated that development of regulators for diacylglycerol/C1-domain interactions can be considered as an alternative target to regulate the activities of the PKC enzymes.[21-23] PH-domain targeting lipid-based drug, 3-deoxy phosphatidylinositol ether lipid (DPIEL) and PHT-427 showed usefulness for the treatment of cancer.[16-19] PITENINs inhibit the PI(3,4,5)P_3 binding of AKT1/PDK1-PH-domains and down-regulate PI3K-PDK1-AKT1 pathways. PITENINs also inhibit the membrane localization and PI(3,4,5)P_3 binding of the ARNO/GRP1 PH-domain due to its inhibition of ARF6 activation, an important mediator of cytoskeleton and cell motility. The PITENINs also suppressed tumour growth in a mouse cancer model.[2, 24] Therefore, inhibition of PIP/PH domain interactions is considered as a potential approach to regulate the target protein activates.

Design of Oxadiazole Based Small Molecule Inhibitors- In this study, we describe the development of 4-Amino-1,2,5-oxadiazole-based antagonists, **GPI**s for PI(3,4,5)P_3-PH-domain binding. 1,2,5-Oxadiazole substituents have been used as a building block for several biologically active small molecules for the treatment of cancer, arthritis and others disorders. The **GPI**s are water soluble non-lipid compounds with polyamine functionalities. Our studies demonstrate that **GPI**s strongly interact with PH-domain and inhibit the PI(3,4,5)P_3-protein binding under liposomal environment. These compounds at lower concentrations showed certain degree of selective inhibitory effect towards different PH-domains used for the current study. The hydroxyl group and oxadiazole moiety of the compounds play a crucial role in

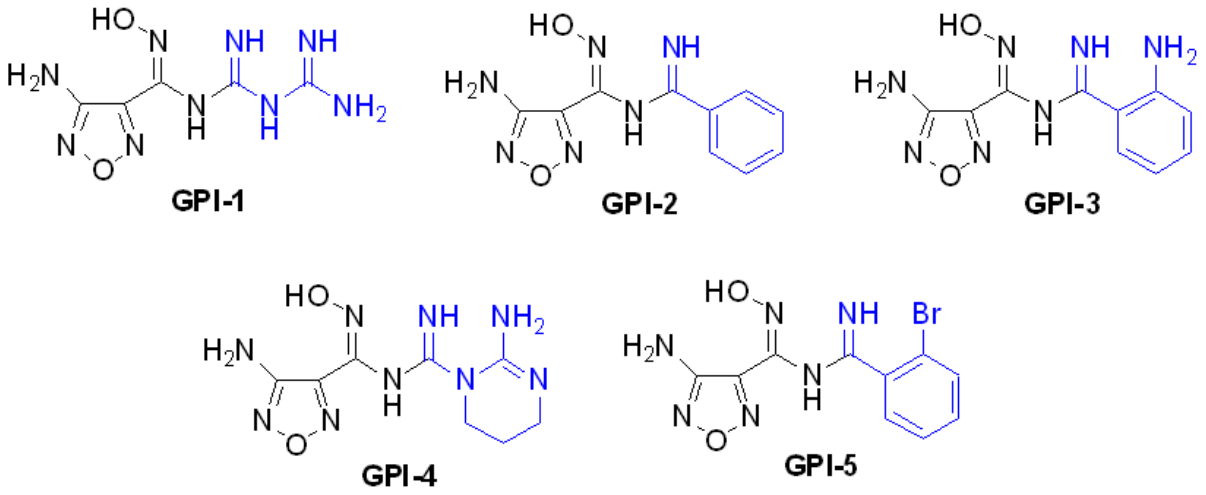

Figure 4.1.1: Structures of the compounds (**GPI**s) used in the present study.

distinguishing the PH-domains. Our studies also demonstrate that the potent compounds do not show significant cytotoxicity and induce reduction of phosphorylated AKT expression level in MDA-MB-231 cancer cell lines. Therefore, we developed a new class of nonlipid antagonist for PI(3,4,5)P_3/AKT-PH domain interactions. These results give us strong encouragement for this PH-domain directed drug discovery strategy.

4.2 Results and Discussion

surface plasmon resonance (SPR)-based competitive binding assay — To screen the efficiency of the synthesized compounds (Figure 4.1.1) in inhibiting the PI(3,4,5)P_3/PH-domain interaction, we used surface plasmon resonance (SPR)-based competitive binding assay, an practical method for quantitative measurement of binding or inhibition parameters.[4, 15, 25, 26] SPR measurements were carried out using parallel two-flow-channel systems and proteins were passed over control channel to active channels (at a rate of 30 μL/min) coated with PC/PE/PS (60:20:20) and PC/PE/PS/PIP (57:20:20:3) liposome, respectively. Control experiments were performed to remove the effect of non-specific binding of proteins on the sensor surface and effect of only compound binding on the liposome surface. PI(3,4,5)P_3 selectivity of the PH domains were tested using these experimental conditions. The efficacy of the compounds in inhibiting PI(3,4,5)P_3/AKT1-PH domain interactions was first determined by calculating their percent of inhibition. The compounds **GPI-1** and **GPI-4** with 50 μM concentration showed 95% and 92% inhibitory effect, respectively. The results suggest that compounds **GPI-1** and **GPI-4** strongly inhibit

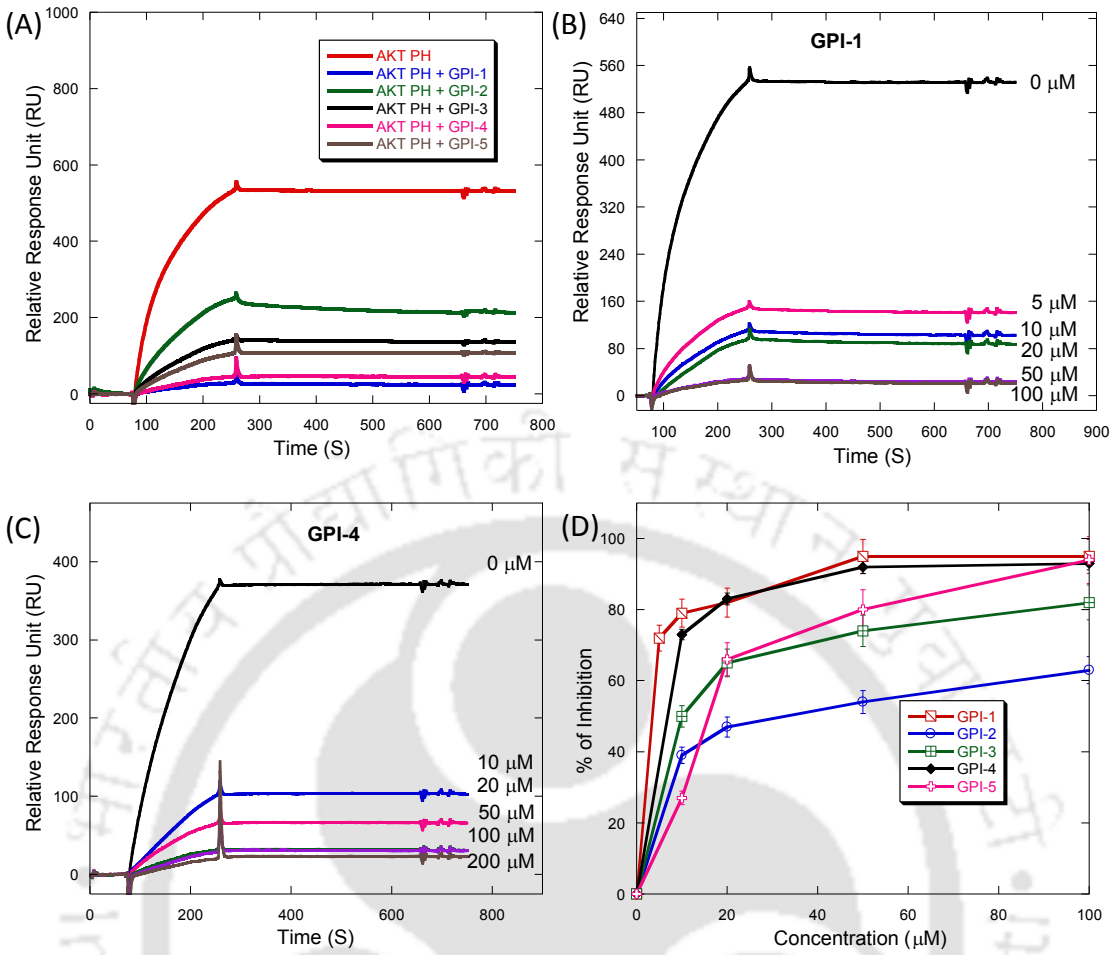

Figure 4.2.1. Screening of PI(3,4,5)P_3/AKT1-PH domain (500 nM) interaction selectivity by compounds (50 μM) (A). Surface plasmon resonance sensorgrams of PI(3,4,5)P_3 binding AKT1-PH domain in the presence of increasing concentration of compounds **GPI-1** (B) and **GPI-4** (C). Selectivity analysis (% of inhibition) of the compounds for PI(3,4,5)P_3/AKT1-PH domain inhibition (D). PC/PE/PS/PI(3,4,5)P_3 (57:20:20:3) and PC/PE/PS (60:20:20) vesicles were used as active and the control surface, respectively. Values represent the mean ± SD from triplicate measurements

the interaction of AKT1 PH-domain with the PI(3,4,5)P_3 containing liposome (Table 4.2.1 and Figure 4.2.1). Whereas, other compounds show moderate competitive inhibitory effect for PI(3,4,5)P_3/AKT1 PH-domain interaction (Figure 4.2.2). For better understanding of their inhibition efficacies, the SPR-based competitive binding analyses were also performed in a concentration (0-200 μM) dependent manner (Figure 4.2.1). Relative response unit (RU) of the sensorgrams for AKT1 PH-domain decreases in the presence of increasing concentration of the compounds. Calculated IC_{50} values of **GPI**-1 (1.85 μM) and **GPI**-4 (3.23 μM) suggested strong interaction phenomenon of the compounds with AKT1 PH-domain.

Table 4.2.1. Relative Inhibitory Activity of the Compounds Measured by Competitive-Surface Plasmon Resonance Analysis

Compound	Relative inhibitory activity (%)			IC_{50} values (μM)		
	AKT1-PH	GRP1-PH	BTK-PH	AKT1-PH	GRP1-PH	BTK-PH
GPI-1	95 ± 3	56 ± 3	40 ± 3	1.85 ± 0.12	24.92 ± 1.02	10.91 ± 0.89
GPI-2	54 ± 2	55 ± 3	-	7.19 ± 0.26	11.51 ± 0.69	-
GPI-3	74 ± 3	59 ± 5	79 ± 5	8.61 ± 0.21	16.63 ± 0.58	3.18 ± 0.29
GPI-4	92 ± 4	67 ± 3	11 ± 2	3.23 ± 0.16	11.54 ± 0.31	46.51 ± 1.59
GPI-5	80 ± 2	-	-	16.35 ± 0.35	-	-

Protein, 500 nM; % of inhibition was calculated using 50 μM compound concentration; measurements were performed in 20 mM HEPES buffer at pH 7.4 containing 160 mM KCl; NM, not measured. Values represent the mean ± SD from triplicate measurements.

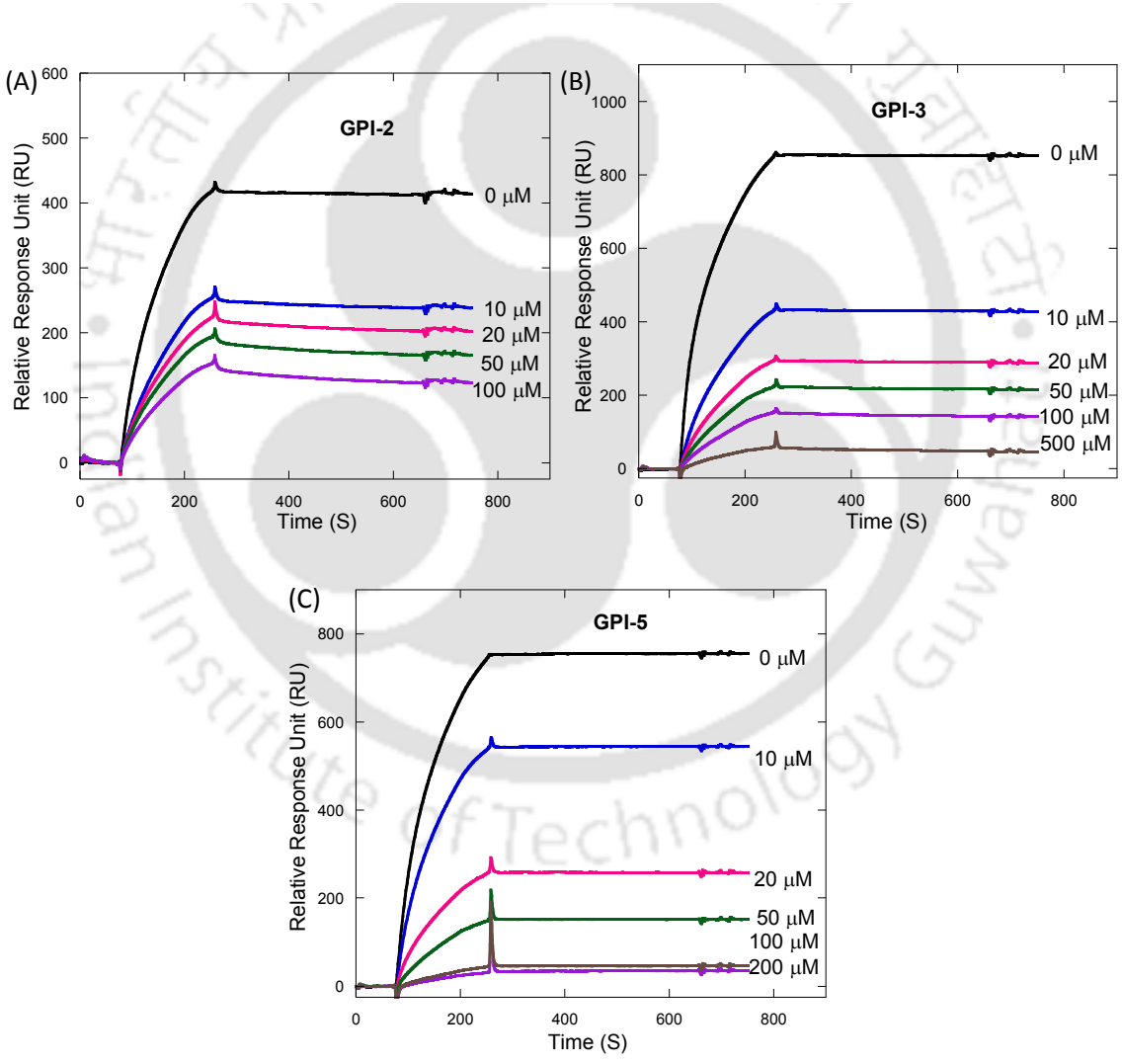

Figure 4.2.2. The inhibitory effects of compounds on the interaction between AKT1-PH domain and PI(3,4,5)P_3. Representative SPR sensorgrams of AKT1-PH domain binding to the PI(3,4,5)P_3 containing liposomes in the presence of increasing concentrations of the compounds **GPI-2** (A), **GPI-3** (B) and **GPI-5** (C).

To determine the selectivity of the compounds in inhibiting PI(3,4,5)P_3/AKT1 PH-domain interaction, we also measured their inhibitory effect on BTK and GRP1 PH-domains, which are known to interact specifically with the PI(3,4,5)P_3 lipids.[9] We also determined the inhibitory effects of compounds on Tapp1 and PLCδ1-PH domains, which selectively interact with the PI(3,4)P_2 and PI(4,5)P_2 lipids respectively.[9, 11] The IC_{50} values of **GPI-1** and **GPI-4** for Tapp1-(28 and 5 μM, respectively) and PLCδ1-PH domains (54 and 28 μM, respectively) were relatively much higher (Table 4.2.2). Therefore, the competitive SPR analysis suggest that compounds **GPI-1** and **GPI-4** have certain degree of selectivity towards PI(3,4,5)P_3 binding AKT1 PH-domain over other PI(3,4)P_2 and PI(4,5)P_2 binding PH-domains.

Table 4.2.2. Relative Inhibitory Activity of the Compounds Measured by Competitive-Surface Plasmon Resonance Analysis

Compound	Relative inhibitory activity (%)		IC_{50} values (μM)	
	Tapp1-PH	PLCδ1-PH	Tapp1-PH	PLCδ1-PH
GPI-1	28 ± 3	54 ± 6	8.5 ± 0.99	9.6 ± 1.71
GPI-3	18 ± 2	46 ± 3	22.1 ± 2.49	3.4 ± 0.41
GPI-4	5 ± 2	28 ± 3	286 ± 19.6	34 ± 3.39

Competitive protein-to-membrane Förster resonance energy transfer analyses- Competitive protein-to-membrane Förster resonance energy transfer (FRET) analyses were also performed for further understanding of the selectivity of these compounds **GPI-1** and **GPI-4** in inhibiting the PI(3,4,5)P_3/AKT1 PH-domain interactions. Trp-residue (W80) present at the membrane binding surface of the AKT1 PH-domain can act as FRET donor, and membrane-embedded dansyl-PE (dPE) serve as the FRET acceptor for this assay. The FRET-signal at 505 nm wavelength decreased with an increase in compound concentrations. However, detailed spectral analysis revealed an associated reduction of Trp-fluorescence signal at 340 nm wavelength (Figure 4.2.3). Control experiment for the change in Trp-fluorescence signal and dPE fluorescence signal demonstrated that both the compounds interact with AKT1-PH domain in solution and reduce fluorescence signal at 340 nm wavelength. Therefore, the reduction in FRET-signal could be primarily due to compound dependent Trp-fluorescence quenching of the protein and subsequent dislocation of protein from bilayer surface. Further detail analyses are required to distinguish their respective contribution in altering the FRET-signal. However, this assay supports that at least a portion of the compounds in solution specifically interact with the AKT1 PH-domain.

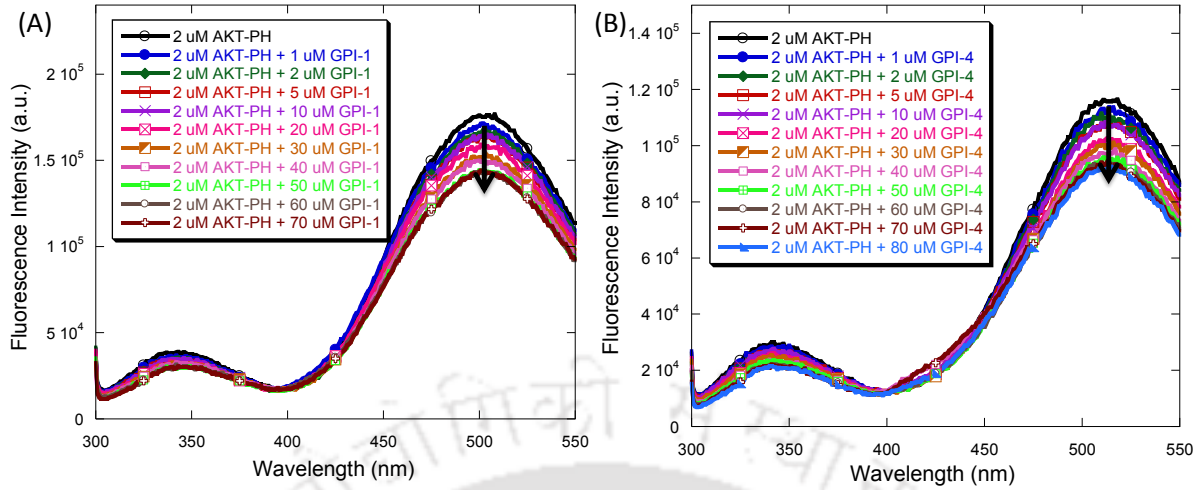

Figure 4.2.3. Representative protein-to-membrane FRET experiment under liposomal environment. Addition of increased concentration of compounds, **GPI-1** (A) and **GPI-4** (B) to AKT1-PH domain (2 μM) bound to the active liposome (PC/PE/PS/dPE/PI(3,4,5)P_3 (56/20/20/1/3)) decreases the FRET signal at 509 nm. All the measurements were performed in 20 mM Tris, pH 7.4 containing 160 mM NaCl. Compound concentrations were varied from 0 to 70 μM.

Liposome pull-down assay- Liposome pull-down assay was also used for qualitative determination of the effect of potent compounds on PI(3,4,5)P_3/AKT1 PH-domain interactions. The binding of GST-tagged AKT1-PH domain (50 μM) to (PC/PE/PS/PI(3,4,5)P_3 (57:20:20:3)) liposome was determined in the absence or presence of compounds (50 μM), **GPI-1** and **GPI-4**. The SDS-PAGE gel image showed that the binding of AKT1-PH domain to PI(3,4,5)P_3 containing liposomes was almost completely diminished by both the compounds, **GPI-1** and **GPI-4** and AKT1-PH domain got displaced from PI(3,4,5)P_3 containing liposomes under the experimental conditions (Figure 4.2.4).

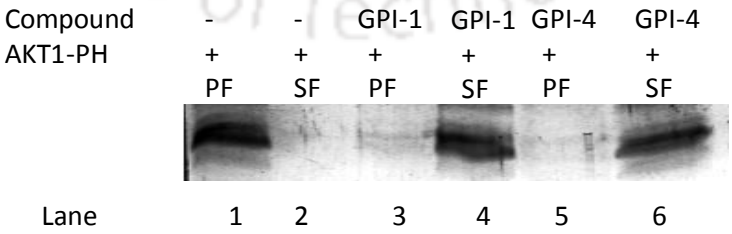

Figure 4.2.4. Coomassie blue stained SDS-PAGE gel images of liposome binding assay. PC/PE/PS/PI(3,4,5)P_3 (57:20:20:3) liposome was used for AKT1-PH domain binding study. Lanes 1, 3 and 5 were liposome bound fraction and 2, 4 and 6 were unbound fraction of AKT1-PH domain. Compound **GPI-1** and **GPI-4** were used as

inhibitor. Liposome concentration 100 μM; Protein concentration 8 μM; Compound concentration, 50 μM; PF, palate fraction; SF, soluble fraction.

Isothermal titration calorimetric (ITC) measurements- Additionally, isothermal titration calorimetric (ITC) measurements were performed to understand the direct binding mechanism and thermodynamic parameters of the compounds **GPI-1** and **GPI-4** with the AKT1 PH-domain. Titration plots of the compounds with AKT1 PH-domain revealed an exothermic reaction with two-step binding mechanism (Figure 4.2.5). The higher negative value of the enthalpy change than the entropy change for this **GPI**/AKT1 PH domain interaction could be due to the hydrogen bond formation and Van der Waals interactions between the compounds and cationic groove of the PIP- and PS-binding sites of the AKT1 PH-domain. Hee-Yong Kim and co-workers recently described that AKT1 PH-domain also contains a phosphatidylserine (PS) binding site next to the IP4 binding site.[27] Therefore, ITC analysis clearly suggests that the compounds in solution can probably interact with the AKT1 PH-domain through both of its PIP and PS-binding sites.

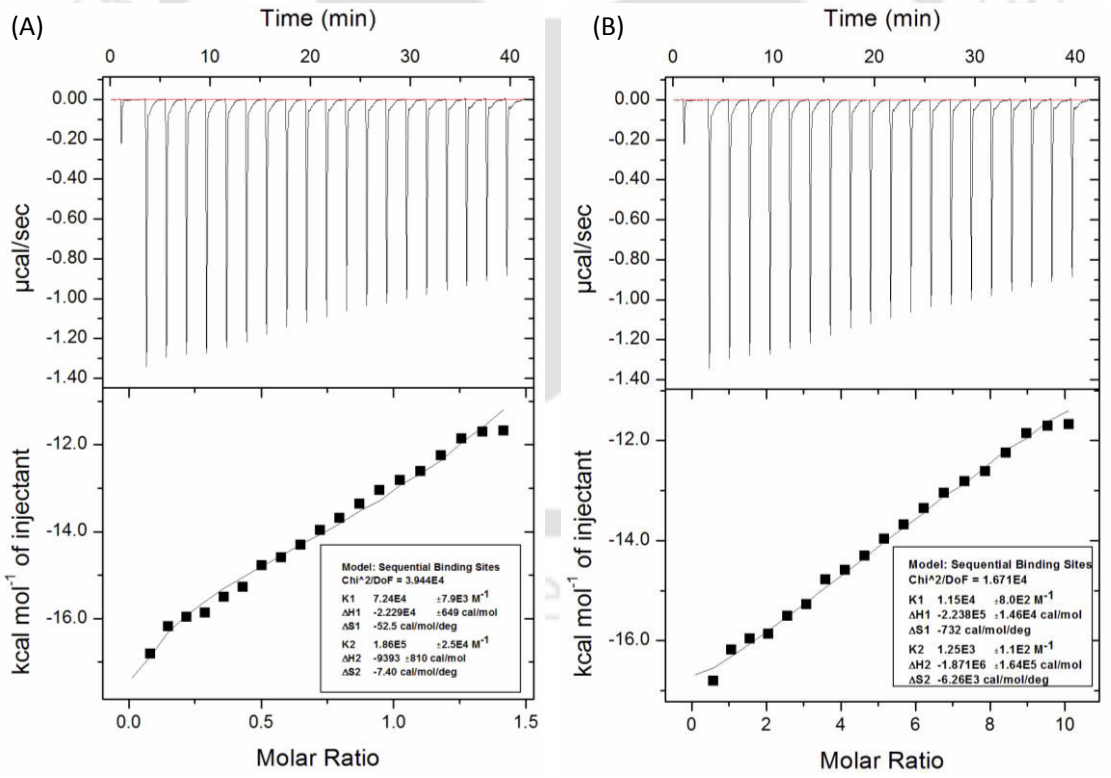

Figure 4.2.5. Representative isothermal titration calorimetric plots of AKT1 PH-domain with potent compounds. Original titration and integrated peak areas of AKT1 PH-domain with **GPI-1** (A) and **GPI-4** (B).

Molecular Docking Analysis—The competitive inhibition and binding assays clearly

revealed that the compounds differentially perturb the PI(3,4,5)P_3/AKT1 PH-domain interaction, suggesting their divergent strength of interaction with the AKT1 PH domain. However, structural analysis showed that all these compounds have 4-amino-N′-hydroxy-

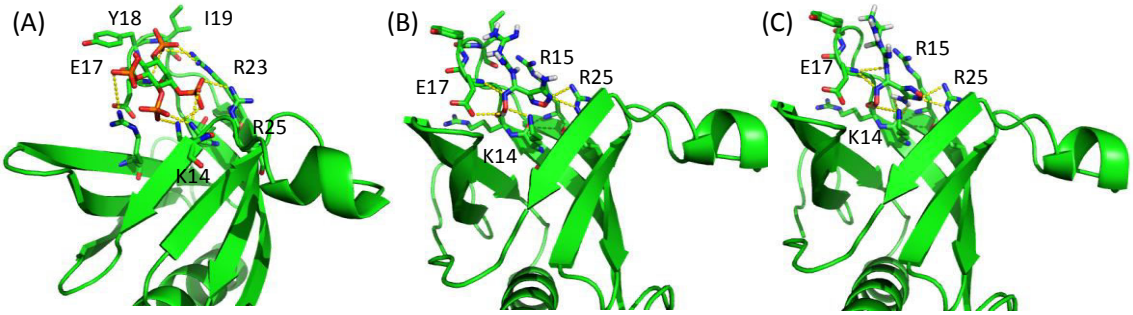

Figure 4.2.6. Structure of AKT1-PH domain (1H10) in complex with IP4 (A). Model structures of ligands **GPI-1** (B) and **GPI-4** (C) docked into the PI-binding site of the AKT1-PH domain. Residues involved in interactions through hydrogen bond formation are shown using dashed lines (yellow).

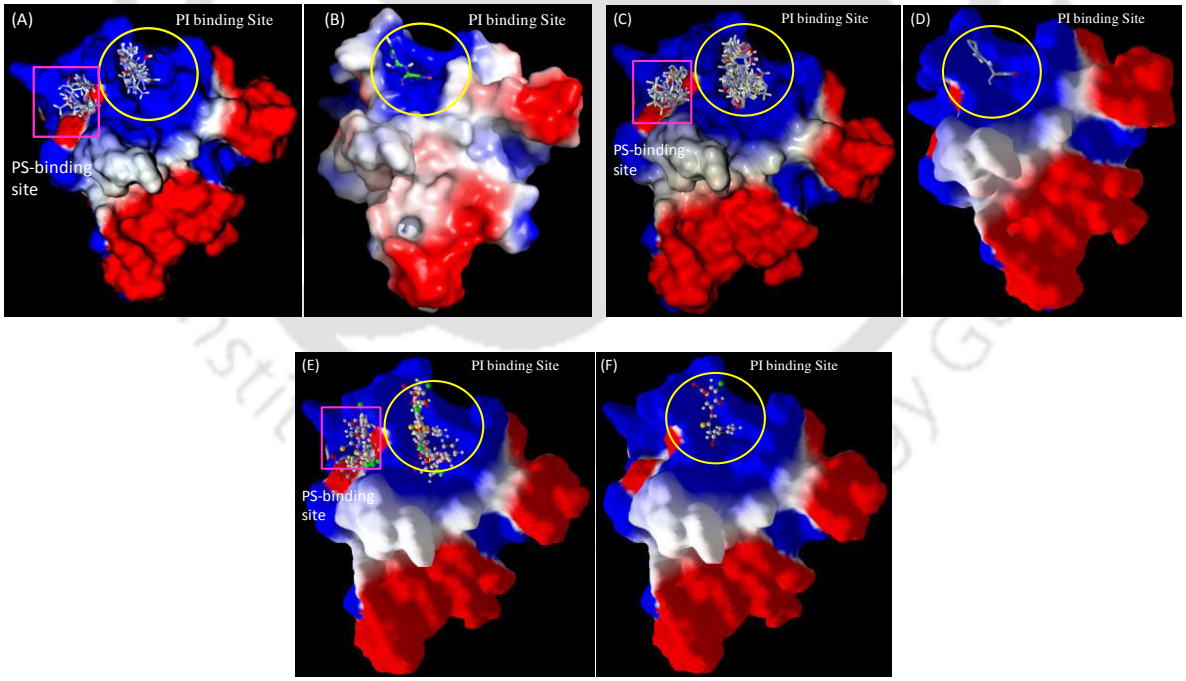

Figure 4.2.7. Surface representation of the docking complexes AKT1-PH/**GPI-1** (A, B), AKT1-PH/**GPI-4** (C, D) and AKT1-PH/**PIT-1** (E, F) both in IP4- (yellow circle) and PS- (pink square box) binding sites. Overall surface of AKT1-PH domain was colored according to the electrostatic potential (blue, positively charged; red, negatively charged; white, neutral) using PyMOL software.

1,2,5-oxadiazole-3-carboximidamide moiety, consequently to understand their interaction properties with the PH-domains and clarify the probable binding mechanism for different inhibitory effects, we performed molecular docking analysis. The reported co-crystal structure of AKT1-PH domain (1H10) in complex with inositol 1,3,4,5-tetrakisphosphate (IP_4) presents a detail insight of the ligand interaction modes.[28] Structure-activity relationship studies of the AKT enzyme and isolated PH domain described that the phosphate groups of IP_4 preferably interact with the K14, E17, Y18, I19, R23, R25, N53 and R86 residues through hydrogen bond formation. Molecular docking analysis revealed that the 4-amino-N′-hydroxy-1,2,5-oxadiazole-3-carboximidamide derivatives preferably interact with the IP_4 binding site of the AKT1 PH-domain. The oxadiazole ring and N′-hydroxy moiety of the compounds could be responsible for their interaction with the cationic groove of the AKT1 PH-domain (Figure 4.2.6 and 4.2.7). Calculated in-silico interaction energies between the ligands and AKT1 PH-domain protein are of high negative values, suggesting acceptable docking poses for further analysis (Table 4.2.3). Further detail analysis of the docking results revealed that the probable binding sites of the ligands are not that specific, as that of IP4 to AKT1 PH-domain. Blind-docking analysis data showed that the 60-70% of the docked poses of the ligands preferentially interact with the AKT1 PH-domain through its IP4 binding site (Figure 4.2.7). The docking results showed that the compounds can also interact with the AKT1 PH-domain through its PS-binding site, which is consistent with the two-step binding mechanism determined by the ITC measurements.

Table 4.2.3. Theoretically calculated Interaction Energy between Ligand and PH-domains

Protein	Ligand	Interaction energy between ligand and Protein (kcal/mol)		Hydrogen bonding energy (kcal/mol)	
		PIP-binding site	Non PIP-binding site	PIP-binding site	Non PIP-binding site
AKT1-PH Domain	**GPI-1**	-096.413	-086.471	-18.895	-14.628
		-094.055	-086.289	-17.347	-15.559
		-092.162	-083.097	-18.140	-13.026
	GPI-2	-118.573	-108.961	-23.223	-27.636
		-111.341	-108.642	-20.653	-16.525
		-110.922	-103.784	-19.252	-18.999
	GPI-3	-127.659	-118.369	-24.080	-27.361
		-126.770	-112.789	-28.646	-15.482
		-125.818	-120.384	-23.513	-23.033
	GPI-4	-118.527	-115.097	-25.753	-15.362
		-119.380	-116.788	-18.622	-21.403
		-117.506	-111.003	-16.348	-14.046

	GPI-5	-122.965	-114.062	-24.391	-12.146
		-115.767	-109.465	-19.299	-15.455
		-115.395	-109.266	-23.840	-08.255
	GPI-1	-92.8201	-	-21.959	-
		-90.6866	-	-19.842	-
		-89.9794	-	-22.223	-
	GPI-2	-113.564	-	-24.156	-
		-112.836	-	-22.030	-
		-112.737	-	-25.896	-
	GPI-3	-131.210	-	-28.362	-
Grp1-PH		-129.856	-	-28.363	-
Domain		-122.495	-	-29.276	-
	GPI-4	-126.288	-	-23.785	-
		-124.609	-	-18.588	-
		-124.401	-	-22.979	-
	GPI-5	-131.210	-	-28.362	-
		-129.856	-	-28.363	-
		-122.495	-	-29.276	-
	GPI-1	-112.621	-140.259	-23.995	-20.284
		-110.963	-138.152	-23.616	-23.426
BTK-PH		-101.816	-136.625	-10.688	-20.842
Domain	**GPI-4**	-127.118	-152.321	-21.303	-20.958
		-126.359	-141.947	-23.870	-23.407
		-125.421	-141.484	-25.414	-25.204

Structural Change Measurement- To understand the effect of compounds on the structural integrity of the isolated AKT1-PH domain, circular dichroism (CD) spectral analysis was performed. The CD spectra of the protein in the absence/presence of **GPI-1** and **GPI-4** are

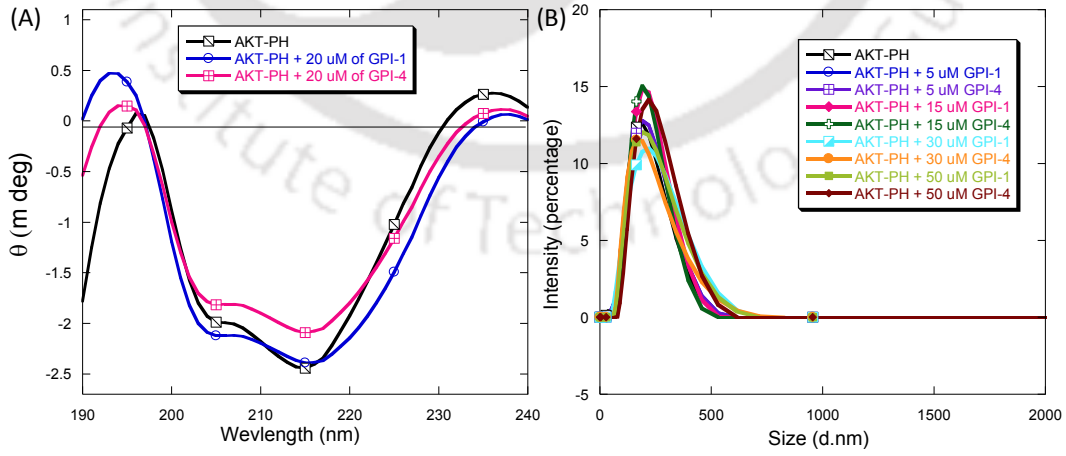

Figure 4.2.8. Effect of compounds on the secondary structural content of the AKT1-PH domain. Far-UV CD spectra of AKT1-PH domain in the absence and presence of compounds (20 μM) in 10 mM phosphate–containing 10 mM NaCl buffer (pH 7.2) (A). Size distribution of AKT1-PH domain in the absence or presence of compounds (20 μM, at t = 5 min) in aqueous solution (20 mM Tris–HCl buffer, pH 7.4, containing 0.16 M NaCl) at 25 °C (B).

shown in Figure 4.2.8A. The spectral analysis revealed that in the presence of compounds there is a weak change in their secondary structural pattern of AKT1 PH-domain in the far-UV CD region. The change in β-sheet contents is little bit higher in the presence of both **GPI-1** and **GPI-4**, indicating direct interactions of the compounds with AKT1 PH-domain. The PIP and/or PS-binding site of AKT1-PH domain is composed of seven β-sheets and connecting loop regions. Analysis of the crystal structure reveals that AKT1-PH domain is enriched with β-sheet, indicating any change in helical content of AKT1-PH domain would be small and change in CD-signal in the range of 225-200 nm might be suppressed by the change in β-sheet content. Therefore, our CD analysis clearly showed that the ligand binding partially alter the secondary structure of the AKT1 PH-domain. In order to ascertain that ligand binding does not induce any significant structural change (such as oligomerization) of the AKT1 PH-domain protein, we also performed dynamic light scattering (DLS) measurements in aqueous solution (at 25 °C, in 20 mM Tris–HCl buffer, pH 7.4, containing 0.16 M NaCl). The results showed a monomodal (PDI = 0.158 -0.186) size distribution of AKT1 PH-domain around a mean hydrodynamic diameter (d_h) of 190–240 nm in the presence of varying compound concentrations (Figure 4.2.8). The DLS measurements clearly indicate that compounds **GPI-1** and **GPI-4** do not induce protein aggregation under the experimental conditions.

Membrane Interaction Measurement- The effects of compounds on dynamics and fluidity of the lipid bilayer were measured by fluorescence anisotropy of 1,6-diphenyl-1,3,5-hexatriene (DPH) and 1,2-diphytanoyl-*sn*-glycero-3-phosphoethanolamine-N-(7-nitro-2-1,3-benzoxadiazol-4-yl) (NBD-PE) under liposomal environment.[29, 30] The DPH and NBD probes are generally localized within the hydrophobic core and at the membrane interface of the lipid bilayers, respectively. Therefore, changes in fluorescence anisotropy values of DPH and NBD probe would be useful in monitoring the alteration of membrane fluidity influenced by membrane-active compounds. The variations in DPH anisotropy values affected by the compounds are not that significant (Table 4.2.4). However, the anisotropy of NBD was affected in the presence of compounds, indicating a weak effect on membrane dynamics and fluidity (Figure 4.2.9A). NBD probe of the NBD-PE lipid preferentially localize at the membrane-water interface, hence the change in anisotropy values in the presence of compounds indicate that the compounds weakly interact with the lipid headgroups. Zeta-potential measurements in the absence and presence of the potent compounds indicate that the compounds have a very weak effect on the surface charge of the liposome in aqueous

solution (Figure 4.2.9B). Therefore, stronger protein binding of the compounds is the predominant factor for their higher inhibitory effect for PI(3,4,5)P_3/AKT1-PH domain interaction.

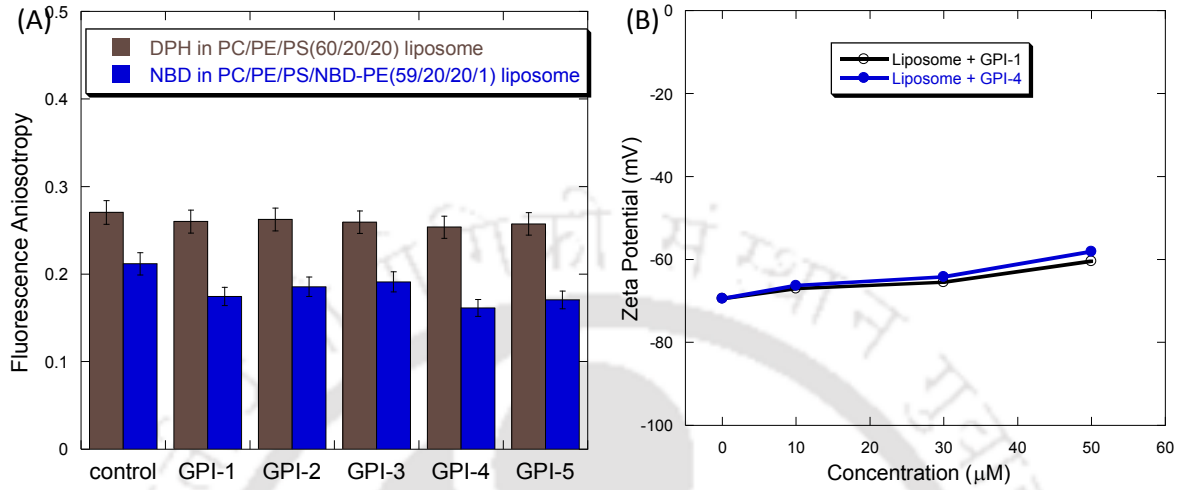

Figure 4.2.9. Fluorescence anisotropy of DPH and NBD-PE embedded in PC/PE/PS (60:20:20) and PC/PE/PS/NBD-PE (59:20:20:1) liposomes for compounds (A). Control: no ligand was added to the liposomes. Zeta potential of the PC/PE/PS/PI(3,4,5)P_3 (57:20:20:3) liposomes in the presence of compounds with different concentrations (B). 100 μL of liposomes from 0.5 mg/mL of total lipid was used for all measurements. Values represent the mean ± SD from triplicate measurements.

Table 4.2.4. Anisotropy Values of the Membrane Sensitive Probes in the Presence and Absence of the compounds

Compound	Anisotropy of DPH	Anisotropy of NBD-PE
liposome	0.2704 ± 0.0128	0.2117 ± 0.0128
GPI-1	0.2599 ± 0.0286	0.1744 ± 0.0262
GPI-2	0.2625 ± 0.0122	0.1855 ± 0.0248
GPI-3	0.2595 ± 0.0135	0.1909 ± 0.0011
GPI-4	0.2536 ± 0.0025	0.1614 ± 0.0026
GPI-5	0.2574 ± 0.0116	0.1704 ± 0.0125

Values in parentheses indicate standard deviations.

Biological Activity Studies — To measure cellular activities of the compounds, we first tested their cytotoxic effects using standard MTT assay. Results showed that all the compounds had minimal toxic effect on MDA-MB-231 cells (Figure 4.2.10A). For example, 100 μM of **GPI-1** inhibited the cell proliferation of MDA-MB-231 only by 10% respectively. All other compounds showed the maximum inhibition of cell proliferation approximately 20% for both the cell lines (Figure 4.2.10A). Therefore, the compounds showed minimal

cytotoxic effect on MDA-MB-231 cells. We also examined the effect of these compounds on PI3K-AKT signalling pathway. The potent compounds showed preferential binding to the AKT-PH domain, which may alter the activity of AKT enzyme. In this regard, the kinase activity of AKT enzyme was studied by measuring the phosphorylation level and expression level of AKT enzyme in MDA-MB-231 cells. The inhibition in growth of cells by the compounds were less than 25% and almost constant within the concentration range of 0.1 to

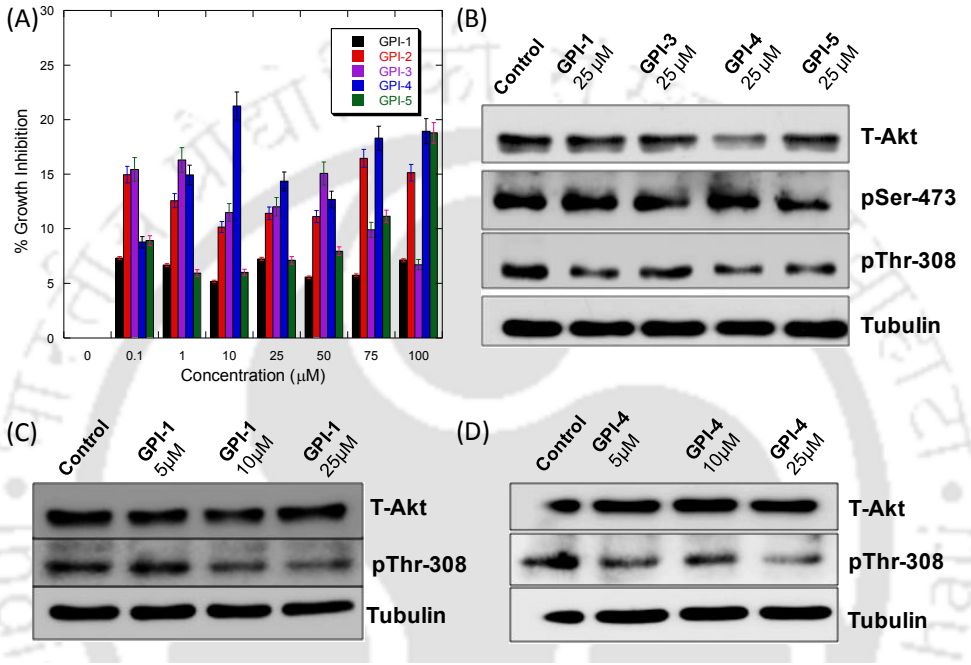

Figure 4.2.10. In vitro cytotoxicity of the compounds in human breast (MDA-MB-231) cancer cell line (A). Compounds inhibit AKT signalling pathway in MDA-MB-231 cells. MDA-MB-231 cells were treated with the compounds (25 μM) for 48 h, and the indicated PI(3,4,5)P_3-dependent phosphorylation events were evaluated by immunoblot analysis (B). MDA-MB-231 cells were treated with the **GPI-1** and **GPI-4** with different concentrations (5, 10 and 25 μM) for 48 h, and the indicated PI(3,4,5)P_3-dependent phosphorylation events were evaluated by immunoblot analysis (C and D). All the immunoblot images were presented in grey scale for better clarity.

100 μM. The kinase activity of the AKT enzyme was initially performed with 25 μM compounds (Figure 4.2.10B) and then **GPI-1** and **GPI-4** were tested in a concentration dependent manner. Figure 4.2.10C and D showed that compound **GPI-4** has moderate effect on expression level of phospho threonine-308 of AKT enzyme. The changes in the expression level of phospho threonine-308 of AKT enzyme in the absence and presence of the compounds were semi-quantized by using ImageJ software. These data support that **GPI-4** has moderate effect on PI3K-AKT signaling pathway without inducing too much cytotoxic

side effects.

Discussion

PI3K-AKT signalling pathway is described as one of the most frequently deregulated pathways and associated with several human diseases including cancer and diabetes. In this regards, AKT has emerged as an attractive therapeutic target.[4, 6, 15, 31, 32] Recent reports showed that, development of specific inhibitors targeting the catalytic domain of the kinase enzymes is considered as quite challenging. There are several protein kinases and their catalytic domain is highly homologous. Several potent inhibitors of AKT enzyme turn out to be relatively toxic, probably due to the uncontrolled inhibition of other ser/threonine kinases.[15, 33] On the contrary, developed inhibitors for the PIP/PH domain interaction of AKT enzyme are comparatively nontoxic and present an improved therapeutic strategy. It is demonstrated that AKT enzyme get fully activated at the membrane interface through its binding with PI(3,4,5)P_3 lipid.[2, 4, 5, 16, 19] In this regard, inhibition of PI(3,4,5)P_3/AKT PH domain interactions could offer an alternate and improved therapeutic strategy for several diseases associated with PI3K-signaliing pathways. In recent years few research groups have already identified phosphate or non-phosphate containing small molecules as being potent inhibitors for PIP-interacting AKT1 PH domain. Selective inhibition of PI(3,4,5)P_3/AKT PH-domains interactions by small molecules like PITENINs, tirucallic acids, TCN-P, NSC348900 and others down regulate PI3K-PDK1-AKT pathways, suppress tumour growth, inhibits AKT-dependent phosphorylation, induce apoptosis in cancer cells.[2, 4, 15, 17, 34]

In this report we describe 4-amino-1,2,5-oxadiazole analogues as a new class of small molecule antagonist for PI(3,4,5)P_3 binding PH-domains. All molecules were designed such a way, that there must be 1,2,5-oxadiazole ring and N′-hydroxy moiety which are critical in forming more hydrogen bond with their binding partners and can be fitted inside the shallow binding pocket of the AKT1 PH-domain. The guanidine/biguanide/benzimidamide moieties were installed to understand their impact in hydrogen bond formation with the amino acid residues within the PH-domain binding pocket. Thus, the impact of this study is to elucidate the inhibitory mechanism of PI(3,4,5)P_3/PH domain interaction by 4-amino-1,2,5-oxadiazole analogues. The guanidine/biguanide/ benzimidamide moieties are present in several bioactive molecules including metformin which is used as drug for type 2 diabetes. Recent studies identified that metformin also acts as an anticancer agent.[35-37] The 4-amino-1,2,5-oxadiazole moiety containing compounds are potent inhibitor of immunosuppressive enzyme indoleamine 2,3-dioxygenase which are currently in clinical trials.[38]

SPR-based competitive binding study clearly indicates that the potent compounds strongly interacts with the PH-domains through its PIPs binding site. Compound **GPI-1** and **GPI-4** showed relatively stronger inhibition capabilities for PI(3,4,5)P_3/AKT1 PH domain interactions. SPR-based competitive binding analyses of the compounds with other PIP binding PH domain like Tapp1, PLCδ1, BTK and GRP1 clearly showed that **GPI-1** and **GPI-4** selectively interact with the AKT1-PH domain. We hypothesize that interaction pattern of the compounds with the amino acid residues present inside and/or outside the binding site, stability of the protein-compound complexes, effect of compound on membrane or their cooperative effect could be accountable for this differential inhibitory effect. These compounds can also differentially influence the in vitro PI(3,4,5)P_3 interaction properties of the AKT1, BTK and GRP1 proteins under the similar experimental conditions. The higher binding affinity of **GPI-1** and **GPI-4** for AKT1 PH-domain over the other PH- domains including GRP1, BTK, PLCδ1 and Tapp1 proteins could be due to its true selectivity for proper orientation of oxadiazole ring within the PIP-binding pocket of the AKT1 PH-domain, although its β1/β2 loop region contains fewer basic residues than the BTK and GRP1 PH-domains.

Molecular docking analyses suggest no clear differences in number of hydrogen bond formation between the compounds and AKT1 PH domain. However, SPR and FRET-based competitive binding study, ITC measurements and liposme pull down assay of the potent compounds clearly showed that these ligands strongly interact with the AKT1 PH-domain. We therefore presume that in addition to the 4-amino-N′-hydroxy-1,2,5-oxadiazole-3-carboximidamide moiety the guanidine/biguanide/ benzimidamide moiety of the ligands might be involved in interaction with the amino acid residues of the AKT1 PH-domain through bridging water molecule, which was not considered during the molecular docking analysis. Hence, the difference in their binding affinity values could be due to the strength of direct hydrogen bonding through oxadiazole ring and N′-hydroxy moiety and also due to the hydrogen bonding through the bridging water molecules.

The ITC measurements, which were used to understand the binding parameters for direct protein-ligand interactions, pointed out that compounds **GPI-1** and **GPI-4** followed a two-step binding mechanism for their interactions with AKT1-PH domain. We hypothesizes that, the ligands are interacting with AKT1 PH domain through its IP4 and PS-binding sites. In-silico interaction energies for ligands with the PIP-binding site of AKT1 PH-domain protein are of higher negative values than that of with the PS-binding site. However, this non-specific ligand binding to the AKT1 PH-domain could also change the protein-conformation

allowing it to show stronger competitive inhibition of the PI(3,4,5)P_3/AKT1 PH-domain interaction than the expected ones. Molecular docking analysis of PIT-1 (PITenins), a reported strong antagonist of PI(3,4,5)P_3/AKT1 PH-domain interactions also showed probable interaction through both IP4 and PS-binding sites.[2] Therefore, **GPI-1** and **GPI-4** could bind to both IP4- and PS-binding sites of the AKT1 PH-domain but with preference for IP4- binding site at lower compound concentrations. Recent studies demonstrated that AKT activation require not only PI(3,4,5)P_3 but also membrane localized PS lipid. The PS lipid supports PI(3,4,5)P_3 binding of AKT PH-domain and involved in PI(3,4,5)P_3-dependent interdomain conformational change for Thr-308 and Ser-473 phosphorylation. Perturbation of PS binding to the PH-domain alters the AKT signalling pathways.[27] Therefore we presume that binding of these compounds to the PS-binding site of the AKT1-PH domain could alter its PI(3,4,5)P_3 binding and AKT-phosphorylation activities. However, further detailed analyses including mutational studies are required to understand the exact binding site of these compounds.

Stronger binding of the compounds to protein can also alter the structure of AKT1 PH-domain, which could forbid the protein to interact with the PI(3,4,5)P_3 containing membranes.[39] CD and DLS measurements showed that stronger binding of the potent compounds have a very weak effect on the secondary structure of AKT1 PH domain and there was no protein aggregation under the experimental conditions. It is important to note that the inhibition/binding properties of the compounds were measured under liposomal environments. Stronger binding affinity values of the compounds could be also as a result of their direct interaction with the liposomes, which can alter the membrane dynamics and inhibit the PH-domains to interact with the membranes. The membrane composition used to measure the efficacy of the compounds in inhibiting respective PIP/PH domain interactions contains anionic lipids PS and PIP. There is a possibility that guanidine/biguanide/benzimidamide moiety of the compounds could interact with the anionic lipids present in the membrane. This interaction could block the protein binding to the membrane and allow the *in vitro* measurements to show high inhibitory effect by the compounds in a concentration dependent manner. Anisotropy and surface potential measurements demonstrate that theses water soluble compounds weakly interact with the interfacial region of the liposome and preferably localize in the bulk phase of the solution and its pharmacophores are accessible for PH-domain binding under the experimental conditions. Therefore, stronger binding of the potent compounds with the AKT1 PH domain perturbs its PI(3,4,5)P_3-dependent membrane association, which is essential for it activity in initiating a

range of local responses, like accumulating signalling complexes, initiating protein kinase cascades and others.

Cytotoxicity measurements of the compounds in breast cancer cells (MDA-MB-231) showed that the compounds have low toxicity, which is one of the key requirements in developing selective PIP/protein interactions in controlling the activities of the target enzymes. The kinase activity of the AKT enzyme was moderately altered in the presence of **GPI-4** in MDA-MB-231 cells. The change in kinase activity of the enzyme in the presence of compound **GPI-4**, correlates well with its PH domain binding or inhibition of PI(3,4,5)P_3/AKT-PH domain interaction abilities. However, *in vitro* inhibition efficiency of the compounds is not in the same order with their cellular kinase activities. Additional biological studies are required to understand their potency in inhibiting AKT kinase activity. The 4-amino-1,2,5-oxadiazole moiety provide a good template to develop more potent AKT enzyme inhibitor.

Conclusion

Targeting the specific enzymes of PI3K-signalling pathway, which would show limited side effects, is considered as future direction of anticancer drug discovery. To this end, this study demonstrate the identification of non-lipid based compounds with 4-amino-N′-hydroxy-1,2,5-oxadiazole-3-carboximidamide moiety that strongly interact with the PI(3,4,5)P_3 binding of AKT1 PH-domain, but weakly interact with the PI(3,4)P_2 and PI(4,5)P_2 binding PH domains. The potent compounds also weakly interact with the liposome through its interfacial region. Cellular measurements showed that the potent compounds have weak cytotoxicity and moderate inhibition effect on AKT-kinase activity. These results suggest the inhibition of PI(3,4,5)P_3 dependent membrane recruitment and AKT enzyme activity by these potent compounds. Our findings imply that the 4-amino-N′-hydroxy-1,2,5-oxadiazole-3-carboximidamide moiety can be used as a template in developing non-phosphate-based potential inhibitors for PIP-binding proteins.

4.3 Experimental Section

Materials: As described in chapter 2**.**

Protein Purification: The AKT1 (homo sapiens; 1-121 amino acid), BTK (homo sapiens; 2-170 amino acid), GRP1 (mus musculus, 1-127 amino acid), Tapp1 (homo sapiens; 180-305 amino acid) and PLCδ1 (rattus norvegicus, 1-131 amino acid) PH-domains were expressed in

E. coli cells (BL21-DE3) and purified using methods similar to those reported earlier.[9,40] The plasmids were generous gift from Prof. Wonhwa Cho (University of Illinois at Chicago, IL, USA).

Surface Plasmon Resonance (SPR) Assay: All surface plasmon resonance (SPR) measurements were performed (at 25 °C, in 20 mM HEPES buffer, pH 7.4, containing 0.16 M KCl, flow rate of 30 µL/min) using a lipid-coated L1 sensorchip in the Biacore-X100 (GE Healthcare) system as described earlier.[9, 25, 26, 40] Vesicles for SPR analysis were prepared at a concentration of 0.5 mg/mL in 20 mM HEPES buffer, pH 7.4, containing 0.16 M KCl, and were vortexed vigorously and passed through a 100-nm polycarbonate filter using an Avanti MiniExtruder (Avanti Polar Lipids, Alabaster, AL) according to the manufacturer's protocol. After washing the sensor chip surface with the running buffer (20 mM HEPES, pH 7.4, containing 0.16 M KCl), PC/PE/PS/PIP (57:20:20:3) and PC/PE/PS (60:20:20) vesicles were injected at 5 µL/min to the active surface and the control surface, respectively, to achieve similar response unit (RU) values (3500-4000 RU). To minimize nonspecific adsorption the control surface was also coated with 40 µL of BSA (0.1 mg/ml in the running buffer) at a flow rate of 5 µL/min, and equilibrated for 20 min, before the injection of protein. The competitive inhibitory effects of each compound were determined by measuring the change in response unit (RU) of the SPR sensorgrams of PH-domains (500 nM) in the absence/presence of compounds (0-200 µM). The compounds were equilibrated with respective PH-domain for 30 minutes before any SPR measurements. The decrease in RU value of each sensorgram with various compound concentrations was measured to calculate % of inhibition efficiency. The inhibition potencies were calculated as (1-(RU of protein mixed with compounds/ RU of protein only)) × 100%. The RU value after 180 sec of injection was considered for % of inhibition efficiency calculations.

In–silico Molecular Docking Analysis: Computational docking and scoring studies of the interaction of the compounds with PH-domains were performed using AutoDock 4 (The Scripps Research Institute, La Jolla, USA) and Molegro Virtual Docker software, version 4.3.0 (Molegro ApS, Aarhus, Denmark) with essentially the same results.[21-23] The crystal structure of AKT1 PH (1-116 amino acids, PDB code: 1H10), [28] BTK PH (1-169 amino acids, PDB code: 1B55) [41] and GRP1 (261-386 amino acids, PDB code: 1FGY) [42] were utilized for docking experiment. To generate apo-protein, the ligands were removed from the co-crystal structures and then they were processed by energy minimization. The energy

minimized three-dimensional structure of ligands was prepared by using the GlycoBioChem PRODRG2 Server (http://davapc1.bioch.dundee.ac.uk/prodrg/). The GROningen MAchine for Chemical Simulations (GROMACS) library of three-atom combination geometries employing a combination of short molecular dynamics simulations and energy minimizations were utilized for the conversion of 2D molecular structures to 3D structures. The original blind docking parameters were used in combination with an evaluation scheme based on Gibbs free energy change (ΔG). In each docking run, one hundred docked structures were generated for individual ligand. Energetically favoured docked conformations were evaluated on the basis of moledock and re-rank score. The docking poses were exported and examined with PyMOL software (The PyMol Molecular Graphics System, Version 1.0r1, Schrödinger, LLC.). The residues surrounding the compounds were also analyzed using LigPlot provided by the European Bioinformatics Institute.

Circular Dichroism Studies: The circular dichroism (CD) spectra of the protein samples were measured using JASCO J-815 CD spectropolarimeter at room temperature. CD spectra of AKT1 PH-domain in the absence and presence of complexes (1 : 3 molar ratio of the AKT1 PH-domain to the compounds) were obtained in the wavelength range of 190–245 nm in 10 mM phosphate–containing 10 mM NaCl buffer (pH 7.2).[39, 40]

Anisotropy Measurement: Fluorescence anisotropy measurements were performed on a Fluoromax-4 spectrofluorometer at 25 °C. The anisotropies of DPH and NBD-PE under liposomal environment were measured according to the reported procedure. [21, 43] The fluorescence probe DPH was incorporated into the PC/PE/PS (60/20/20) liposome (100 µL of 0.5 mg/mL of total lipid) by adding the dye dissolved in THF (1 mM) to vesicles up to a final concentration of 1.25 µM. The NBD-PE probe was incorporated to the PC/PE/PS/NBD-PE (59/20/20/1) liposome using our earlier mentioned procedure.[22] After 30 min of incubation at room temperature, DPH (λ_{ex} = 355 nm; λ_{em} = 430 nm) and NBD (λ_{ex} = 460 nm; λ_{em} = 535 nm) fluorescence anisotropies were measured. The concentration of compounds was 15 µM. The degree of anisotropy in the DPH/NBD fluorescence of the probes were calculated using equation 1, at the peak of the fluorescence spectrum, where I_{VV} and I_{VH} are the fluorescence intensities of the emitted light polarized parallel and perpendicular to the excited light, respectively, and $G = I_{VH}/I_{HH}$ is the instrumental grating factor.

$$r = \frac{(I_{VV} - GI_{VH})}{(I_{VV} + 2GI_{VH})} \quad (1)$$

Dynamic Light Scattering Measurement: The dynamic light scattering (DLS) experiment was carried out to determine the degree of aggregation of AKT1 PH-domain protein with varying concentration of compounds in aqueous medium (at 25 °C, in 20 mM Tris–HCl buffer, pH 7.4, containing 0.16 M NaCl) using a Zetasizer Nano ZS90 (Malvern, Westborough, MA) light scattering spectrometer equipped with a He–Ne laser working at 4 mW (λ_0 = 632.8 nm).[40, 44] The reduced glutathione content in protein samples were removed using a PD-10 desalting column (Sigma, St. Louis MO). Before performing any measurements dust or other particles were removed from sample solutions through syringe filtration technique (0.22 μm) and equilibrated for 10 min before performing any measurement (at least 11 runs were performed for each sample, all measurements were performed in triplicates). The scattering intensity was measured at 90° (right angle) to the incident beam.

Zeta-Potential Measurement: The zeta-potential measurements of the liposomes in the absence and presence of the compounds were carried out in aqueous medium (at 25 °C, in 20 mM Tris–HCl buffer, pH 7.4, containing 0.16 M NaCl) using a Zetasizer Nano ZS90 (Malvern, Westborough, MA) light scattering spectrometer equipped with a He–Ne laser working at 4 mW (λ_0 = 632.8 nm).[45, 46] Unilamellar vesicles composed of PC/PE/PS/PI(3,4,5)P_3 (57:20:20:3) lipids were prepared in 20 mM Tris–HCl buffer, pH 7.4, containing 0.16 M NaCl by vigorous vortexing and extruding through a polycarbonate filter (100-nm) using an Avanti Mini-Extruder. 100 μL of liposomes from 0.5 mg/mL of total lipid was used for zeta-potential measurements. All the measurements were performed three times per sample and averaged to give the final value.

Förster Resonance Energy Transfer (FRET) Measurements: Analysis of protein-to-membrane Förster resonance energy transfer (FRET) based binding assay was used to detect the specificity of the compounds for PH-domain binding through PIP-binding site. In this assay, membrane-bound AKT1 PH-domain was displaced from liposomes by the addition of the compound. The vesicles composed of PC/PE/PS/dPE (55/20/20/5) and PC/PE/PS/dPE/PIP (52/20/20/5/3) was used as control and for ligands, respectively. The FRET-signal due to PIP-dependent protein binding to the liposomes was corrected with non-

specific fluorescence signal originated from control liposome (PC/PE/PS/dPE) and protein interactions. Control experiments were also performed to test the effect of only compounds on the fluorescence of dPE. The stock solution of compounds was titrated into the sample containing AKT1 PH-domain (1 μM) and excess liposome (100 μM total lipid) in a buffer solution (20 mM Tris–HCl buffer, pH 7.4, containing 0.16 M NaCl) at room temperature. The competitive displacement of protein from the membrane was monitored using protein-to-membrane FRET-signal (λ_{ex} = 280 nm and λ_{em} = 505 nm). Control experiments were performed to measure the dilution effect under similar experimental condition and the increasing background emission arising from direct dPE excitation.[21, 22]

Isothermal Titration Calorimetry (ITC) Measurements: Thermodynamic parameters of protein-ligand interactions were measured using ITC-200 microcalorimeter from Microcal (Northampton, MA, USA). AKT1 PH-domain (200 μM), after dialysis with 20 mM HEPES buffer, pH 7.4, containing 0.16 M NaCl, was titrated against compounds (2 mM) dissolved in the final dialysate. A typical titration involved injecting 20 injection volumes (2 μL) of compound into the sample cell containing AKT1 PH-domain (201.6 μL) at 2.0 min intervals with continuous stirring (at 25 °C with stirring speed of 500 rpm). The heat of dilution data corresponding to individual injections were analyzed using a sequential binding model with two binding sites considering both PIP and PS-binding sites per AKT1 PH-domain monomer with the system running Microcal Origin 7.0 software. The data points obtained from the ITC measurements were first fitted with different models and the best fit was obtained using sequential binding model with two binding sites. The ΔH and ΔS values were obtained using a nonlinear least-square fit of the data. Gibbs free energy (ΔG) was calculated by using Gibbs equation: $\Delta G = \Delta H - T\Delta S$.

Liposome Binding Assay: Inhibition of PI(3,4,5)P_3/AKT1-PH domain interaction by the compounds was further determined by liposome pull-down assay according to the reported procedures.[40, 45, 47] Liposomes of PC/PE/PS/PI(3,4,5)P_3 (57:20:20:3) in 20 mM Tris buffer, pH 7.4, containing 150 mM NaCl, 170 mM sucrose, pH 7.4 buffer solution were prepared by sonication, followed by extrusion through 0.1mm pore size polycarbonate filters. The suspension was pelleted down at 100000**g**, 4 °C, for 20 minutes and resuspended in binding buffer (20 mM Tris buffer, pH 7.4, containing 100 mM KCl, 5 mM $MgCl_2$). Purified AKT1-PH domain (8 μM) was incubated with sucrose-loaded vesicles (40 μg in 100 μL) for 30 min in the presence of binding buffer containing 0.3 mg mL^{-1} BSA. Membrane-bound

protein was separated from free protein by centrifugation at 100000*g* for 30 min at 4 °C. Protein of supernatant and pellet fractions was analyzed by SDS-PAGE gel.

***In vitro* Cytotoxicity Assay:** The *in vitro* toxicity of the compounds was determined in human breast cancer cell line (MDA-MB-231). Cells were cultured according to the American Type Culture Collection (ATCC) instructions. MDA-MB-231 cells were grown in RPMI1640 media supplemented with 10% Fetal Bovine Serum, 100 U/mL penicillin and 100 µg/mL streptomycin at 37°C and 5% CO_2 atmosphere under humid condition. Cytotoxic effect of the compounds (**GPI-1** to **5**) were determined by 3-(4, 5 dimethylthiazol-2-yl)-2-5 diphenyl tetrazolium bromide (MTT) assay as described previously.[48] Briefly, cells (3×10^3/per well) were seeded one day prior the treatment of the compounds. Then cells were treated with different concentrations (1 – 100 µM) of compounds for 48 hours. At the end of incubation, MTT solution (20 µl of 5 mg/ml of stock) was added to the media and incubated for 4 hours in the CO_2 incubator. Finally media containing MTT solution was replaced with 100 µl of MTT solvent (5 mM HCl and 0.1% Triton X-100 in iso-propanol) and incubated at room temperature for 15 minutes with gentle rocking. Then absorbance was measured at 590 nm using a Thermo pierce plate reader. The percentage of viable cells was calculated as the mean with respect to the vehicle treated cells and considered to be 100%. All the compounds were dissolved in DMSO and maximum 0.01% DMSO was used for the experiments. This experiment was repeated three times. The data from cancer cell lines were acquired from three independent cell passages and the IC_{50} values were calculated from the plot of cell viability *vs.* concentration of compounds.

Immunoblot analysis: Cells were collected at the end of treatment and washed with ice cold PBS. Then, whole cell extracts were prepared using lysis buffer (50 mM Tris buffer of pH 7.4, 250 mM NaCl, 50 mM NaF, 0.5 mM Na_3VO_4, 5 mM EDTA and 0.5% Triton-X 100 contain protease inhibitor cocktail). Cells were lysed in ice for 30 minutes and then lysates were clarified by centrifugation at 13000 rpm for 15 minutes at 4 °C. The supernatants were transferred to the fresh tubes and protein concentration was measured by using Bradford reagent as described previously.[2] Then equal amount of whole cell lysates were resolved by SDS-PAGE and transferred to PVDF membrane and probed with indicated antibodies.

References

1. I. Vivanco and C. L. Sawyers, *Nat. Rev. Cancer*, 2002, **2**, 489-501.
2. B. Miao, I. Skidan, J. Yang, A. Lugovskoy, M. Reibarkh, K. Long, T. Brazell, K. A. Durugkar, J. Maki, C. V. Ramana, B. Schaffhausen, G. Wagner, V. Torchilin, J. Yuan and A. Degterev, *Proc. Natl. Acad. Sci. USA*, 2010, **107**, 20126-20131.
3. P. Workman, P. A. Clarke, F. I. Raynaud and R. L. van Montfort, *Cancer Res.*, 2010, **70**, 2146-2157.
4. N. Berndt, H. Yang, B. Trinczek, S. Betzi, Z. Zhang, B. Wu, N. J. Lawrence, M. Pellecchia, E. Schonbrunn, J. Q. Cheng and S. M. Sebti, *Cell Death Differ.*, 2010, **17**, 1795-1804.
5. L. Catley, T. Hideshima, D. Chauhan, P. Neri, P. Tassone, R. Bronson, W. Song, Y. T. Tai, N. C. Munshi and K. C. Anderson, *Exp Hematol*, 2007, **35**, 1038-1046.
6. B. D. Manning and L. C. Cantley, *Cell*, 2007, **129**, 1261-1274.
7. W. Cho, *Sci. STKE*, 2006, pe7.
8. W. Cho and R. V. Stahelin, *Annu. Rev. Biophys. Biomol. Struct.*, 2005, **34**, 119-151.
9. D. Manna, A. Albanese, W. S. Park and W. Cho, *J. Biol. Chem.*, 2007, **282**, 32093-32105.
10. W. S. Park, W. D. Heo, J. H. Whalen, N. A. O'Rourke, H. M. Bryan, T. Meyer and M. N. Teruel, *Mol. Cell*, 2008, **30**, 381-392.
11. M. A. Lemmon, *Nat. Rev. Mol. Cell. Biol.*, 2008, **9**, 99-111.
12. C. Peifer and D. R. Alessi, *Chem. Med. Chem.*, 2008, **3**, 1810-1838.
13. L. Yang, H. C. Dan, M. Sun, Q. Liu, X. M. Sun, R. I. Feldman, A. D. Hamilton, M. Polokoff, S. V. Nicosia, M. Herlyn, S. M. Sebti and J. Q. Cheng, *Cancer Res.*, 2004, **64**, 4394-4399.
14. K. D. Courtney, R. B. Corcoran and J. A. Engelman, *J. Clinic. Oncol.*, 2010, **28**, 1075-1083.
15. D. Mahadevan, G. Powis, E. A. Mash, B. George, V. M. Gokhale, S. Zhang, K. Shakalya, L. Du-Cuny, M. Berggren, M. A. Ali, U. Jana, N. Ihle, S. Moses, C. Franklin, S. Narayan, N. Shirahatti and E. J. Meuillet, *Mol. Cancer Ther.*, 2008, **7**, 2621-2632.
16. E. J. Meuillet, N. Ihle, A. F. Baker, J. M. Gard, C. Stamper, R. Williams, A. Coon, D. Mahadevan, B. L. George, L. Kirkpatrick and G. Powis, *Oncol. Res.*, 2004, **14**, 513-527.
17. A. C. Estrada, T. Syrovets, K. Pitterle, O. Lunov, B. Buchele, J. Schimana-Pfeifer, T. Schmidt, S. A. Morad and T. Simmet, *Mol. Pharmacol.*, 2010, **77**, 378-387.
18. C. R. McNamara and A. Degterev, *Future Med. Chem.*, 2011, **3**, 549-565.

19. E. J. Meuillet, S. Zuohe, R. Lemos, N. Ihle, J. Kingston, R. Watkins, S. A. Moses, S. Zhang, L. Du-Cuny, R. Herbst, J. J. Jacoby, L. L. Zhou, A. M. Ahad, E. A. Mash, D. L. Kirkpatrick and G. Powis, *Mol. Cancer Ther.*, 2010, **9**, 706-717.
20. J. K. Morrow, L. Du-Cuny, L. Chen, E. J. Meuillet, E. A. Mash, G. Powis and S. X. Zhang, *Recent Patents on Anti-Cancer Drug Discovery*, 2011, **6**, 146-159.
21. D. Talukdar, S. Panda, R. Borah and D. Manna, J. Phys. Chem. B, 2014, **118**, 7541-7553.
22. N. Mamidi, R. Borah, N. Sinha, C. Jana and D. Manna, *J. Phys. Chem. B*, 2012, **116**, 10684-10692.
23. N. Mamidi, S. Gorai, R. Mukherjee and D. Manna, *Mol. Biosyst.*, 2012, **8**, 1275-1285.
24. Y. Kommagalla, S. Cornea, R. Riehle, V. Torchilin, A. Degterev and C. V. Ramana, *Med. chem. comm.*, 2014, **5**, 1359-1363.
25. Y. Yoon, *Bioorg. Med. Chem. Lett.*, 2014, **24**, 2334-2339.
26. Y. Kim and Y. Yoon, *Bioorg. Med. Chem. Lett.*, 2014, **24**, 2256-2262.
27. B. X. Huang, M. Akbar, K. Kevala and H. Y. Kim, *J. Cell Biol.*, 2011, **192**, 979-992.
28. C. C. Thomas, M. Deak, D. R. Alessi and D. M. van Aalten, *Curr. Biol.*, 2002, **12**, 1256-1262.
29. D. Tang, D. Borchman, N. Harris and S. Pierangeli, *Biochim. Biophys. Acta*, 1998, **1372**, 45-54.
30. D. K. Hincha, A. E. Oliver and J. H. Crowe, *Biophys. J.*, 1999, **77**, 2024-2034.
31. W. S. Chen, P. Z. Xu, K. Gottlob, M. L. Chen, K. Sokol, T. Shiyanova, I. Roninson, W. Weng, R. Suzuki, K. Tobe, T. Kadowaki and N. Hay, *Genes Dev.*, 2001, **15**, 2203-2208.
32. T. L. Yuan and L. C. Cantley, *Oncogene*, 2008, **27**, 5497-5510.
33. C. C. Kumar and V. Madison, *Oncogene*, 2005, **24**, 7493-7501.
34. M. Hussein, M. Bettio, A. Schmitz, J. S. Hannam, J. Theis, G. Mayer, S. Dosa, M. Gutschow and M. Famulok, *Angew. Chem. Int. Ed. Engl.*, 2013, **52**, 9529-9533.
35. V. N. Anisimov, *Curr. Drug. Targets.*, 2015.
36. D. R. Morales and A. D. Morris, *Annu. Rev. Med.*, 2015, **66**, 17-29.
37. D. Li, *J Diabetes*, 2011, **3**, 320-327.
38. E. W. Yue, B. Douty, B. Wayland, M. Bower, X. Liu, L. Leffet, Q. Wang, K. J. Bowman, M. J. Hansbury, C. Liu, M. Wei, Y. Li, R. Wynn, T. C. Burn, H. K. Koblish, J. S. Fridman, B. Metcalf, P. A. Scherle and A. P. Combs, *J. Med. Chem.*, 2009, **52**, 7364-7367.
39. C. C. Milburn, M. Deak, S. M. Kelly, N. C. Price, D. R. Alessi and D. M. Van Aalten, *Biochem J.*, 2003, **375**, 531-538.

40. S. Gorai, P. R. Bagdi, R. Borah, D. Paul, M. K. Santra, A. T. Khan and D. Manna, *Biochem. Biophys. Rep*., 2015, **2**, 75-86.

41. E. Baraldi, K. Djinovic Carugo, M. Hyvonen, P. L. Surdo, A. M. Riley, B. V. Potter, R. O'Brien, J. E. Ladbury and M. Saraste, *Structure*, 1999, **7**, 449-460.

42. S. E. Lietzke, S. Bose, T. Cronin, J. Klarlund, A. Chawla, M. P. Czech and D. G. Lambright, *Mol. Cell*., 2000, **6**, 385-394.

43. O. Raifman, S. Kolusheva, M. J. Comin, N. Kedei, N. E. Lewin, P. M. Blumberg, V. E. Marquez and R. Jelinek, *FEBS J*., 2010, **277**, 233-243.

44. R. Borah, D. Talukdar, S. Gorai, D. Bain and D. Manna, *RSC Adv*., 2014, **4**, 25520-25531.

45. N. Mamidi, S. Gorai, B. Ravi and D. Manna, *RSC Adv*., 2014, **4**, 21971-21978.

46. J. E. Johnson, J. Giorgione and A. C. Newton, *Biochemistry*, 2000, **39**, 11360-11369.

47. O. Lorenzo, S. Urbe and M. J. Clague, *J. Cell Sci*., 2005, **118**, 2005-2012.

48. P. Kumar, S. Gorai, M. K. Santra, B. Mondal and D. Manna, *Dalton Trans*., 2012, **41**, 7573-7581.

CHAPTER 5

Insights into the Inhibitory mechanism of Triazole-Based Small Molecules on Phosphatidylinositol-4,5-bisphosphate Binding Pleckstrin Homology Domain

This chapter describes rational design, synthesis and biophysical study of Triazole-based small molecules are novel inhibitors of phosphatidylinositol-4,5-bisphosphate binding pleckstrin homology domain. The SPR based competitive binding, FRET, lipid pull-down assay and cellular localization studies confirm the inhibition of PH domain of PLCδ to membrane targeting. In-sillico docking study gives us total binding mode of these synthesised small molecules to PLCδ1-PH domain.

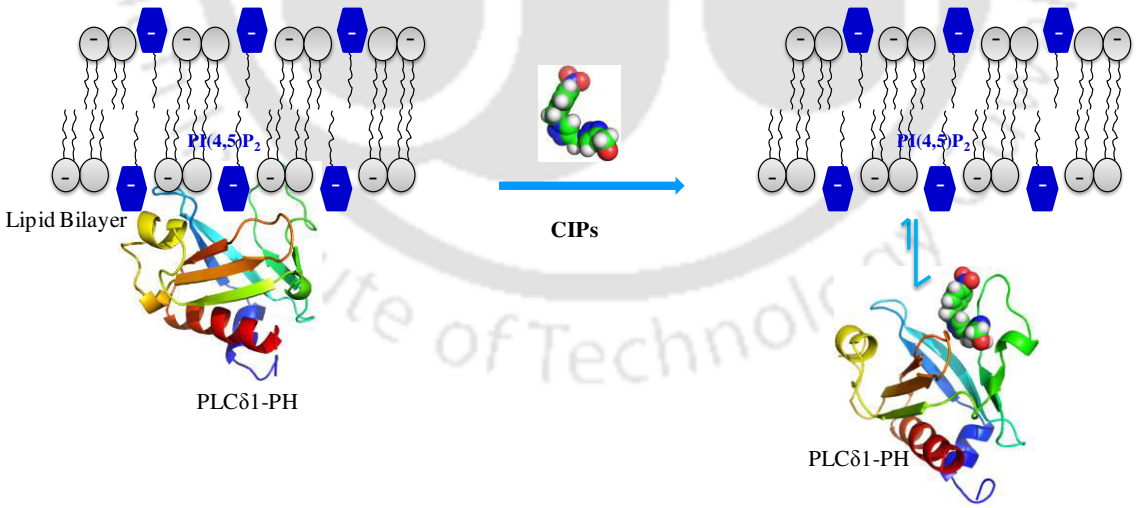

5.1. Background and Focus of the Present Work

In response to specific stimuli, various cytosolic proteins are reversibly recruited to the cellular membranes and form dynamic signalling complexes with specific lipid molecules, including phosphatidylinositols (PIPs). The PIPs lipids have drawn much attention due to its various cellular functions through a plethora of effector proteins.[1-4] A number of human diseases which are directly or indirectly linked with PIP-binding/metabolism have been identified and become an exciting therapeutic target in biomedical research.[2, 3, 5-8] Phosphatidylinositol-4,5-bisphosphate ($PI(4,5)P_2$) is the most abundant PIP in the plasma membrane (PM). Hydrolysis of $PI(4,5)P_2$ to diacylglycerol (DAG) and inositol-1,4,5-trisphosphate ($I(1,4,5)P_3$) by activated phospholipase C (PLC) enzymes is one of the crucial cellular signaling pathways that regulates Ca^{2+} release from endoplasmic reticulum (ER) and protein kinase C (PKC) activator DAG. Various membrane receptors including G-protein-coupled receptors (GPCRs) strongly interact with PLC enzyme and regulate $PI(4,5)P_2$ turnover and consequent downstream cell signaling pathways. $PI(4,5)P_2$ regulates several proteins including PLCδ, Ras GTPase activating protein (RasGAP) and pleckstrin, which mediate a wide verity of cellular process.[9-12] Improper cellular functions of these effectors proteins are associated with disorder such as neurodegenerative, cardiovascular diseases and others.[13, 14] The PI-kinase I/II and SH2-containing Inositol-5′-Phosphatase (SHIP), phosphatase and tensin homolog (PTEN) enzymes phosphorylate phosphatidylinositol-4-phosphate (PI(4)P)/phosphatidylinositol-5-phosphate (PI(5)P) and dephosphorylate phosphatidylinositol-3,4,5-trisphosphate ($PI(3,4,5)P_3$), respectively to generate $PI(4,5)P_2$ at the inner PM in responses to various stimuli.[15, 16] $PI(4,5)P_2$ is phosphorylated by class I PI-3-kinase to form $PI(3,4,5)P_3$, which regulates cellular functions of several crucial signaling proteins including AKT.

The $PI(4,5)P_2$ generation recruits several proteins to the PM through their interaction with pleckstrin homology (PH)- or other PIP-binding modules. This $PI(4,5)P_2$-dependent membrane association of the lipid binding modules are necessary and sufficient for activation and proper functioning of the effector proteins including PLCδ. PLCδ activation proceeds after $PI(4,5)P_2$-binding of the PH domain at the inner PM that reorient the EF-hands–C2 domain–TIM barrel unit so that the catalytic domain is in a productive orientation relative to the membrane. Recent studies reported that in addition to PH domain, C2 domain of PLCδ also interacts with the membrane and plays an important role in PLCδ activation.[17-19] .

Design of Triazole Based Small Molecule Inhibitors- However, development of inhibitors for PIP/PH-domain interactions to regulate enzyme activities had not been substantially described yet. Using the similar hypothesis, we recently demonstrated that development of DAG-responsive C1 domain based activator can be considered as an alternative target to regulate the activities of the PKC enzymes.[26-28] Emmanuelle Meuillet and coworkers demonstrated that PH-domain targeting lipid-based drug, 3-deoxy phosphatidylinositol ether lipid (DPIEL) and PHT-427 can be useful for the treatment of cancer and other human diseases.[22, 29] Alexei Degterev and co-workers demonstrated that small molecules like PITENINs can inhibit the PI(3,4,5)P_3 binding of AKT1/PDK1-PH-domains resulting in down-regulation of PI3-Kinase/PDK1/AKT1 pathways.[8] So far there are only a few PLC regulators that play a significant role in understanding the PI(4,5)P_2 mediated cellular signaling pathways.[18, 19] Neomycin is known as a regulator of PI(4,5)P_2-PLC enzyme interactions and PLC induced PI(4,5)P_2 hydrolysis at the cellular membranes. However neomycin directly interacts with the PI(4,5)P_2 molecules present at the membrane through an electrostatic interaction and blocks PLCδ enzyme activity.[19] However, there is no report of PH domain specific PLC regulator.

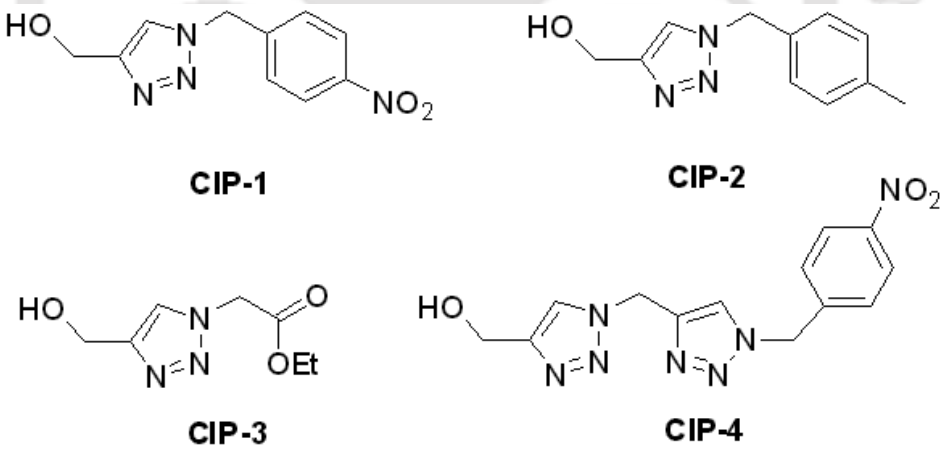

Figure 5.1.1. Structure of synthesized triazole-based small molecules

In this regard our current study describes the development of 1,2,3-triazol-4-yl methanol-based antagonists, **CIP**s for PI(4,5)P_2/PLCδ1-PH domain binding. These compounds at lower concentrations showed certain degree of selective inhibitory effect towards different PH-domains used for the current study. The 1,2,3-triazol-4-yl methanol moiety and nitro group of the compounds play a crucial role in distinguishing the PH-domains. Potent compound, **CIP-**

4 can competitively interact with the PLCδ1-PH domain and displace it from PM to cytoplasm. We believe that these non-lipid potent compounds would be able to inhibit PI(4,5)P_2 targeted PIP-binding proteins/enzyme under cellular environment and regulate its cellular signaling pathways.

5.2. RESULTS AND DISCUSSION

PIP signalling pathway is considered as one of the most commonly deregulated pathways in several human diseases including cancer.[5, 21, 40, 41] For this reason development of potent and specific inhibitors for the effector proteins associated with this PIP-kinase/phosphatase pathway is highly demanding in the drug discovery and related research fields.[42] However, targeting the catalytic domain of these enzymes to develop inhibitor remained quite challenging. For example, several potent inhibitors of AKT1 enzyme turn out to be relatively toxic, presumably due to the inhibition of other ser/threonine kinases.[21, 43] On the other hand, small molecules such as DPIEL and perifosine, developed for the inhibition of PIP/PH-domain interaction are comparatively nontoxic and offer a better therapeutic strategy than inhibitors for ATP-site.[22, 41] In recent years, studies have been carried out to identify phosphate or nonphosphate containing small molecules as being inhibitors for PIP-binding domains.[8, 21, 44, 45]

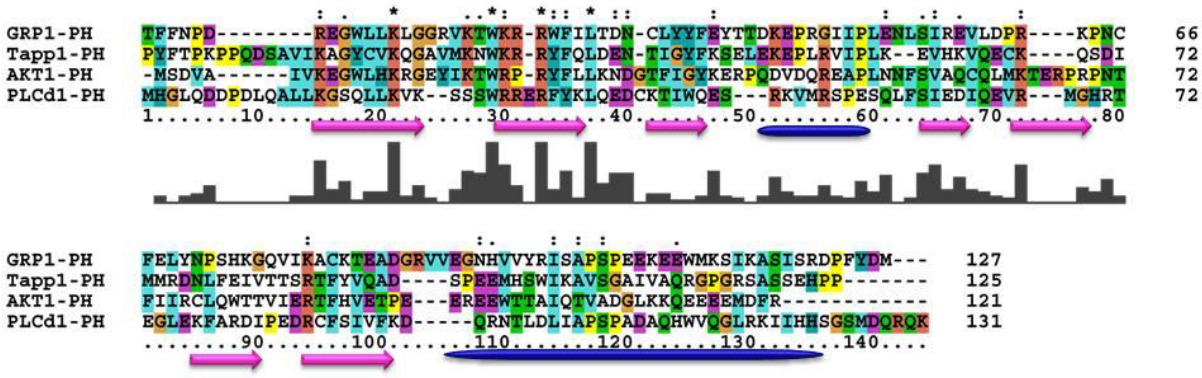

Figure 5.2.1: Amino-acid sequence alignment of the AKT1, GRP1, TAPP1, PLCδ1-PH domains are shown using Clustal X. Secondary structural elements of the PH domains are shown below the alignments with colored pink (β-sheets) or blue (α-helices). PH domain residues forming the cationic patch at its base are labelled with chocolate squares.

It is well documented that stimulated PLCδ1 enzyme hydrolyze PI(4,5)P_2 to DAG and IP_3, which acts as second messengers. Deregulation of PLC enzyme activity is related with

diverse diseases including cancer, cardiovascular diseases.[46-48] Therefore, development of small molecule-based inhibitors is considered as potential pharmacological tools to investigate the roles PLC enzyme in diseases and can be used as candidates for drug discovery. The interaction of PH domain with $PI(4,5)P_2$ at the inner PM is essential for PLCδ enzyme to hydrolyze $PI(4,5)P_2$.[18, 19, 49] In this regard, we have synthesized 1,2,3-triazol-4-yl methanol derivatives targeting the $PI(4,5)P_2$ binding PH-domain of PLCδ1-PH domain (Figure 5.1.1). The compounds were synthesized according to the reported procedure using CuO nanoparticles as catalyst.[50-52] Typically, all molecules were designed such a way, that there must be 1,2,3-triazol-4-yl methanol moiety, which are critical in forming more hydrogen bond with their binding partners and can be fitted inside the shallow positively charged binding pocket of the PLCδ1-PH domain (Figure 5.2.1). The nitro group and an additional triazole ring were installed to understand their impact in hydrogen bond formation with the amino acid residues within the PH-domain binding pocket. Thus, the impact of this study is not only inhibition constant measurement but also elucidate their binding mechanism.

Surface Plasmon Resonance based-competitive Binding Assay—We first measured the efficiency of the compounds in disrupting the PIP/PH domain interaction, by using SPR-based competitive binding assay, an useful technique for quantitative determination of binding and/or inhibition affinities in real-time.[21, 30] All SPR measurements were performed using two parallel flow-channel systems (control and active channel). Liposomes of PC/PE/PS (60/20/20) and PC/PE/PS/PIP (57/20/20/3) were coated on control and active channel, respectively. For all measurements only protein or protein equilibrated with **CIP** compounds were passed over control channel to active channels. To remove any non-specific binding of protein on the liposomal surface, RU of control channel was subtracted from RU of active channel. Control experiments with only compound binding on the liposome surfaces showed almost no effect on RU of protein. PIP selectivity, of the respective PH domains was also tested under similar experimental conditions. The calculated % of inhibition values from SPR measurements showed that compounds **CIP-1** and **CIP-4** strongly interact with the PLCδ1-PH domain and inhibits its binding with the $PI(4,5)P_2$ lipid under liposomal environment (Figure 5.2.2A). The compounds **CIP-1** and **CIP-4** with 5 μM concentration showed 83% and 72% inhibitory effect for $PI(4,5)P_2$/PLCδ1-PH domain interactions, respectively (Table 5.2.1). For further understanding of this inhibitory effect of the compounds on $PI(4,5)P_2$/PLCδ1-PH domain interaction, we also carried out SPR

measurements in a concentration dependent manner (Figure 5.2.2B,C). The analysis clearly showed that the relative RU values of the SPR sensorgrams of PLCδ1-PH domain decrease as a function of concentration of the compounds. These results clearly suggest that the compounds, **CIP-1** and **CIP-4** could affect the $PI(4,5)P_2$ /PLCδ1-PH domain interaction, either by blocking the binding site or by altering the protein conformation.

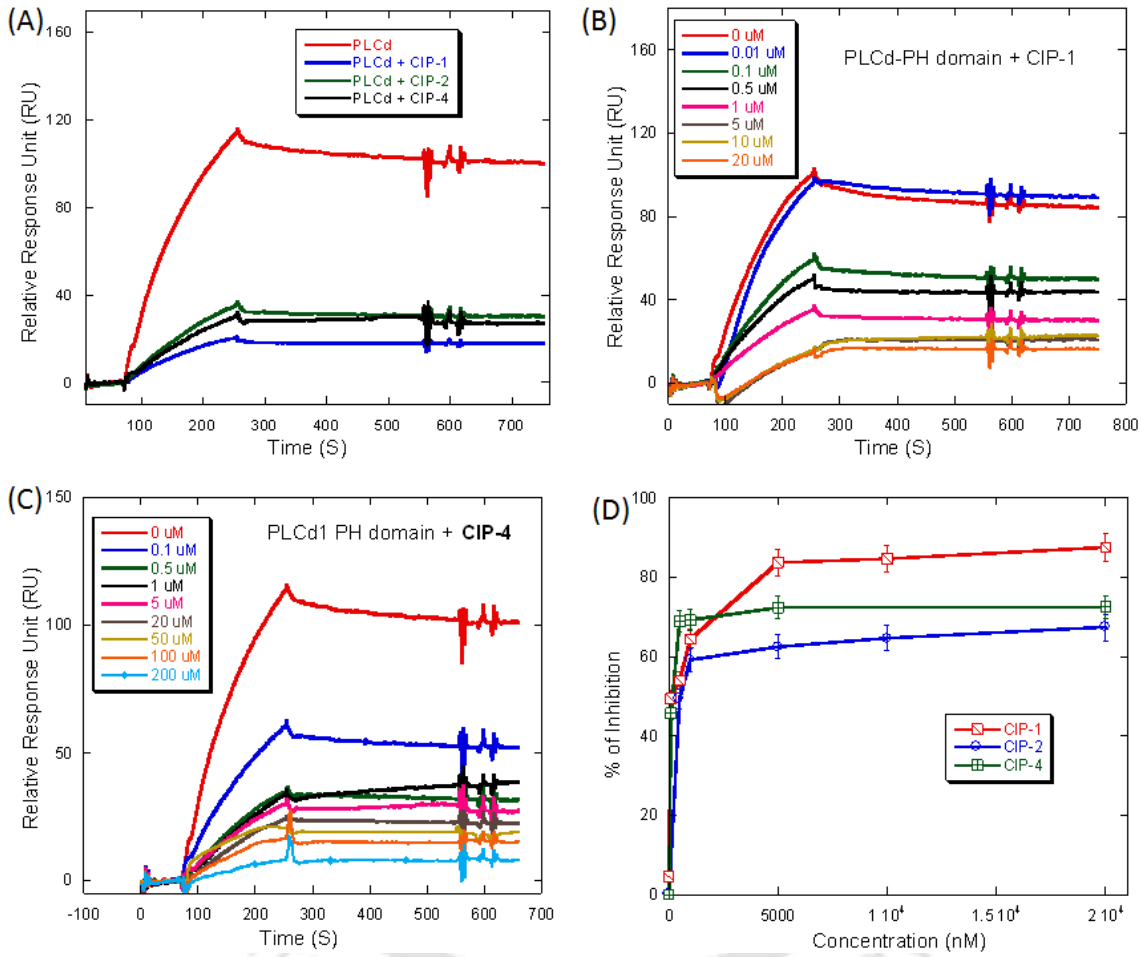

Figure 5.2.2. Screening of PI(4,5)P2/PLCδ1-PH domain (500 nM) interaction selectivity by compounds (5 µM) (A). Surface plasmon resonance sensorgrams of PI(4,5)P2 binding PLCδ1-PH domain in the presence of increasing concentration of compounds **CIP-1** (B) and **CIP-4** (C). Selectivity analysis (% of inhibition) of the compounds for PI(4,5)P2/PLCδ1-PH domain inhibition (D). PC/PE/PS/PI(4,5)P2 (57/20/20/3) and PC/PE/PS (60/20/20) vesicles were used as active and the control surface, respectively. Values represent the mean ± SD from triplicate measurements.

Table 5.2.1. Relative Inhibitory Activity of the Compounds Measured by Competitive-Surface Plasmon Resonance Analysis

Protein	Relative inhibitory activity (%)				IC_{50} values (nM)			
	CIP-1	**CIP-2**	**CIP-3**	**CIP-4**	**CIP-1**	**CIP-2**	**CIP-3**	**CIP-4**
PLCδ1-PH	83 ± 4	62 ± 3	-	72 ± 3	113 ± 7	159 ± 11	-	53 ± 9
TAPP1-PH	18 ± 2	41 ± 4	-	21 ± 2	647 ± 33	106 ± 8	-	1112 ± 78
AKT1-PH	44 ± 2	55 ± 2	4 ± 1	33 ± 3	175 ± 21	315 ± 32	NM	3799 ± 98
GRP1-PH	56 ± 3	58 ± 5	-	52 ± 4	145 ± 11	216 ± 9	-	789 ± 35

Protein, 500 nM; % of inhibition was calculated using 5 μM compound concentration; measurements were performed in 20 mM HEPES buffer at pH 7.4 containing 160 mM KCl; NM, not measured. Values represent the mean ± SD from triplicate measurements.

The calculated IC_{50} values for **CIP-1** and **CIP-4** compounds were 113 and 53 nM, respectively for the $PI(4,5)P_2$/PLCδ1-PH domain interaction, indicating their strong binding pattern under experimental conditions. PLCδ1-PH domain is reported as cellular marker of $PI(4,5)P_2$ lipid.[2, 9, 15, 19] To determine the selectivity of potent compounds in inhibiting the $PI(4,5)P_2$/PLCδ1-PH domain interaction, we also measured their inhibitory effect on other PIPs binding PH-domains (Figure 5.2.3). It is well documented that AKT1-PH domain strongly interact with both $PI(3,4,5)P_3$ and $PI(3,4)P_2$, whereas GRP1 and TAPP1-PH domains selectively interacts with $PI(3,4,5)P_3$ and $PI(3,4)P_2$ respectively.[23]

We measured the inhibitory effects of compounds **CIP-1** and **CIP-4** on $PI(3,4,5)P_3$/AKT1-PH domain (IC_{50} values were 175 and 3799 nM, respectively), $PI(3,4,5)P_3$/GRP1- PH domain (IC_{50} values were 159 and 789 nM, respectively) and $PI(3,4)P_2$/TAPP1-PH domain (IC_{50} values were 647 and 1112 nM, respectively) interactions (Table 5.2.2). Concentration dependent % of inhibition values of **CIP-4** for different PIP/PH domain interactions were shown in Table 5.2.2.

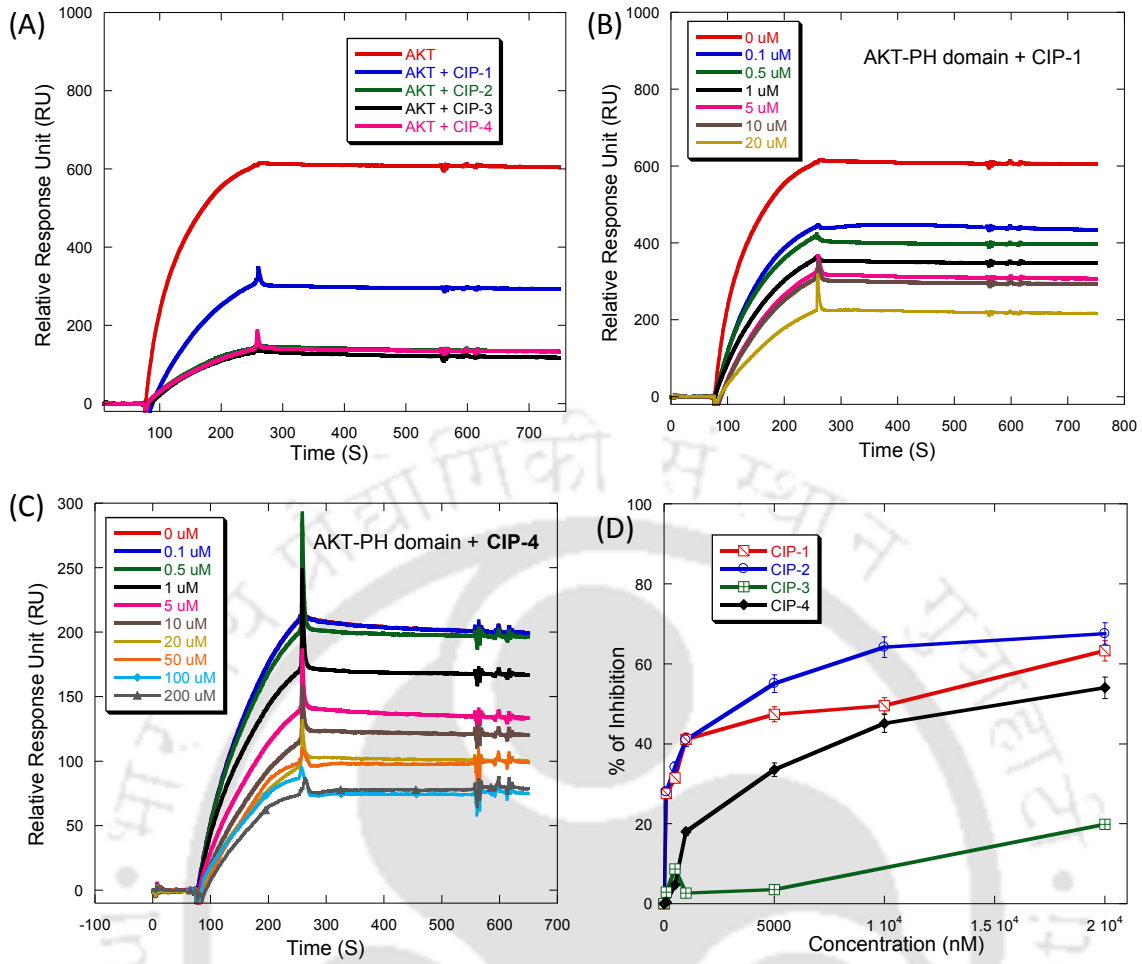

Figure 5.2.3. The inhibitory effects of compound on the interaction between AKT1-PH domain and PI(3,4,5)P_3. Specificity screening of PI(3,4,5)P_3/AKT1-PH domain (500 nM) inhibition by compounds (5 μM). Surface plasmon resonance sensorgrams of PI(3,4,5)P_3 binding AKT1-PH domain in the presence of increasing concentration of compounds **CIP-1** and **CIP-4**. Specificity analysis (% of inhibition) of the compounds for PI(3,4,5)P_3/AKT1-PH domain inhibition. Values represent the mean ± SD from triplicate measurements.

Table 5.2.2. Calculation of relative inhibitory effect of compound **CIP-4**

Compound,	**Relative inhibitory activity (%)**			
CIP-4	PLCδ1-PH	TAPP1-PH	AKT1-PH	GRP1-PH
5 μM	72 ± 3	21 ± 3	33 ± 3	52 ± 4
50 μM	82 ± 7	29 ± 5	52 ± 5	64 ± 8
200 μM	93 ± 5	47 ± 8	64 ± 7	64 ± 11

These results suggest that compound **CIP-4** have certain degree of selectivity for PI(4,5)P_2 binding PLCδ1-PH domain over PI(3,4)P_2 and PI(3,4,5)P_3 binding PH-domains. Therefore, this competitive binding study suggests that at least a fraction of this potent compound specifically interacts with the PH-domains through its PIPs binding site. However, differential inhibitory effects of the compounds on PIP/PH-domain interactions could be due to their interaction pattern with the amino acid residues within and/or outside the PIP-binding pocket, stability of the compound-PH-domain complexes, effect of compound on membrane bilayer or their synergistic effect. Hence, additional studies are required to determine the specificities and understand their binding mechanism of these compounds for diverse PIP-binding PH-domains.

Molecular Docking Analysis—The SPR-based competitive binding assay showed that the compounds differentially inhibit the PI(4,5)P_2/PLCδ1-PH domain interaction under the similar experimental conditions. The relative inhibitory activity of compound **CIP-4** for PI(4,5)P_2/PLCδ1-PH domain was much higher than other PIP-binding PH-domains, which indicate that **CIP-4** was able to distinguish different PH-domains tested under the similar experimental conditions. Structural analysis revealed that all these tested compounds contain 1,2,3-triazol-4-yl methanol moiety, consequently to elucidate the probable binding mode for different inhibitory efficacies, molecular docking analysis was performed.

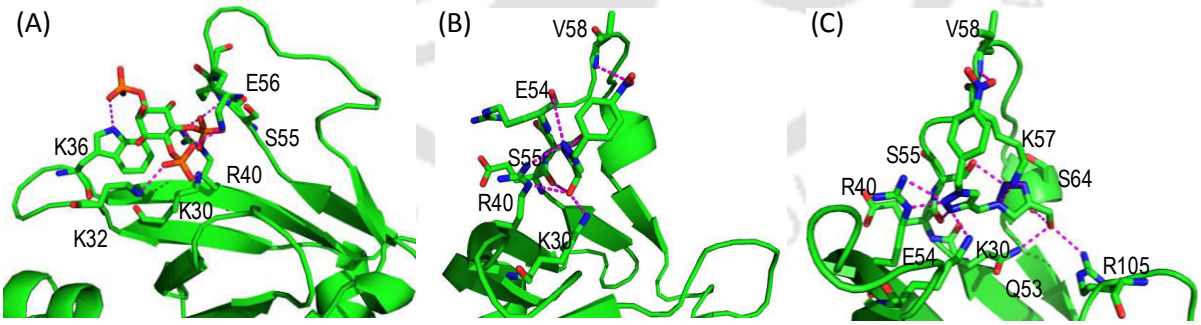

Figure 5.2.4. Structure of PLCδ1-PH domain (1MAI) in complex with IP3 (A). Model structures of ligands **CIP-1** (B) and **CIP-4** (C) docked into the PIP-binding site of the PLCδ1-PH domain (1MAI). Residues involved in interactions through hydrogen bond formation are shown using dashed lines (pink).

The reported crystal structure of PLCδ1-PH domain (1MAI) in complex with inositol 1,4,5-triphosphate (IP_3) provides a detail insight into the mode of ligand interactions within the

binding pocket.[32] Structural analysis and structure-activity studies showed that phosphate groups attached to myo-inositol ring of IP_3 preferably interact with the K30, K32, W36, R40, S55, R56 and R57 residues through hydrogen bond formation.[10, 15, 19, 32] Blind molecular docking analysis demonstrated that the 1,2,3-triazol-4-yl methanol derivatives preferably interact with PLCδ1-PH domain through its the IP3 binding site. The triazol ring,

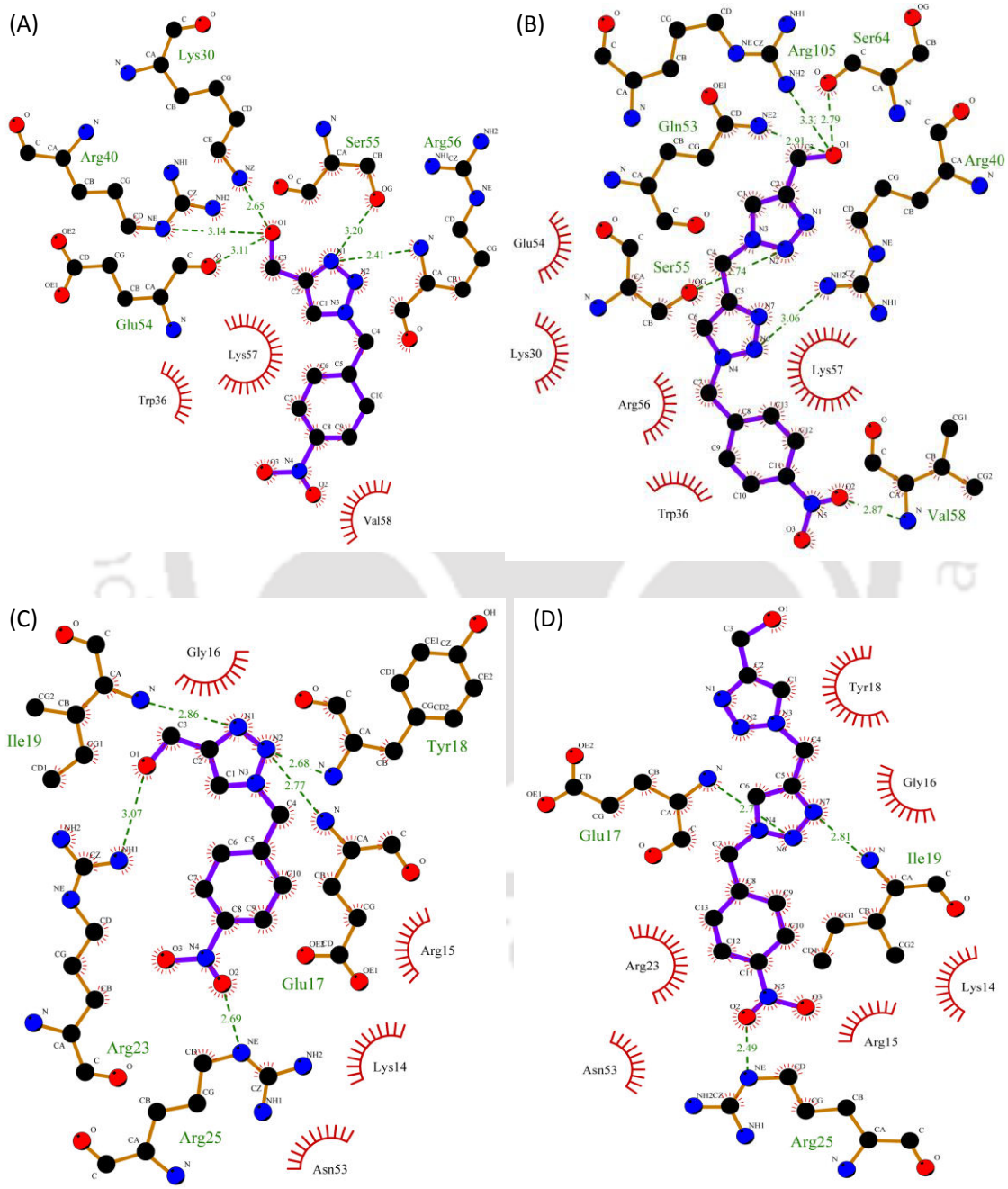

Figure 5.2.5. Lig-plot analysis of **CIP-1** and **CIP-4** docked into PIP binding site of PLCδ1-PH (A, C) and AKT1-PH (B, D) domains, respectively. Residues involved in interactions through hydrogen bond formation are shown using dashed lines.

hydroxy and nitro groups of the compounds could be mainly responsible for their interaction with the cationic groove of the PLCδ1-PH domain (Figure 5.2.4). For further analysis best docking poses were selected based on the number of interactions with the protein, similarity of docking orientation and position within the PIP-binding site of the protein. The calculated in-silico interaction energies between the ligands and PLCδ1-PH domain protein are of high negative values, suggesting acceptable docking poses for further analysis (Table 5.2.3). The docking poses showed that the pharmacophores of compounds **CIP-1** and **CIP-4** could form hydrogen bonds with the side chain or backbone carbonyls/amide protons of PLCδ1-PH domain through its IP_3 binding site (Figure 5.2.4 and Figure 5.2.5).

Table 5.2.3. Theoretically Calculated Interaction Energy between Ligand and PH-domains

Protein	Ligand	Interaction energy between ligand and Protein (kcal/mol)	Hydrogen bonding energy (kcal/mol)
PLCδ1-PH Domain	**CIP-1**	-102.5011	-20.4174
		-99.9215	-20.8066
		-98.4244	-17.8983
	CIP-4	-129.5161	-21.1872
		-126.2811	-18.4781
		-122.6232	-24.3443
AKT1-PH Domian	**CIP-1**	-107.3021	-20.7979
		-101.1464	-21.1471
		-99.4748	-19.5755
	CIP-4	-133.9121	-20.2021
		-131.4982	-20.0973
		-129.3274	-19.1821

However, the docking results did not show any significant difference in their number of interactions or interacting residues. **CIP-1** and **CIP-4** showed 5 and 6-hydrogen bond formation with the PLCδ1-PH domain, respectively (Figure 5.2.4). Calculated IC_{50} values of the compounds showed that **CIP-4** has approximately 2-fold stronger binding affinity than **CIP-1**. Therefore, strength of interactions and surface area of the compounds may be important criterion in showing stronger binding properties. We also performed molecular docking analysis of these ligands with AKT1-PH domain (1H10)[31]. The docking results showed that the ligands specifically interact with the AKT1-PH domain through its PIP-binding site in a similar pattern as with PLCδ1-PH domain. In particular, compound **CIP-4** forms only 3-hydrogen bonding with AKT1-PH domain, which was also reflected in its IC_{50}

values. Therefore, the molecular docking analysis predicts that these ligands interact with the PH-domain preferably through their PIP-binding site.

Structural Change Measurement: Lower IC_{50} values of the compounds could be due to the structural change of the PH-domains in the presence of the compounds that could prohibit the PH-domains to interact with the PIP containing membranes. In this regard, we performed circular dichroism (CD) spectral analysis to understand whether interactions of compounds with the PH-domains alter the structural integrity or not. The CD spectra of the PLCδ1-PH domain in the absence/presence of compounds **CIP-1** and **CIP-4** are shown in Figure 5.2.6A. The negative ellipticity in the range of 225-200 nm and the positive ellipticity around 195 nm

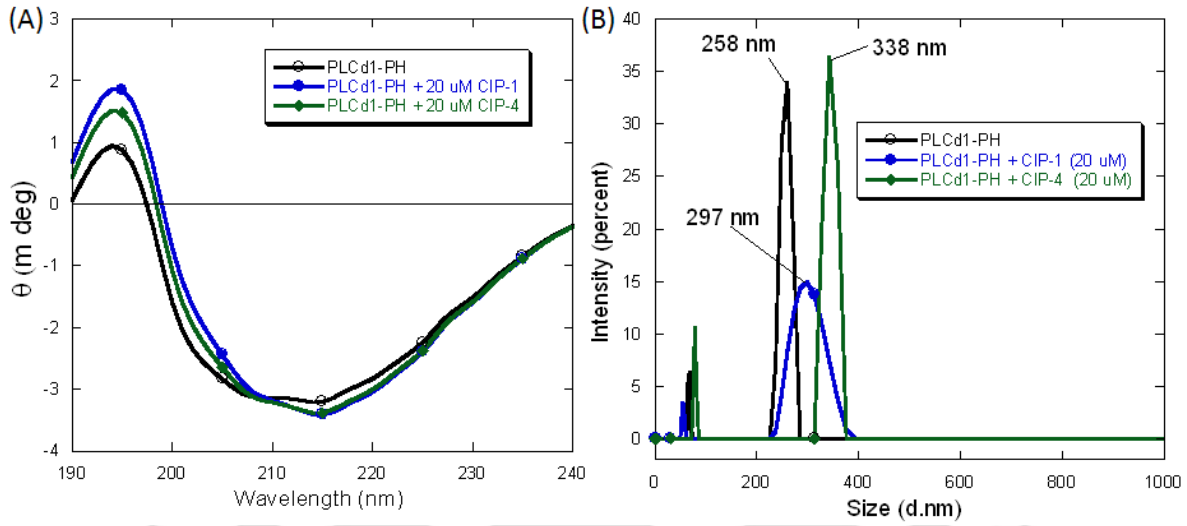

Figure 5.2.6. Effect of compounds on the secondary structural content of the PLCδ1-PH domain. Far-UV CD spectra of PLCδ1-PH domain in the absence and presence of compounds (20 μM) in 10 mM phosphate–containing 10 mM NaCl buffer (pH 7.2) (A). Size distribution of PLCδ1-PH domain in the absence or presence of compounds (20 μM, at t = 5 min) in aqueous solution (PBS buffer pH 7.0) at 25 °C (B).

are the characteristic of protein secondary structural features such as α-helix and β-sheet. The spectral data showed that in the presence of compounds **CIP-1** and **CIP-4** there is almost no change in their secondary structural pattern of PLCδ1-PH domain in the far UV-CD spectrum. The change in beta sheet content is little bit higher in the presence of **CIP-4** than **CIP-1**, which is in correlation with the IC_{50} values. However, larger change in β-sheet content of the PLCδ1-PH domain indicates that the compounds interact with the PH-domain though it's PIP-binding site which is composed of seven β-sheets and connecting loop regions. It is important to mention that any increase in helical content of the PLCδ1-PH

domain upon ligand binding would be small and that any increase in CD-signal in the range of 225-200 nm might be obscured by the change in contribution from high β-sheet content of the PH-domain structure. In addition our dynamic light scattering (DLS) measurements data also pointed out that the compounds did not alter the hydrodynamic sphere of the protein (Figure 5.2.6B). Therefore, our CD and DLS measurements clearly showed that the ligand binding does not significantly alter the secondary structure of the PLCδ1-PH domain.

Membrane Interaction Measurement: Another possibility of the lower IC_{50} values of the compounds could be also due to their interaction with the membrane as was seen in the case of neomycin.[19] It can be assumed that direct interaction of the compounds with the PIP-containing liposomes can alter the membrane dynamics and inhibit the PH-domains to interact with the membranes. Therefore, to understand whether the compounds alter the

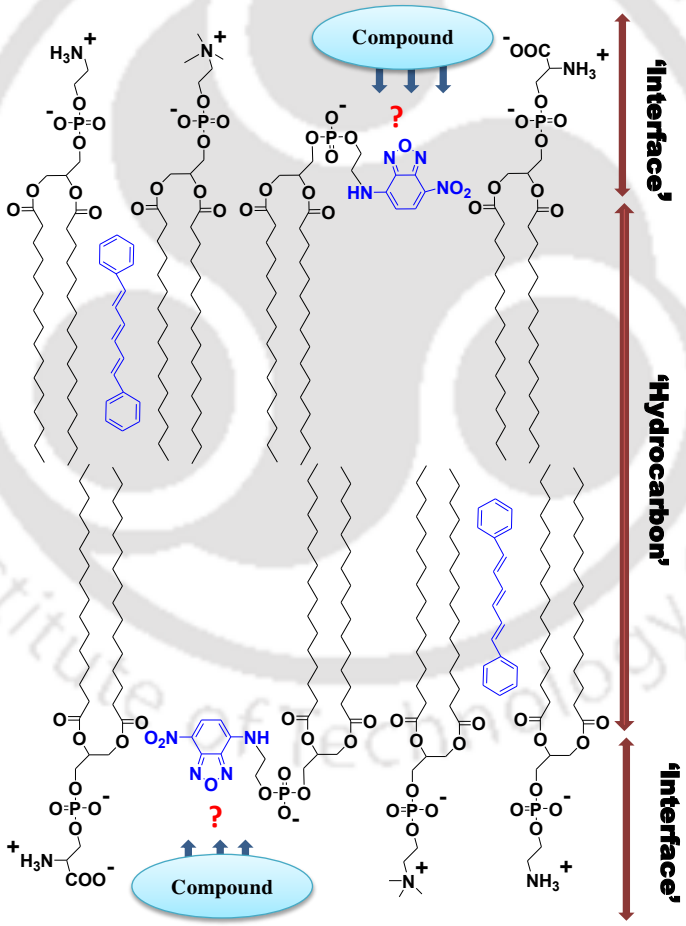

Figure 5.2.7. Schematic representation of DPH and NBD-PE localization in the lipid membrane. The DPH (in blue) localize in the hydrophobic core of the lipid bilayer. The NBD (in blue) group of NBD-PE lipid localize at the interface of the lipid bilayer.

membrane dynamics of lipids and fluidity of the lipid bilayer, we measured the fluorescence anisotropy of 1,6-diphenyl-1,3,5-hexatriene (DPH) and 1,2-diphytanoyl-*sn*-glycero-3-phosphoethanolamine-N-(7-nitro-2-1,3-benzoxadiazol-4-yl) (NBD-PE) under liposomal environment.[28, 34] The membrane composition (PC/PE/PS/PIP) used for the SPR studies contain anionic lipids like PS and PIP. We presume that the interaction of the triazole and nitro groups of the compounds with the anionic lipids could alter the membrane organization

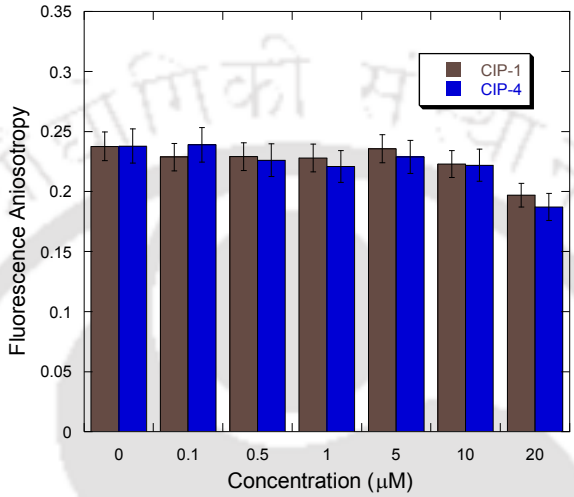

Figure 5.2.8. Anisotropy values of NBD-PE in the absence and presence of the compounds with different concentrations. Values represent the mean ± SD from triplicate measurements.

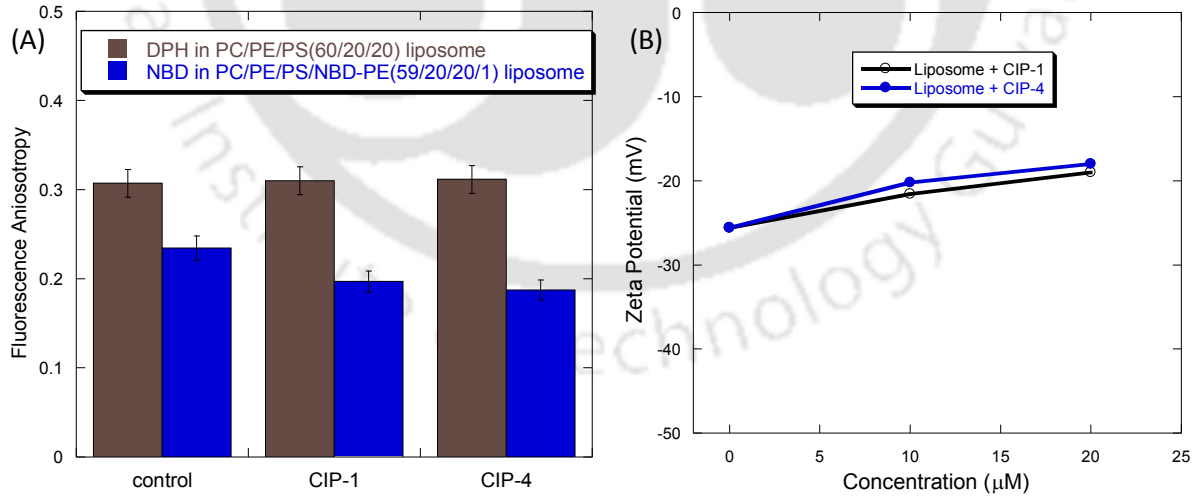

Figure 5.2.9. Fluorescence anisotropy of DPH and NBD-PE embedded in PC/PE/PS (60/20/20) and PC/PE/PS/NBD-PE (59/20/20/1) liposomes for compounds (A). Control: no ligand was added to the liposomes. Zeta potential of the PC/PE/PS/PI(4,5)P_2 (57/20/20/3) liposomes in the presence of compounds with different concentrations (B). 100 μL of liposomes from 0.5 mg/mL of total lipid was used for all measurements. Values represent the mean ± SD from triplicate measurements.

by blocking the protein binding under the liposomal environment and allowing the competitive-SPR measurements to show high inhibitory effect by the compounds. The DPH molecules generally embedded within the hydrophobic core of the lipid bilayer, NBD of NBD-PE is presumed to be mainly localized at the membrane interface (Figure 5.2.7) therefore changes in fluorescence anisotropy values can be useful in evaluating the modulation of lipid-bilayer fluidity induced by membrane-active compounds. Figure 5.2.9 and Table 5.2.4 represent the change in anisotropy values of DPH and NBD-PE molecules in

Table 5.2.4. Anisotropy Values of the Membrane Sensitive Probes in the Absence and Presence of the Compounds

Compound	Anisotropy of DPH	Anisotropy of NBD-PE
liposome	0.30706 ± 0.00829	0.22764 ± 0.05691
CIP-1	0.31004 ± 0.01141	0.19695 ± 0.02564
CIP-4	0.32135 ± 0.01148	0.18729 ± 0.06543

Values represent the mean ± SD from triplicate measurements.

the presence of anionic hybrid lipids under liposomal environment. NBD fluorescence anisotropy was also measured in the presence of different compound concentrations (Figure 5.2.8). The variations in DPH fluorescence anisotropy values affected by the compounds are very small, indicating almost no change in ordering of the core of lipid bilayer. However, NBD fluorescence anisotropy values get affected only at higher concentrations of the compounds. This indicates that ordering of the interfacial region of the lipid bilayer get affected by the compounds only at higher concentrations. The anisotropy measurements were performed at 25 ºC, which is much above the phase transition temperature of PC/PE/PS (60/20/20) lipid bilayers. Therefore, the lipids are in liquid-crystal (LC) phase at 25 ºC and the partition coefficients of DPH/NBD-PE are expected to be higher than solid-gel (SG) phase.[28, 53] We also measured the change in surface potential of the liposomes (PC/PE/PS/PI(4,5)P_2) in the absence and presence of the compounds, to determine whether their interaction could alter the surface charge of the liposmes. The results clearly showed that the compounds have weak effect on the surface potential values of the liposomes, indicating their weak interaction pattern with membrane surface (Figure 5.2.9). Therefore, the stronger inhibitory effects of the compounds are predominantly due to its stronger binding with the respective PH-domains.

Förster Resonance Energy Transfer Analysis- The membrane binding surface, surrounding the PIP-binding site of the PH domain allows PLCδ1 to interact with the cellular

membranes.[37] This PI(4,5)P_2 dependent membrane interaction of the PLCδ1-PH domain activates PLCδ1 enzyme.[17] Therefore, for further understanding of the selectivity of these compounds in inhibition of the PI(4,5)P_2/PH-domain interactions, we performed competitive-protein to membrane Förster resonance energy transfer (FRET) analysis. One of the Trp-residues (W27) is localized close to the PI(4,5)P_2 binding site of the PLCδ1-PH domain and provides as FRET donor, and a low density of membrane-embedded, dPE lipid serve as the FRET acceptor. In this assay we first allowed the PH-domain to bind the dPE labeled PI(4,5)P_2 containing liposomes, then the compounds were added to confirm that they interact with the PH-domain through its PIP-binding site. The decrease in fluorescence signal at 505 nm wavelength, in the presence of compounds confirmed its binding to PLCδ1-PH domain under liposomal environment (Figure 5.2.10). However, detailed spectral analysis showed a concomitant decrease of Trp-fluorescence signal (at 340 nm). Our control experiment showed

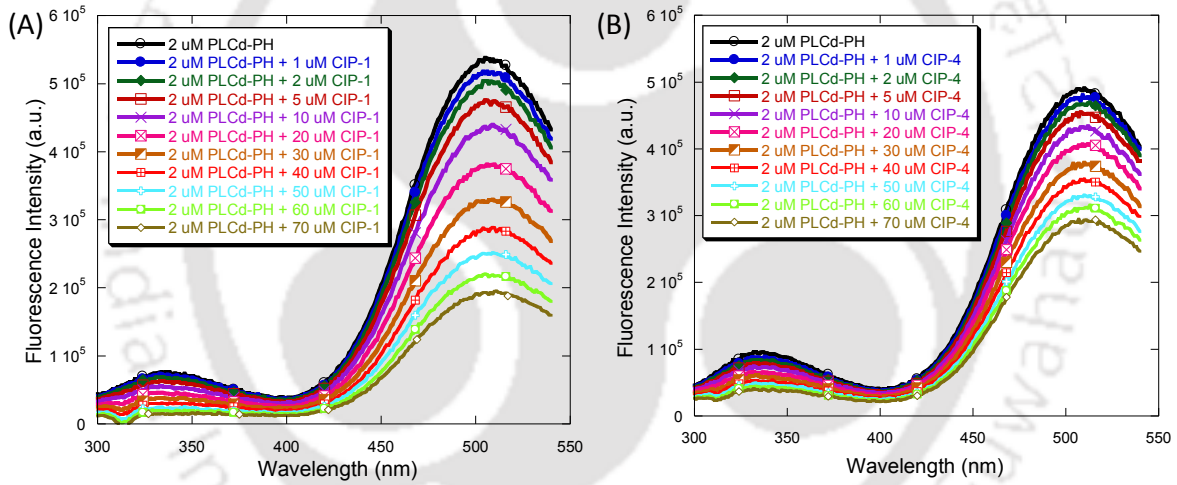

Figure 5.2.10. Representative protein-to-membrane FRET experiment under liposomal environment. Addition of increased concentration of compounds, **CIP-1** (A) and **CIP-4** (B) to PLCδ1-PH domain (2 μM) bound to the active liposome (PC/PE/PS/dPE/PI(4,5)P_2 (56/20/20/1/3)) decreases the FRET signal at 509 nm. All the measurements were performed in 20 mM Tris, pH 7.4 containing 160 mM NaCl. Compound concentrations were varied from 0 to 70 μM.

that the compounds directly interact with the PLCδ1-PH domain in solution. Therefore, the decrease in protein-to-membrane FRET signal could be predominantly due to compound dependent Trp-fluorescence quenching of the protein and subsequent displacement of protein from bilayer surface to the bulk solution. Overall, this assay also confirms that the compounds in solution specifically interact with the PH-domain.

Isothermal Titration Calorimetric Measurements- To better understand the binding mechanism of the compounds, **CIP-1** and **CIP-4** with the PLCδ1-PH and AKT1-PH domains, we performed isothermal titration calorimetric (ITC) measurements. Representative titration plots of both the compounds with PLCδ1-PH domain showed an exothermic reaction

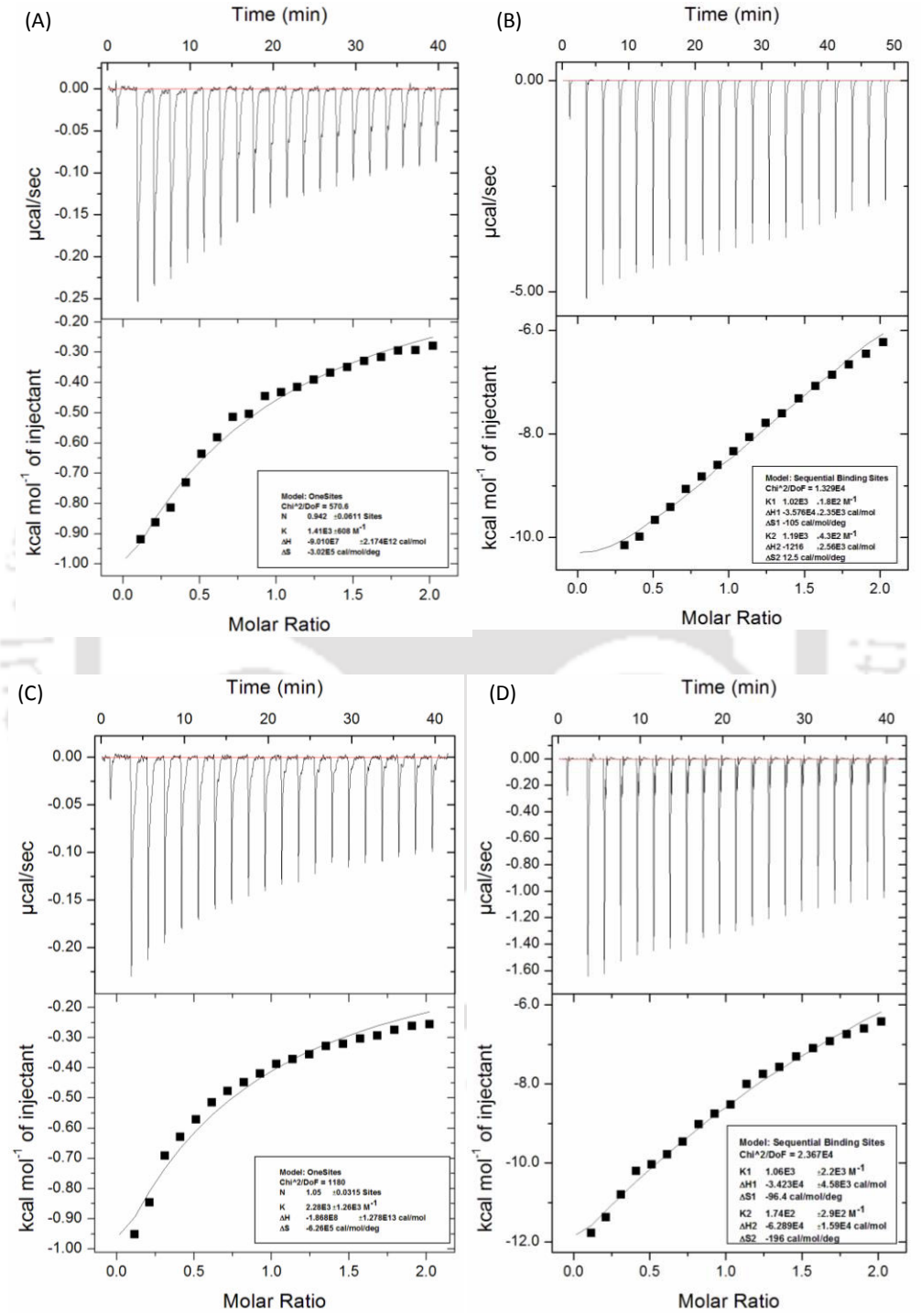

Figure 5.2.11. Isothermal calorimetric titration of PLCδ1-PH and AKT1-PH domains with compounds. Original titration and integrated peak areas of PLCδ1-PH and AKT1-PH domain with **CIP-1** (A and B) and **CIP-4** (C and D), respectively.

with one-step binding mechanism (Figure 5.2.11). This indicates that stronger hydrogen bond formation and van der Waals interactions between the compounds and cationic groove present inside the PIP- binding site of the PLCδ1-PH domain are predominant factors for their interactions. The binding parameters are in accordance with spectroscopic and molecular docking analysis results. Interactions of both the compounds with AKT1-PH domain followed an exothermic reaction with two-step binding mechanism (Figure 5.2.11). However, both the compounds have weaker binding affinity for AKT1-PH domain in comparison with the PLCδ1-PH domain. Therefore, ITC analysis clearly suggests that the compounds in solution interact with the PLCδ1-PH and AKT1-PH domain.

Lipid-Pull down Assay: The inhibition of PI(4,5)P_2/PLCδ1-PH domain interaction under liposomal environment was also qualitatively determined by lipid pull-down assay.[27, 38, 39] The binding of PLCδ1-PH domain (50 μM) with PI(4,5)P_2 containing liposomes (PC/PE/PS/PI(4,5)P_2 (57:20:20:3)) were measured in the absence or presence of compounds (100 μM), **CIP-1** and **CIP-4** at physiological pH. The coomassie blue staining of the SDS-PAGE gel clearly showed that the PLCδ1-PH domain binding to the PI(4,5)P_2 containing liposomes was almost completely diminished by the compound **CIP-4** (Figure 5.2.12A).

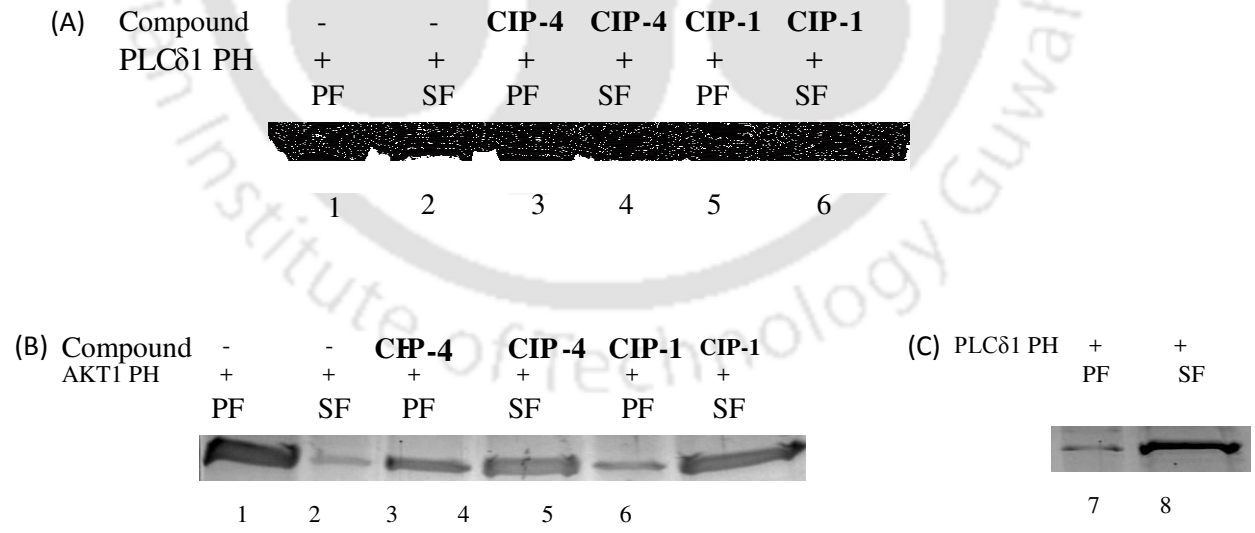

Figure 5.2.12. Coomassie blue stained SDS-PAGE gel images of liposome binding assay. PC/PE/PS/PI(4,5)P2 or PC/PE/PS/PI(3,4,5)P_3 (57/20/20/3) liposomes were used for PLCδ1-PH domain or AKT-PH domain binding study respectively. Lanes 1, 3 and 5 were liposome bound fraction and 2, 4 and 6 were unbound fraction of PLCδ1-PH domain in the presence of compound **CIP-1** and **CIP-4** (A). Lanes 1, 3 and 5 were liposome bound fraction and 2, 4 and 6 were unbound fraction of AKT1-PH domain in the presence of compound **CIP-1** and

CIP-4 (B). PC/PE/PS (60/20/20) was used as control liposome. Lane 7 and 8 were liposome bound and unbound fraction of PLCδ1-PH domain (C). Liposome concentration 100 μM; Protein concentration 50 μM; Compound concentration, 100 μM; PF, palate fraction; SF, soluble fraction.

However, compound **CIP-1** was not that efficient in displacing the PLCδ1-PH domain from its liposome bound state. The inhibition of $PI(3,4,5)P_3$/AKT1-PH domain interaction by the potent compounds was also measured using similar methods. Visual inspection of coomassie blue stained SDS-PAGE gel images revealed that compound **CIP-1** inhibit the $PI(3,4,5)P_3$/AKT1-PH domain interaction more strongly than compound **CIP-4**, under similar experimental conditions (Figure 5.2.12B). Control experiment showed that PLCδ1-PH domain has very weak binding affinity for PC/PE/PS liposome (Figure 5.2.12C). Hence, the liposome-pull down assay results indicate that the PLCδ1-PH domain strongly interact with $PI(4,5)P_2$ containing liposomes and **CIP-4** strongly inhibit the $PI(4,5)P_2$/PLCδ1-PH domain interaction.

Cellular Translocation of PLCδ1-PH domain: To demonstrate the physiological significance of our *in vitro* inhibition/binding studies that show potent compounds strongly interact with PLCδ1-PH domain and inhibits its specific interactions with $PI(4,5)P_2$ under liposomal environment, we measured membrane displacement of GFP-tagged PLCδ1-PH domain in A549 cells. As reported earlier $PI(4,5)P_2$ is mostly present at the inner PM of cells, hence expression of cDNA of GFP-tagged PLCδ1-PH domain allow this protein to be localized at the PM.[9, 15, 54] Freshly prepared compound solutions were added after 24 hours of transfection of cDNA. Cells were treated with compounds for 30 min and then fixed with 4% paraformaldehyde for immunofluorescence study. All measurements were performed for minimum three times with more than 10 cells were monitored for each measurement. In general, more than 80% of cell population showed similar behaviors with respect to PM displacement of PLCδ1-PH domain.The extent of displacement of PLCδ1-PH domain from PM was monitored in the presence of compounds **CIP-1** and **CIP-4** (0 - 100 μM) in a concentration dependent manner (Figure 5.2.13). Confocal microscopic images clearly showed that external addition of **CIP-4** can efficiently displace localized PLCδ1-PH domain from PM. Whereas, extent of displacement of PLCδ1-PH domain from PM is lower by compound **CIP-1**, which is accordance with their *in vitro* binding affinities/IC_{50} values. The results indicate that the $PI(4,5)P_2$/PLCδ1-PH domain interaction is indeed inhibited by the potent compounds under cellular environment.

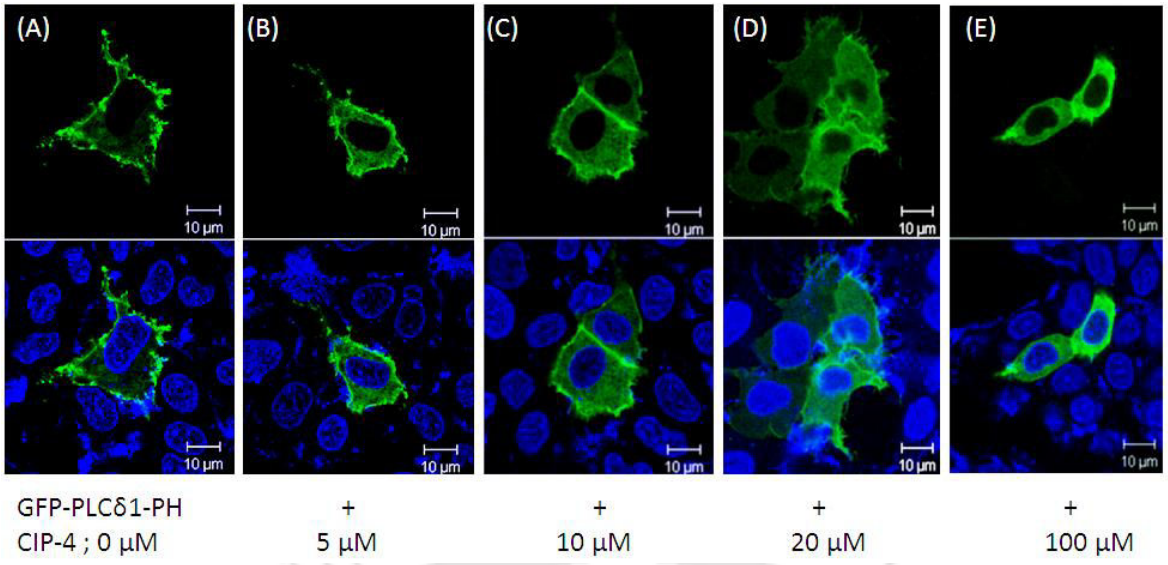

Figure 5.2.13. Effect of compound on cellular localization of GFP-tagged PLCδ1-PH domain in A549 cells. Representative cellular localization pattern of GFP-tagged PLCδ1-PH domain in the absence or presence of compound **CIP-4** with different concentrations, 0 (A), 5 (B), 10 (C), 20 (D) and 100 µM (E). The compound was treated in A549 cells for 30 min and then cells were fixed with 4% paraformaldehyde for immunofluorescence study.

Present study described that compounds with 1,2,3-triazol-4-yl methanol moiety had moderate to strong inhibition of the PI(4,5)P_2 binding to the PLCδ1-PH domain. Through biophysical analyses demonstrate that the interactions between the potent compounds and lipid bilayer are very weak in nature. The compounds preferably localize in the bulk phase of the solution and its pharmacophores are accessible for PH-domain binding under the experimental conditions. The 1,2,3-triazol-4-yl methanol moiety and nitro group are crucial for their interaction with the PH-domains. These compounds have stronger binding affinity for several PH domains, but their affinity differences are negligible except for compound **CIP-4**. The higher binding affinity of **CIP-4** for PLCδ1-PH domain over the other PH-domains including AKT1, TAPP1 and GRP1 proteins could be due to its true selectivity. We hypothesize that stronger binding of the compounds with the PLCδ1-PH domain block its membrane association and PI(4,5)P_2 binding, which is essential for its activity in hydrolyzing PI(4,5)P_2 to IP_3 and DAG under cellular environment. However, the stronger binding affinity and selectivity for PLCδ1-PH domain of compound **CIP-4** over **CIP-1** could be because of the presence of additional triazole ring, which not only provide additional hydrogen bonding with the amino acid residues within the PIP binding pocket but also the surface area of the liagnd required for stronger inhibition of PI(4,5)P_2/ PLCδ1-PH domain interactions.

Recently, neomycin is reported as inhibitor of $PI(4,5)P_2$ binding PLC enzyme, which regulates $PI(4,5)P_2$ hydrolysis at the cellular membranes, but the mechanism of its activity is quite different than compound **CIP-4**.[19] Strong electrostatic interactions between neomycin and $PI(4,5)P_2$ molecules present at the membranes regulate PLC enzyme activity. However, direct binding of neomycin to $PI(4,5)P_2$ can alter biological activities of several other proteins/enzymes including protein kinase C. U73122, ATA are among other reported inhibitors of PLC enzyme, but these compounds targets catalytic site of the enzyme.[55, 56] Whereas, our experimental results show that **CIP-4** is selective and presumably interact with the PH domain of PLCδ1 enzyme through its PIP/IP_3 binding site. In this regard, we hypothesize that selective PLC enzyme activity can be also controlled by these types of compounds, which directly interacts with the PIP-binding domains not with the PIPs. However, further biological studies, including enzyme activity assay, are required to understand the $PI(4,5)P_2$/PH domain inhibition potency of compound **CIP-4** and regulation of PLC enzyme activity.

Conclusion

Taken together, our results show that 1,2,3-triazol-4-yl methanol derivatives strongly interact with PH-domain of PLCδ1, AKT1 and GRP1 proteins but weakly interact with the model membranes. Potent compound **CIP-4** efficiently displaces $PI(4,5)P_2$ from its binding sites of the PH-domains, but failed to displace $PI(3,4)P_2$ and $PI(3,4,5)P_3$ effectively from their respective PH-domain binding pockets, indicating its selectivity for $PI(4,5)P_2$/PH-domain interactions. The interactions of the potent compounds with the PLCδ1-PH domain are exothermic and preferentially interact through its PIP binding site without altering its secondary structure content. The molecular docking analysis indicates that the presence of two triazol moieties and nitro group are essential for their interaction with the PH-domains. The results suggest that these small molecules seem to act principally by binding to the PH-domain and preventing the recruitment to the cellular membranes, where these effector proteins are primarily activated. Our findings also suggest that the 1,2,3-triazol-4-yl methanol moiety can be used to develop nonphosphate-based potential regulators for $PI(4,5)P_2$ binding PH and other lipid binding domains containing proteins.

5.3. Experimental Section

As described in chapter 4 section 4.3

REFERENCES

[1] W. Cho, *Sci. STKE*, 2006, pp. pe7.

[2] W. Cho and R.V. Stahelin, *Annu. Rev. Biophys. Biomol. Struct.*, 2005, **34**, 119-151.

[3] M.A. Lemmon, Nat. Rev. Mol. Cell Biol., 2008, **9**, 99-111.

[4] J.C. Holthuis and T.P. Levine, *Nat. Rev. Mol. Cell Biol.*, 2005, **6**, 209-220.

[5] T.L. Yuan and L.C. Cantley, *Oncogene*, 2008, **27**, 5497-5510.

[6] P. Malaney, R.R. Pathak, B. Xue, V.N. Uversky and V. Dave, *Sci. Rep.,* 2013, **3**, 2035.

[7] S. Sriskantharajah, N. Hamblin, S. Worsley, A.R. Calver, E.M. Hessel and A. Amour, *Ann. N. Y. Acad. Sci.*, 2013, **1280**, 35-39.

[8] B. Miao, I. Skidan, J. Yang, A. Lugovskoy, M. Reibarkh, K. Long, T. Brazell, K.A. Durugkar, J. Maki, C.V. Ramana, B. Schaffhausen, G. Wagner, V. Torchilin, J. Yuan and A. Degterev, *Proc. Natl. Acad. Sci. USA,*2010, **107,** 20126-20131.

[9] K. Itsuki, Y. Imai, H. Hase, Y. Okamura, R. Inoue and M.X. Mori, *J. Gen. Physiol.*, 2014, **143**, 183-201.

[10] T.J. Kubiseski, Y.M. Chook, W.E. Parris, M. Rozakis-Adcock and T. Pawson, *J Biol Chem*, 1997, **272**, 1799-1804.

[11] B. Sot, E. Behrmann, S. Raunser and A. Wittinghofer, *Proc. Natl. Acad. Sci. USA*, 2013, **110**, 111-116.

[12] J. Gomez-Rodriguez, E.A. Wohlfert, R. Handon, F. Meylan, J.Z. Wu, S.M. Anderson, M.R. Kirby, Y. Belkaid and P.L. Schwartzberg, *J. Exp. Med.*, 2014, **211**, 529-543.

[13] J. Shi, L. Birnbaumer, W.A. Large and A.P. Albert, *FASEB J.*, 2014, **28**, 244-255.

[14] L. Trovo, T. Ahmed, Z. Callaerts-Vegh, A. Buzzi, C. Bagni, M. Chuah, T. Vandendriessche, R. D'Hooge, D. Balschun and C.G. Dotti, *Nat. Neurosci.*, 2013, **16**, 449-455.

[15] A. Gericke, N.R. Leslie, M. Losche and A.H. Ross, *Adv. Exp. Med. Biol.*, 2013, **991**, 85-104.

[16] L.S. Ehrlich, G.N. Medina, S. Photiadis, P.B. Whittredge, S. Watanabe, J.W. Taraska and C.A. Carter, *Front. Microbiol.*, 2014, **5**, 234.

[17] J.H. Hurley and J.A. Grobler, *Curr. Opin. Struct. Biol.*, 1997, **7**, 557-565.

[18] S. Scarlata, R. Gupta, P. Garcia, H. Keach, S. Shah, C.R. Kasireddy, R. Bittman and M.J. Rebecchi, *Biochemistry*, 1996, **35**, 14882-14888.

[19] C. Wang, X.N. Du, Q.Z. Jia and H.L. Zhang, *Acta Pharmacol. Sin.*, 2005, **26**, 1485-1491.

[20] K.D. Courtney, R.B. Corcoran and J.A. Engelman, *J. Clinic. Oncol.*, 2010, **28**, 1075-1083.

[21] D. Mahadevan, G. Powis, E.A. Mash, B. George, V.M. Gokhale, S. Zhang, K. Shakalya, L. Du-Cuny, M. Berggren, M.A. Ali, U. Jana, N. Ihle, S. Moses, C. Franklin, S. Narayan, N. Shirahatti and E.J. Meuillet, *Mol. Cancer Ther.*, 2008, **7**, 2621-2632.

[22] E.J. Meuillet, N. Ihle, A.F. Baker, J.M. Gard, C. Stamper, R. Williams, A. Coon, D. Mahadevan, B.L. George, L. Kirkpatrick and G. Powis, *Oncol. Res.*, 2004, **14**, 513-527.

[23] D. Manna, A. Albanese, W.S. Park and W. Cho, *J. Biol. Chem.*, 2007, **282**, 32093-32105.

[24] C.R. McNamara and A. Degterev, *Future Med. Chem.*, 2011, **3**, 549-565.

[25] B. Vanhaesebroeck, L. Stephens and P. Hawkins, *Nat. Rev. Mol. Cell Biol.*, 2012, **13**, 195-203.

[26] N. Mamidi, R. Borah, N. Sinha, C. Jana and D. Manna, *J. Phys. Chem. B*, 2012, **116**, 10684-10692.

[27] N. Mamidi, S. Gorai, J. Sahoo and D. Manna, *Chem. Phys. Lipids*, 2012, **165**, 320-330.

[28] D. Talukdar, S. Panda, R. Borah and D. Manna, *J. Phys. Chem. B*, 2014, **118**, 7541-7553.

[29] E.J. Meuillet, S. Zuohe, R. Lemos, N. Ihle, J. Kingston, R. Watkins, S.A. Moses, S. Zhang, L. Du-Cuny, R. Herbst, J.J. Jacoby, L.L. Zhou, A.M. Ahad, E.A. Mash, D.L. Kirkpatrick and G. Powis, *Mol. Cancer Ther.*, 2010, **9**, 706-717.

[30] Y. Yoon, *Bioorg. Med. Chem. Lett.*, 2014, **24**, 2334-2339.

[31] C.C. Thomas, M. Deak, D.R. Alessi and D.M. van Aalten, *Curr. Biol.*, 2002, **12**, 1256-1262.

[32] K.M. Ferguson, M.A. Lemmon, J. Schlessinger and P.B. Sigler, *Cell*, 1995, **83**, 1037-1046.

[33] C.C. Milburn, M. Deak, S.M. Kelly, N.C. Price, D.R. Alessi and D.M. Van Aalten, *Biochem. J.*, 2003, **375**, 531-538.

[34] O. Raifman, S. Kolusheva, M.J. Comin, N. Kedei, N.E. Lewin, P.M. Blumberg, V.E. Marquez and R. Jelinek, *FEBS J.*, 2010, **277**, 233-243.

[35] R. Borah, D. Talukdar, S. Gorai, D. Bain and D. Manna, *RSC Advances*, 2014, **4**, 25520-25531.

[36] N. Mamidi, S. Gorai, B. Ravi and D. Manna, *RSC. Advances*, 2014, **4,** 21971-21978.

[37] M.A. Lemmon, K.M. Ferguson, R. O'Brien, P.B. Sigler and J. Schlessinger, *Proc. Natl. Acad. Sci. USA*, 1995, **92**, 10472-10476.

[38] J.E. Johnson, J. Giorgione and A.C. Newton, *Biochemistry*, 2000, **39**, 11360-11369.

[39] O. Lorenzo, S. Urbe, and M.J. Clague, *J. Cell. Sci*., 2005, **118**, 2005-2012.

[40] R. Katso, K. Okkenhaug, K. Ahmadi, S. White, J. Timms and M.D. Waterfield, *Annu. Rev. Cell. Dev. Biol.,* 2001, **17**, 615-675.

[41] L. Catley, T. Hideshima, D. Chauhan, P. Neri, P. Tassone, R. Bronson, W. Song, Y.T. Tai, N.C. Munshi and K.C. Anderson, *Exp. Hematol*., 2007, **35**, 1038-1046.

[42] P. Workman, P.A. Clarke, F.I. Raynaud and R.L. van Montfort, *Cancer Res*., 2010, **70**, 2146-2157.

[43] C.C. Kumar and V. Madison, *Oncogene*, 2005, **24**, 7493-7501.

[44] M. Hussein, M. Bettio, A. Schmitz, J.S. Hannam, J. Theis, G. Mayer, S. Dosa, M. Gutschow and M. Famulok, *Angew. Chem. Int. Ed. Engl*., 2013, **52**, 9529-9533.

[45] A.C. Estrada, T. Syrovets, K. Pitterle, O. Lunov, B. Buchele, J. Schimana-Pfeifer, T. Schmidt, S.A. Morad and T. Simmet, *Mol. Pharmacol*., 2010, **77**, 378-387.

[46] W. Huang, M. Barrett, N. Hajicek, S. Hicks, T.K. Harden, J. Sondek and Q. Zhang, *J. Biol. Chem.,*2013, **288**, 5840-5848.

[47] G. Sala, F. Dituri, C. Raimondi, S. Previdi, T. Maffucci, M. Mazzoletti, C. Rossi, M. Iezzi, R. Lattanzio, M. Piantelli, S. Iacobelli, M. Broggini and M. Falasca, *Cancer Res*., 2008, **68**, 10187-10196.

[48] L. Zhang, S. Malik, G.G. Kelley, M.S. Kapiloff and A.V. Smrcka, *J. Biol. Chem*., 2011, **286**, 23012-23021.

[49] J.H. Hurley and S. Misra, *Annu. Rev. Biophys. Biomol. Struct*., 2000, **29**, 49-79.

[50] C. Deraedt, N. Pinaud and D. Astruc, *J. Am. Chem. Soc*., 2014, **136**, 12092-12098.

[51] P.R. Bagdi, R.S. Basha, P.K. Baruah and A.T. Khan, *Rsc. Advances*, 2014, **4**, 10652-10659.

[52] H.A. Stefani, M.F.Z.J. Amaral, F. Manarin, R.A. Ando, N.C.S. Silva and E. Juaristi, *Tett. Lett*., 2011, **52**, 6883-6886.

[53] G. van Meer, D.R. Voelker and G.W. Feigenson, *Nat. Rev. Mol. Cell Biol*., 2008, **9**, 112-124.

[54] D. Manna, N. Bhardwaj, M.S. Vora, R.V. Stahelin, H. Lu and W. Cho, *J. Biol. Chem*., 2008, **283**, 26047-26058.

[55] N.E. Wilsher, W.J. Court, R. Ruddle, Y.M. Newbatt, W. Aherne, P.W. Sheldrake, N.P. Jones, M. Katan, S.A. Eccles and F.I. Raynaud, *Drug. Metab. Dispos*., 2007, **35**, 1017-1022.

[56] R.R. Klein, D.M. Bourdon, C.L. Costales, C.D. Wagner, W.L. White, J.D. Williams, S.N. Hicks, J. Sondek and D.R. Thakker, *J. Biol. Chem*., 2011, **286**, 12407-12416.

Conclusions and Scope for future work

Most of the phosphoinositides binding domains have been characterized as a specific PIP interacting module and this interaction is necessary and sufficient for their membrane targeting and localization. Among the large number of PIP interacting domains known so far, only a small number of them have been successfully characterized. Therefore in this thesis, we have determined the membrane binding properties of Tks5-PX and Lpd-PH domain and also have developed PIP/PH domain interaction based small molecule inhibitors. *Invitro* binding parameters have been measured using surface plasmon resonance, FRET-based competitive binding assay and also role of the hydrophobic amino acid residues in membrane binding have been determined by monolayer penetration measurements. The significance of *invitro* binding parameters has been further elucidated by cellular colocalization and/or translocation studies.

We have successfully investigated the phosphoinositide binding nature of Tks5-PX and Lpd-PH domain. In **chapter 2**, we have determined the roles of cationic and hydrophobic amino acid residues of Tks5-PX domain in membrane binding. FRET-based competitive binding as well as SPR binding measurements demonstrates that Tks5-PX domain has dual binding specificity to both PI(3)P and PI(3,4)P_2 lipids. Also our studies show that R42/R93 cationic residues are the main phosphoinositide binding partners. Monolayer measurements suggest that the hydrophobic residues present at the binding surface of Tks5-PX also play important role in membrane binding by partial membrane penetration. Cellular localization patterns of the PX domain and its mutants in normal A549 cells are consistent with their *in vitro* membrane binding properties. PX domain colocalizes with PI(3)P binding cellular marker at the early endosomal membranes and translocate to the plasma membrane upon stimulation with platelet-derived growth factor. In **chapter 3**, we have quantitatively determined the binding parameters of Lpd-PH domain employing the similar biophysical studies as performed in chapter 2. FRET analysis and SPR measurements showed that Lpd-PH domain strongly interact with the PI(3,4)P_2 lipid containing membranes but monolayer penetration measurements exhibited its inability to penetrate significantly into the membrane even in presence of the PI(3,4)P_2 lipid. From the *in vitro* binding measurements it has been demonstrated that K32/R34 residues are the key PI(3,4)P_2 binding residues. Our cellular studies showed that GFP-fused Lpd-PH domain localize at the plasma membrane in PDGF-stimulated A549 cells. However, the mutation of main PI(3,4)P_2 binding residues, K32/R34

completely abolished the membrane translocation. Overall, our combined theoretical and experimental analyses showed that the cationic residues present at the membrane binding surface of Lpd-PH domain predominantly regulates the PI(3,4)P_2-dependent membrane binding of Lpd protein.

This lipid-protein interaction is crucial for the activation of host protein and the understanding of its binding property is the key step for the enzyme specific drug development. In this regard, next two chapters focused on the development of PIP/PH-domain interaction based small molecule inhibitors. In **chapter 4**, we have described the development of 4-Amino-1,2,5-oxadiazole-based antagonists, **GPI**s for PI(3,4,5)P_3-PH-domain binding and determined their inhibitory effect by using competitive-surface plasmon resonance (SPR) analysis (IC_{50} ranges from 1.85 to 16.35 μM for PI(3,4,5)P_3/AKT1-PH-domain binding assay). Our study also demonstrated that these non-lipid based compounds with 4-amino-N′-hydroxy-1,2,5-oxadiazole-3-carboximidamide moiety strongly interact with the PI(3,4,5)P_3 binding of AKT1-PH-domain, but weakly interact with the PI(3,4)P_2 and PI(4,5)P_2 binding PH domains. The potent compounds also interact weakly with the liposome through its interfacial region. Cellular measurements showed that the potent compounds have weak cytotoxicity and moderate inhibition effect on AKT-kinase activity. In **chapter 5,** we have employed 1,2,3-triazol-4-yl methanol containing small molecule (**CIPs**) as antagonists for PI(4,5)P_2/PH-domain interaction and have determined their inhibitory effect by using competitive-SPR analysis (IC_{50} ranges from 53 to 159 nM for PI(4,5)P_2/PLCδ1-PH domain binding assay). We have also used PI(3,4,5)P_3, PI(3,4)P_2, PI(4,5)P_2 specific PH-domains to determine binding selectivity of the compounds. Various physicochemical analyses showed that the compounds have weak affect on fluidity of the model membrane but strongly interact with the PLCδ1-PH domains preferably through its PIP binding site. The 1,2,3-triazol-4-yl methanol moiety and nitro group of the compounds are found to be essential for their exothermic interaction with the PH-domains. Potent compounds can efficiently displace PLCδ1-PH domain from PM to cytosol in A549 cells.

Therefore, this thesis demonstrated the membrane binding properties of PX and PH domain containing proteins and has also led to the development of PIP/PH-domain interaction based non-lipid small molecules with minimal side effects. It is noteworthy that this is the first study to show that PH domain could be targeted for the development of inhibitor for PLCδ1 enzyme. This is also the first work to successfully determine (both in *Invitro* and cellular environment) the membrane binding nature of Tks5-PX and Lpd-PH domains. This PIP/PX and/or PH domain binding study is not only impotent for further

understanding of their cellular activity but also for intervening the role of their interaction based small molecule inhibitors. In addition, triazole and oxadiazole moieties are also found to have a wide range of applications as bioactive molecules exhibiting antibacterial, antiviral and anticancer properties. Therefore, this study suggest that the 4-amino-N′-hydroxy-1,2,5-oxadiazole-3-carboximidamide and 1,2,3-triazol-4-yl methanol moiety can be used for the development of nonphosphate-based potential regulators for PIP/PH and other lipid binding domains containing proteins. It is noteworthy to mention that preliminary study performed with one of our 4-amino-N′-hydroxy-1,2,5-oxadiazole-3-carboximidamide moiety containing compound that exhibits potent inhibitory effect of the kinase activity of AKT in various cancer cell lines which encouraged us for further *in vivo* (mice model) study.

Appendix

General reagents- Acetic acid, Hydrochloric acid, methanol, ethanol, potassium acetate, di sodium hydrogen phosphate, chloroform were purchased from SRL and Merck, India.

Molecular biology grade reagents/ enzymes- SDS, Tris-base, EDTA, Agarose, acrylamide, APS, bis-acrylamide, TEMED, IPTG, triton x 100, dNTP, pfu enzyme, DMSO, sodium chloride, potassium chloride, kanamycine, ampiciline, agar, LB broth, T4-DNA ligase, Xho1, Kpn1, Ecor1, DNA and protein marker, Commassie brilliant blue (CBB) R250 and G250, Bradford reagent,

Table A1. Bacterial and Mammalian Cell culture medium

Media	Constituents	Concentration	pH
Luria broth (LB)	Bactotryptone Yeast extract NaCl	1.0% 0.5% 0.5%	7.2
DMEM	DMEM powder with high glucose for 1 lit, 3.7g	-	7.4
DMEM with serum	DMEM, 10% serum, 1x antibiotics	-	7.4

Table A2. List of buffers and solutions

Buffers / Solutions	Compositions
Tris acetate EDTA (TAE) buffer, 50x (100ml)	24.2 g Tris base, 5.71 ml CH_3COOH, 10 ml of 0.5 M EDTA
30% acrylamide-bisacrylamide solution (100 ml)	29.2 g acrylamide, 0.8 g bisacrylamide
Gel running buffer	250 mM Tris base, 250 mM glycine, 0.1% SDS
Sample loading buffer (1X)	50 mM Tris-HCl pH 6.8, 2 % SDS, 10 % glycerol, 1% β-mercaptoethanol, 0.02 % bromophenol blue
Staining solution	50 % methanol, 10 % acetic acid, 0.25 % CBB R250
Destaining solution	30 % methanol, 10 % acetic acid, 60 % water

Table A3. Buffer solutions for plasmid isolation

Buffer	Compositions
Solution I (P1 buffer)	50 mM glucose, 25 mM Tris Hcl, 10 mM EDTA (pH 8.0)
Solution II (P2 buffer)	0.2 N NaOH, 1 % SDS
Solution II (P3 buffer)	5 M potassium acetate, pH adjusted to 4.8 with acetic acid

Table A4. List of primers for Tks5-PX domain mutations

Name	Sequence	Annealing Temp. (°C)
Tks5-PX	XhoI-Forward: 5'- ATT CTC GAG ATT ATG GAT ATG CTC GCC TAC TGC GTG -3' KpnI-Reverse: 5'- ATT CGG TAC CGT GAA GAA CCG GAA GAC TTC GTC -3'	60
TKS5-PX-R42A	Forward: 5'-CAG ACT ATC TAC CGG GCT TAC AGC AAG TTC-3' Reverse: 5'- GTC GAA CTT GCT GTA AGC CCG GTA GAT AGT -3'	56.4
TKS5-PX-R43A	Forwar: 5'- CAG ACT ATC TAC CGG GCC TAC AGC AAG TTC TTC -3' Reverse: 5'- GAA GAA CTT GCT GTA GGC CCG GTA GAT AGT CTG -3'	58
TKS5-PX-K78A	Forward: 5'- TTT CTT CCA GGC GCT ATC CTC TTC CGG AGA -3' Reverse: 5'- TCT CCG GAA GAG GAT AGC GCC TGG AAG AAA -3'	60
TKS5-PX-I79A	Forward: 5'- TTT CTT CCA GGC AAG GCT CTC TTC CGG AGA AGC -3' Reverse: 5'- GCT TCT CCG GAA GAG AGC CTT GCC TGG AAG AAA -3'	61.7
TKS5-PX-L80A/F81A	Forward: 5'- TT CCA GGC AAG ATC GCT GCA CGG AGA AGC CAC AT -3' Reverse: 5'- AT GTG GCT TCT CCG TGC AGC GAT CTT GCC TGG AA –3'	64
TKS5-PX-R82A/R83A	Forward: 5'- AAG ATC CTC TTC GCT GCT AGC CAC ATC -3' Reverse: 5'- GAT GTG GCT AGC AGC GAA GAG GAT CTT -3'	63

TKS5-PX-R93A	Forward: 5'- GAC GTG GCT GTG AAG GCT CTA AAG CCC ATC GAT -3' Reverse: 5'- ATC GAT GGG CTT TAG AGC CTT CAC AGC CAC GTC -3'	59.5

Table A5. List of primers for Lpd-PH domain mutations

Name	Sequence	Annealing Temp (°C)
Lpd-PH	XhoI-Forward: 5'- ATT CTC GAG ATT ATG GAT ATG GTC CTC TTG GAG-3' KpnI-Reverse- 5'- ATT CGG TAC CGT CTG AGA CTC TGG -3'	55
Lpd-PH-K28A	Forward: 5'-TTG AAG GAT GAT GGC GCT AAG TCC TGG AAA AAG-3' Reverse: 5'- AAC TTC CTA CTA CCG CGA TTC AGG ACC GGG GGC-3'	58
Lpd-PH-K24A	Forward: 5'- GTC CTT TGG TTG GCA GAT GAT GGC AAG AAG -3' Reverse: 5'- CTT CTT GCC ATC ATC TGC CAA CCA AAG GAC -3'	58
Lpd-PH-L23R /D25G	Forward: 5'- A GTC CTT TGG CGT AAG GGA GAT GGC AAG AA -3' Reverse: 5'- TT CTT GCC ATC TCC CTT ACG CCA AAG GAC T -3'	59.4
Lpd-PH-K29A/W31A	Forward: 5'-GAT GAT GGC AAG GCA TCC GCA AAA AAG CGT TAT -3' Reverse: 5'- ATA ACG CTT TTT TGC GGA TGC CTT GCC ATC ATC -3'	59
Lpd-PH-K32A /R34A	Forward: 5'- AAG AAG TCC TGG GCA AAG GCA TAT TTT CTC TTG -3' Reverse: 5'- CAA GAG AAA ATA TGC CTT TGC CCA GGA CTT CTT -3'	57
Lpd-PH-K96A	**Forward:** 5'-**CCA CAA ATC CAG AAG AAA GCA CAA TAT ATC AAA**-3' Reverse: 5'- GGT GTT TAG GTC TTC TTT CGT GTT ATA TAG TTT-3'	53
Lpd-PH-K79A	Forward: 5'- CGG AAC AAA TAC GCA GCA CCT ACA GAC -3' Reverse: 5'- GTC TGT AGG TGC TGC GTA TTT GTT CCG -3'	56

List of Publications

1. **S. Gorai,** D. Paul, N. Haloi, R. Borah, M. Santra and D. Manna, (***communicated***)
2. **S. Gorai,** D. Paul, N. Haloi, R. Borah, M. Santra and D. Manna, *Molecular Biosystems*. 2016, **12**, 747-757.
3. **S. Gorai,** S. Paul, S. Ganga, R**.** Borah, M. Santra and D. Manna, *Medicinal chem com.* 2015,**6**, 1798-1808
4. **S. Gorai,** P.R. Bagdi, R. Borah, D. Paul, M. Santra, A.T. Khan and D. Manna, *Biochemistry and Biophysics Reports,* 2015, **2**, 75-83
5. R. Borah, N. Mamidi, S. Panda, **S**. **Gorai,** S. Pathak and D. Manna, *Molecular Biosystems***,** 2015, **11**, 1389-1399
6. R. Borah, D. Talukdar, S. **Gorai,** D. Bain and D. Manna, *RSC Advance,* 2014, **4**, 25520-25531.
7. N. Mamidi, [†] **S. Gorai,** [†] R. Bolledu and D. Manna, *RSC Advances,* 2014, **4**, 21971-21978. [[+]equally contributed]
8. P. Kumar, **S**. **Gorai,** M. Santra, B. Mondal, and D. Manna, *Dalton Transactions***,** 2012, **41**, 7573-7581.
9. N. Mamidi, **S**. **Gorai,** J. Sahoo and D. Manna, *Chemistry and Physics of Lipids***,** 2012, **165**, 320-330.
10. N. Mamidi, S. **Gorai,** R. Mukherjee, and D. Manna, Molecular *Biosystems***.** 2012, **8**, 1275-1285.

Seminar/conference attended

1. **S. Gorai** and D. Manna, "*Mechanistic Insight into the Phosphatidylinositol-binding Properties of TKS5-Phox-Homology Domain*", FICS-2012, IIT Guwahati, India.
2. **S. Gorai** and D. Manna, "*Roles of basic and hydrophobic amino acid residues of TKS5-Phox Homology domain in membrane binding",* ISCB-2014, University of Delhi, India.
3. **S. Gorai** and D. Manna, "*Biophysical Insights into the Inhibitory mechanism of Triazole-Based Small Molecules on Phosphatidylinositol-4,5-bisphosphate Binding Pleckstrin Homology Domain",* ISBOC-2015, IISER PUNE, India.